
Polynomial Context-Truncation Sensitivity in Autoregressive Language Models: Sequential Wyner–Ziv Bounds for KV Cache Compression

Munsik Kim¹

Abstract

We study the rate–distortion limits of online KV cache compression in autoregressive language models, formulating it as sequential Wyner–Ziv source coding on the filtration induced by the model, with the next-step query as decoder side information. Empirically, across four models spanning two families and 0.5–3B parameters, we find that the next-token distribution’s sensitivity to context truncation decays *polynomially* rather than *geometrically*: a power law improves on an exponential fit by an order of magnitude in extrapolation, the fitted exponent is recovered independently from a sink-plus-recent KL measurement, and the decay is verified to be free of positional-encoding artifacts by a position-preserving ablation. Under a corresponding *polynomial truncation-sensitivity* assumption, our main result characterizes the per-token memory requirement of *suffix-only* cache policies: a sliding-window scheme attains distortion ε with window $w = O(\varepsilon^{-1/\alpha})$, and—under an additional two-sided Bayes-risk condition—a converse shows $w = \Omega(\varepsilon^{-1/\alpha})$ is necessary within this policy class, so the scaling is $\Theta(\varepsilon^{-1/\alpha})$ for suffix-only policies. Whether recurrent or propagating cache summaries can beat this scaling is left open. An explicit block-Markov scheme achieves the upper bound; its rate-of-convergence exponent matches the converse under additional forward-decay and regularity hypotheses (not implied by truncation sensitivity alone), and differs by a factor of two otherwise. Empirically, the polynomial law predicts the degradation curves of concrete cache policies: recency-based eviction (sliding, sink-plus-recent) suppresses distortion by roughly two orders of magnitude over random retention at equal budget, with a power-law decay in the budget.

¹Independent Researcher. Correspondence to: Munsik Kim <physicist456@gmail.com>.

Preprint. May 26, 2026.

1. Introduction

Long-context inference with autoregressive language models is bottlenecked by the linear growth of the key-value (KV) cache (Vaswani et al., 2017; Shazeer, 2019; Ainslie et al., 2023). A rich ecosystem of compression schemes has emerged: heavy-hitter eviction (Zhang et al., 2023; Liu et al., 2023), sliding-window attention with attention sinks (Xiao et al., 2024; Jiang et al., 2023), multi-head latent attention (DeepSeek-AI, 2024), and low-bit quantization (Liu et al., 2024; Kang et al., 2024). Each scheme is justified empirically; none is accompanied by a quantitative statement of what is achievable in principle for the online compression problem.

We formulate KV cache compression as a sequential Wyner–Ziv source coding problem on the filtration $\{\mathcal{F}_t\}$ induced by the language model, with the next-step query Q_t serving as decoder side information (Wyner & Ziv, 1976; Witsenhausen, 1980). The sequential setting departs from classical Wyner–Ziv in two ways: the source is non-stationary, and the decoder receives token-level side information.

The truncation-sensitivity question. Classical compression bounds under memory constraints rely on a *mixing* or *ergodicity* condition specifying how quickly the influence of distant past decays. The standard assumption is ρ -mixing or geometric ergodicity of the underlying process:

$$\left| \mathbb{P}(X_t = x \mid X_{1:t-1}) - \mathbb{P}(X_t = x \mid X_{t-w:t-1}) \right| \leq C\rho^w$$

for some $\rho \in [0, 1)$. This form is natural for Markov chains with spectral gap and is mathematically convenient: it yields $\log(1/\varepsilon)$ -size windows for ε accuracy and clean block-Markov coding theorems. However, the form is an assumption about the source, and is not derived from the language-modeling setup.

A central empirical contribution of this work is to test this assumption directly on a trained model. Since the data-generating process of natural language is inaccessible, we instead measure the trained model’s sensitivity to context truncation: $\widehat{\text{TV}}_w := \text{TV}(p_\theta(\cdot \mid X_{1:t-1}), p_\theta(\cdot \mid X_{t-w:t-1}))$, the change in the model’s next-token distribution when conditioning on only the most recent w tokens. On Qwen2.5-

0.5B (Yang et al., 2024), sweeping $w \in \{2, 4, \dots, 256\}$ over 100 prefixes from each of two domains (NLTK Gutenberg books, GitHub Python source), the data are well described by a power law $\widehat{\text{TV}}_w \propto w^{-\alpha}$ (log-RMSE 0.08–0.14) rather than an exponential (log-RMSE 0.20–0.31), with measured exponents $\alpha_{\text{nat}} = 0.44$ and $\alpha_{\text{code}} = 0.38$. We refer to this property as *polynomial truncation sensitivity* to emphasize that it is a property of the trained model under the evaluation distribution, rather than a claim about the underlying data process. The finding is qualitatively consistent with the heavy-tailed statistics of natural language (Piantadosi, 2014) and the power-law spectra observed in scaling-law analyses of large models (Kaplan et al., 2020), both of which would predict polynomial rather than geometric behavior at the model level.

Our contribution. Motivated by the empirical observation, we develop an information-theoretic framework under a *polynomial truncation-sensitivity* assumption (Definition 3.3). The central contribution is a characterization of the *memory requirement* of suffix-only cache policies—tight within that class under a two-sided Bayes-risk condition—together with an explicit achievability scheme, with additional universal and structural extensions deferred to the appendix.

- (C1) *Sequential Wyner–Ziv converse.* For any causal on-line scheme achieving average KL distortion $\leq D$, $\liminf_n \mathbb{E}[R_n] \geq R^*(D)$ (Theorem 4.1), with finite-sample forms in Appendix H (Theorem H.1, Corollary H.2).
- (C2) *Window scaling for suffix-only policies.* A sliding-window scheme achieves TV distortion ε with window $w = O(\varepsilon^{-1/\alpha})$ (Theorem 4.2); a *conditional* converse shows $w = \Omega(\varepsilon^{-1/\alpha})$ is necessary *within the class of suffix-only reconstructions* under a two-sided Bayes-risk sensitivity condition (Definition 4.4, Theorem 4.5). The per-token memory requirement of suffix-only policies is thus $\Theta(\varepsilon^{-1/\alpha})$ (Corollary 4.8). Whether recurrent or propagating cache summaries can achieve a better scaling is an open problem.
- (C3) *Explicit achievability.* A block-Markov random-coding scheme with window $w_n = n^{1/(\alpha+1)}$ achieves distortion within $O(n^{-\alpha/(\alpha+1)})$ of D (Theorem 4.6). Its rate is within $O(n^{-\alpha/(2(\alpha+1))})$ of $R^*(D)$ in general, and within $O(n^{-\alpha/(\alpha+1)})$ —matching the converse exponent—under additional forward-decay and regularity hypotheses *not* implied by truncation sensitivity alone (Theorem L.11). The sharpening replaces an Azuma bound by a Freedman bound that exploits the long-memory growth of the per-block redundancy variance.
- (C4) *Sink-plus-recent implication.* A direct consequence

places sink-plus-recent eviction—a deployed baseline combining attention sinks with a recent-token window—in the rate–distortion hierarchy: under α -polynomial truncation sensitivity, sink-plus-recent with k tokens achieves KL distortion $D = D^* + O(k^{-2\alpha})$ (Corollary 4.9, §4.4). The factor of 2 in the exponent arises from a local quadratic relation $\text{KL} \leq C(\varepsilon_{\min}) \cdot \text{TV}^2$ valid in the bounded-floor regime under bounded log-density (Lemma D.1); the standard Pinsker inequality provides only the converse direction $\text{TV} \leq \sqrt{\text{KL}/2}$. The empirical KL decay is well-fit by a power law with exponents $\alpha_{\text{KL}} \in [0.74, 1.04]$ across the two cross-model domains, satisfying $\alpha_{\text{KL}}/\alpha_{\text{TV}} \in [1.93, 2.38]$, bracketing the factor-of-two value predicted by the local quadratic KL–TV approximation. We interpret this agreement as empirical evidence consistent with the local quadratic approximation, rather than as a deterministic information-theoretic identity: the quadratic exponent requires the bounded-floor condition of Lemma D.1, and the observed ratios are consistent with the measured distributions operating in this bounded-floor regime. The operational-smoothing lemma (Lemma D.3) provides finite KL control when the worst-case floor is vacuous, but it yields only a *linear* KL–TV exponent and therefore does not by itself explain the observed doubling.

Three further results are deferred to the appendix as they are not needed for the main story: a *universal scheme* oblivious to α (Theorem M.1), a continuous-latent intrinsic-dimension lower bound (Theorem O.8), and a multi-layer Lagrangian rate allocation (Theorem O.12).

Implications for deployed compression schemes. The polynomial truncation-sensitivity finding has quantitative implications. Under the classical ρ -mixing assumption, a window of w tokens suppresses distortion exponentially in w , and a few dozen tokens suffice for negligible error. Under α -polynomial sensitivity with $\alpha \approx 0.5$, doubling the window halves the distortion only when $\alpha \approx 1$; smaller α values imply sub-linear improvement and motivate the empirical observation that deployed sliding-window schemes (Mistral’s $w = 4096$, StreamingLLM’s w -plus-sinks) require windows substantially larger than would be predicted under geometric mixing.

Organization. Section 2 situates our framework in the classical information theory, mixing theory, and KV cache compression literature. Section 3 introduces the formal setup. Section 4 states the four core results—the sequential Wyner–Ziv converse, the polynomial sliding-window upper bound, the conditional suffix-only lower bound with explicit achievability, and the sink-plus-recent implication—

and summarizes the deferred universal scheme and structural extensions. Section 5 reports the empirical validation. Section 6 connects to deployed systems, and Section 8 concludes. All proofs are deferred to the appendices.

2. Related Work

Information theory and mixing. Source coding with decoder side information (Wyner & Ziv, 1976) and its indirect (Witsenhausen, 1980) and nonanticipative (Massey, 1990; Charalambous et al., 2013) variants provide the rate-distortion backbone of our setup; rate-distortion dimension (Kawabata & Dembo, 1994) and high-resolution quantization (Bennett, 1948; Gersho, 1979) underlie the intrinsic-dimension result (Theorem O.8). On the source side, strong mixing conditions (Bradley, 2005) give geometric dependence decay ρ^w for spectral-gap Markov chains, whereas *subgeometric/polynomial* mixing (Douc et al., 2009) decays only as $w^{-\alpha}$. We adopt polynomial truncation sensitivity as the operative assumption, motivated by our measurements (§5) and consistent with the heavy-tailed statistics of language (Piantadosi, 2014) and neural scaling laws (Kaplan et al., 2020).

Theoretical analyses of attention. Lipschitz properties of self-attention (Kim et al., 2021; Dasoulas et al., 2021), rank collapse toward a low-rank subspace (Dong et al., 2021), the long-depth clustering limit (Geshkovski et al., 2023), and feed-forward layers as key-value memories (Geva et al., 2021; Phuong & Hutter, 2022) inform our multi-layer analysis (§4) but do not directly characterize mixing.

KV cache compression and empirical observations. Deployed schemes fall into families that our rate-distortion hierarchy organizes under one truncation-sensitivity condition: heavy-hitter eviction (Zhang et al., 2023; Liu et al., 2023; Ge et al., 2024), sliding-window-plus-sinks (Xiao et al., 2024; Jiang et al., 2023), prompt-aware selection (Li et al., 2024; Tang et al., 2024), layer/head-adaptive budgets (Cai et al., 2024; Feng et al., 2024), continuous-latent compression (DeepSeek-AI, 2024), quantization (Liu et al., 2024; Kang et al., 2024), and architectural variants (Ainslie et al., 2023; Shazeer, 2019; Meta AI, 2024). The sink-plus-recent corollary (Corollary 4.9) applies directly to the sliding-window family; the heavy-hitter family requires the additional (empirical) assumption that high-attention tokens approximately coincide with sinks plus recency. Empirically, attention-score concentration on recent tokens and a sink (Xiao et al., 2024) and sublinear effective receptive fields (Chen et al., 2024) are consistent with our finding but do not measure decay exponents; intrinsic-dimension measurements in vision (Pope et al., 2021; Ansuini et al., 2019) serve as order-of-magnitude anchors only.

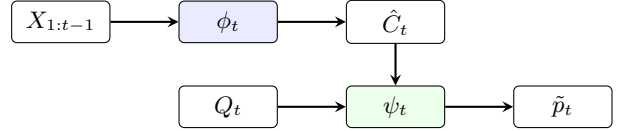


Figure 1. Sequential Wyner–Ziv compression of the KV cache. The encoder ϕ_t maps past tokens to \hat{C}_t ; the decoder ψ_t reconstructs \tilde{p}_t from $(\hat{C}_{\leq t}, Q_t)$. Distortion $D_{\text{KL}}(p_t \parallel \tilde{p}_t)$.

3. Preliminaries and Problem Formulation

Notation. Let $X_1, X_2, \dots \in \mathcal{V}$ denote tokens with $|\mathcal{V}| = V$, and let $\mathcal{F}_t := \sigma(X_1, \dots, X_t)$. The language model is a fixed function f producing logits $Z_t = f(X_{<t})$ via L attention layers; the next-token distribution is $p_t := \text{softmax}(Z_t)$. For each t , the side information is the query vector $Q_t \in \mathbb{R}^k$ computed at the final layer.

On the abstraction of Q_t . We treat Q_t as *idealized exogenous* decoder side information: the decoder receives the query the uncompressed model would compute and reconstructs the next-token distribution from the compressed cache and this query. This is a deliberate simplification: in an actual transformer the query is itself produced from the (possibly compressed) hidden states, so Q_t and $\hat{C}_{\leq t}$ are not strictly independent, and the abstraction collapses the multi-layer query/key/value structure into a single side channel. Our results are thus bounds for this idealized single-channel formulation; a fully recursive layer-wise treatment is a natural extension (§7).

Assumption 3.1 (Bounded logits). There exists $B(n_{\max}) > 0$ such that $\|Z_t\|_{\infty} \leq B(n_{\max})$ a.s. for $t \leq n_{\max}$; consequently, $p_t \geq \epsilon := V^{-1}e^{-2B}$ componentwise.

Online compression. An *online encoder* is a sequence $\phi_t : \mathcal{V}^{t-1} \rightarrow \mathcal{C}_t$ producing codes $\hat{C}_t = \phi_t(X_{1:t-1})$. The encoder is causal in the strict sense that \hat{C}_t depends only on the strict past $X_{<t}$, not on X_t itself; this matches the KV-cache compression setting, where the cache at the time of predicting X_t summarizes the previously generated tokens $X_{<t}$. The compressed filtration is $\hat{\mathcal{F}}_t := \sigma(\hat{C}_1, \dots, \hat{C}_t)$ and satisfies $\hat{\mathcal{F}}_t \subseteq \mathcal{F}_{t-1}$ by construction. The *decoder* produces $\tilde{p}_t := \psi_t(\hat{C}_{\leq t}, Q_t)$. The per-token rate and distortion are

$$R_n := \frac{1}{n} \sum_{t=1}^n H(\hat{C}_t \mid \hat{\mathcal{F}}_{t-1}), \quad D_n := \frac{1}{n} \sum_{t=1}^n D_{\text{KL}}(p_t \parallel \tilde{p}_t).$$

Definition 3.2 (Sequential WZ rate function). An *auxiliary process* $\{U_t\}$ is an \mathcal{F}_t -adapted sequence that is $\hat{\mathcal{F}}_t$ -measurable. The per-step pointwise WZ rate is $\mathcal{R}_t^{\text{WZ}} := I(X_t; U_t \mid \hat{\mathcal{F}}_{t-1}) - I(U_t; Q_t \mid \hat{\mathcal{F}}_{t-1})$. The auxiliary is *D-admissible* if some measurable decoder $\psi_t = g_t(U_t, Q_t)$ achieves $\mathbb{E}[D_{\text{KL}}(p_t \parallel \tilde{p}_t)] \leq D$ on average. The sequential

Wyner–Ziv rate function is

$$R^*(D) := \inf_{\{U_t\}} \inf_{D\text{-admissible}} \liminf_n \frac{1}{n} \sum_{t=1}^n \mathbb{E}[\mathcal{R}_t^{\text{WZ}}].$$

Truncation-sensitivity assumption. The mixing-style condition we adopt below describes the *trained model’s* sensitivity to context truncation, not the mixing of the underlying data process (which is inaccessible). The distinction is important: the quantity we measure and assume properties of is the next-token distribution under the model p_θ , not the marginal of a hypothetical generating process. We make this explicit in the definition.

Definition 3.3 (Polynomial truncation sensitivity). The language model p_θ has α -polynomial truncation sensitivity with constants $C_{\text{TS}} > 0$ and $\alpha > 0$ if, for all t and $w \geq 1$,

$$\text{TV}(p_\theta(\cdot | X_{1:t-1}), p_\theta(\cdot | X_{t-w:t-1})) \leq C_{\text{TS}} w^{-\alpha}$$

almost surely (with respect to the joint distribution of $X_{1:t-1}$ used at evaluation), where $\text{TV}(p, q) := \frac{1}{2} \sum_{x \in \mathcal{V}} |p(x) - q(x)|$.

Remark 3.4 (Equivalent pointwise sufficient condition). A stronger uniform-pointwise bound $\sup_x |p_\theta(x | X_{1:t-1}) - p_\theta(x | X_{t-w:t-1})| \leq C_{\text{ptw}} w^{-\alpha}$ implies Definition 3.3 with $C_{\text{TS}} \leq \frac{V}{2} C_{\text{ptw}}$. The pointwise form is convenient in some proofs (e.g., Lemma J.15) but is generally not necessary; all main results require only the TV form of Definition 3.3.

Remark 3.5 (Naming). We avoid the term “polynomial mixing” in isolation because it suggests a property of the data-generating process. The quantity in Definition 3.3 is a property of the trained model p_θ under the context distribution at evaluation. The condition is what we measure (Section 5) and is the operative condition for our results. The classical ρ -mixing condition for processes is strictly stronger when applied to p_θ : any process with ρ^w truncation sensitivity is α -polynomially sensitive for every $\alpha > 0$, but the converse fails. Theorem 4.2 below recovers the geometric case as the limit $\alpha \rightarrow \infty$.

4. Main Theoretical Results

4.1. Core Result 1: Asymptotic Lower Bound

Theorem 4.1 (Asymptotic lower bound). *Under Assumption 3.1, for any encoder–decoder pair with $\limsup_n \mathbb{E}[D_n] \leq D$,*

$$\liminf_n \mathbb{E}[R_n] \geq R^*(D).$$

The proof (Appendix H) constructs three martingales adapted to the compressed filtration $\{\hat{\mathcal{F}}_t\}$: $M_t^{(1)}$ encoding source entropy, N_t encoding the log-likelihood ratio

of the decoder estimate, and S_t encoding the pointwise Wyner–Ziv rate. The argument is mixing-free—no assumption on α or ρ is needed for the asymptotic lower bound. A finite-sample concentration bound and the corresponding expectation form $\mathbb{E}[R_n] \geq R^*(D) - O(\log n/n)$ are given in Appendix H (Theorem H.1, Corollary H.2).

4.2. Core Result 2: Polynomial Sliding-Window Approximation

The asymptotic bound is uninformative for finite-window schemes. The following result, the main mixing-dependent theorem, replaces the classical geometric bound by a polynomial one.

Theorem 4.2 (Polynomial sliding-window approximation). *Under Assumption 3.1 and the α -polynomial truncation-sensitivity condition (Definition 3.3), the sliding-window compression scheme with window size*

$$w = \left\lceil (C_{\text{TS}}/\varepsilon)^{1/\alpha} \right\rceil$$

achieves $R_w^(D) \leq R^*(D - \varepsilon)$ for any $\varepsilon \in (0, D)$.*

The proof (Appendix J.6, Theorem J.14) adapts the block-Markov coding argument to the polynomial setting (Douc et al., 2009), with block length $B^* = w^{\alpha/2}/(2\sqrt{C_{\text{TS}}})$ balancing rate slack against distortion error. The required window $w \sim \varepsilon^{-1/\alpha}$ is *polynomial* in $1/\varepsilon$, in contrast to the *logarithmic* $w \sim \log(1/\varepsilon)$ under geometric mixing. The exponent depends on whether the target is TV ($w \sim \varepsilon_{\text{TV}}^{-1/\alpha}$) or KL, where the bounded-floor relation $\text{KL} \leq C(\varepsilon_{\text{min}})\text{TV}^2$ (Lemma D.1) gives $w \sim \varepsilon_{\text{KL}}^{-1/(2\alpha)}$. For the empirical $\alpha \in [0.38, 0.58]$ (§5), KL distortion 0.01 requires windows of order 10^2 tokens, consistent with deployed sliding-window schemes (Xiao et al., 2024; Jiang et al., 2023).

Corollary 4.3 (Mixing-sharpened concentration). *Under α -polynomial truncation sensitivity, Theorem H.1 sharpens to $R_n \geq R^*(D) - O(n^{-\alpha/(\alpha+1)}\sqrt{\log n})$, replacing the $1/(1-\rho)$ factor of the geometric case by a polynomial-in- α dependence.*

4.3. Core Result 3: Achievability and Optimal Window Scaling

The lower bound (Theorem 4.1) and the sliding-window approximation (Theorem 4.2) leave open two questions: (a) whether the window size $w \asymp \varepsilon^{-1/\alpha}$ is *necessary*, and (b) whether an explicit causal scheme achieves $R^*(D)$ at a finite rate of convergence. We address both. For (a), the window scaling is optimal *within the suffix-only policy class*, which we establish by a conditional window lower bound (requiring the two-sided Bayes-risk condition of Definition 4.4). For (b), we give an explicit achievability scheme with a non-asymptotic rate; the rate-convergence exponent

matches the converse in window size but leaves a gap in the n -dependence that we state explicitly as a conjecture.

Window scaling for suffix-only policies (tight within the class). The sliding-window approximation (Theorem 4.2) shows $w = O(\varepsilon^{-1/\alpha})$ suffices for TV distortion ε . The following converse shows it is *necessary within the suffix-only class*, under a two-sided sharpening of the truncation-sensitivity condition that we state explicitly as an additional assumption.

Definition 4.4 (Two-sided truncation sensitivity, Bayes-risk form). Let \mathcal{M}_w denote the class of suffix-only reconstructions at step t : distributions q_t measurable with respect to $\sigma(X_{t-w:t-1})$. The model has α -tight truncation sensitivity with constant $c_{\text{TS}} > 0$ if, in addition to Definition 3.3, the Bayes risk of approximating the full-context conditional by the best suffix-only reconstruction is bounded below: for every $w \geq 1$,

$$\liminf_{n \rightarrow \infty} \frac{1}{n} \sum_{t=1}^n \mathbb{E} \left[\inf_{q_t \in \mathcal{M}_w} \text{TV}(p_\theta(\cdot | X_{1:t-1}), q_t) \right] \geq c_{\text{TS}} w^{-\alpha}.$$

This is the operationally relevant lower bound: it asserts directly that *no* window- w reconstruction—not merely the truncated conditional $p_\theta(\cdot | X_{t-w:t-1})$ —can approximate the full conditional better than $c_{\text{TS}} w^{-\alpha}$ on average. It avoids assuming that the truncated conditional is the Bayes-optimal suffix reconstruction (which would require a tower property not guaranteed for trained models under positional-encoding effects). The companion upper bound of Definition 3.3 shows the truncated conditional *achieves* the $w^{-\alpha}$ rate, so the two-sided condition brackets the Bayes risk at $\Theta(w^{-\alpha})$.

Empirically validating the lower-bound half of Definition 4.4 would require estimating the conditional variability among contexts that share a similar length- w suffix—a measurement we do not attempt here and leave to future work; the present evidence (§5) directly supports only the upper-bound half (the $w^{-\alpha}$ decay of $\widehat{\text{TV}}_w$).

Theorem 4.5 (Conditional suffix-only lower bound (Bayes-risk implication)). *Call a scheme suffix-only if its reconstruction at step t is measurable with respect to the truncated context $X_{t-w:t-1}$ alone (equivalently, the codes carry no information about $X_{1:t-w-1}$ beyond what is in the suffix). Under α -tight truncation sensitivity (Definition 4.4), any suffix-only scheme with window w incurs average TV distortion at least $\Omega(w^{-\alpha})$. Consequently, achieving TV distortion ε requires $w = \Omega(\varepsilon^{-1/\alpha})$, matching the sufficiency of Theorem 4.2: the window scaling $w \asymp \varepsilon^{-1/\alpha}$ is optimal within the suffix-only class.*

The proof (Appendix K) is immediate from the Bayes-risk form of Definition 4.4: any suffix-only window- w scheme

produces a reconstruction in the class \mathcal{M}_w , so its distortion is at least the Bayes risk $\inf_{q \in \mathcal{M}_w} \text{TV}(p_\theta(\cdot | X_{1:t-1}), q) \geq c_{\text{TS}} w^{-\alpha}$, with no claim about which reconstruction is optimal. The restriction to suffix-only schemes is essential: a general causal scheme may *propagate* old information through a recurrently updated code (e.g. a running summary in C_t), in which case the last w codes can encode arbitrarily old context and the lower bound need not hold. Our achievability scheme (Theorem 4.6) is itself suffix-only, so the upper and lower bounds apply to the same class and the memory requirement of suffix-only sequential KV-cache compression is $\Theta(\varepsilon^{-1/\alpha})$. Whether a propagating scheme can beat this scaling is an open question.

Explicit achievability (finite- n rate). We complement the window-scaling result with an explicit online scheme and a non-asymptotic analysis.

Theorem 4.6 (Polynomial achievability). *Suppose Assumption 3.1 and α -polynomial truncation sensitivity (Definition 3.3) with $\alpha \in (0, 1]$. There exists a sequence of causal online (suffix-only) encoder–decoder pairs $\{(\phi_t^{(n)}, \psi_t^{(n)})\}$ using window size $w_n = \lceil n^{1/(\alpha+1)} \rceil$ with the following guarantees.*

(a) Expected rate (sharp, no forward-decay hypothesis).

$$\begin{aligned} \mathbb{E}[R_n] &\leq R^*(D) + O(n^{-\alpha/(\alpha+1)} \log n), \\ \mathbb{E}[D_n] &\leq D + O(n^{-\alpha/(\alpha+1)}). \end{aligned}$$

(b) High-probability rate (unconditional). *For any $\delta \in (0, 1)$, with probability $\geq 1 - \delta$,*

$$R_n \leq R^*(D) + O\left(n^{-\alpha/(2(\alpha+1))} (\log n) \sqrt{\log V \cdot \log(1/\delta)}\right).$$

The implicit constants depend on C_{TS}, α, V , and the auxiliary alphabet size, but not on n . For $\alpha > 1$ the distortion exponent saturates at $\min(\alpha, 1)/(\alpha+1)$ (the boundary term $w^{-1} \log w$ then dominates the truncation term $w^{-\alpha}$).

The proof (Appendix L) is a block-Markov random-coding construction with three ingredients: a window-restricted covering lemma (Lemma L.2); the block-typicality stability lemma (Lemma J.16), controlling the truncation bias; and a redundancy-accumulation bound (Lemma L.9). The window $w_n = n^{1/(\alpha+1)}$ balances the truncation bias against the codebook redundancy.

Remark 4.7 (Three rate guarantees and what each requires). The distortion exponent $\alpha/(\alpha+1)$ matches the converse window scaling unconditionally. The rate guarantees separate by hypothesis: (a) in expectation the sharp exponent $\alpha/(\alpha+1)$ holds with no forward-decay hypothesis (only the finite-memory covering regularity of Assumption L.1); (b)

in high probability an Azuma–Hoeffding bound gives the looser $\alpha/(2(\alpha + 1))$; and (c) the sharp exponent is restored in high probability only under the forward covariance-decay condition (\dagger), which is *not* implied by truncation sensitivity (Theorem L.11; details in Appendix L).

Corollary 4.8 (Memory characterization for suffix-only policies). *Under α -tight truncation sensitivity (Definition 4.4), the minimal window size (equivalently, the per-token KV-cache memory) required for average TV distortion ε by a suffix-only policy is $\Theta(\varepsilon^{-1/\alpha})$, with matching upper (Theorem 4.2) and lower (Theorem 4.5) bounds within that class. Under the additional bounded-floor condition of Lemma D.1, the corresponding KL-distortion memory scaling is $\Theta(\varepsilon_{\text{KL}}^{-1/(2\alpha)})$ via the local quadratic KL–TV relation. The characterization does not preclude that a more general propagating (non-suffix-only) scheme achieves a smaller window; establishing or refuting this is an open problem.*

Additional results (deferred to the appendix). Two further results round out the framework but are not needed for the main story. (i) A *universal scheme*, oblivious to α , attains the rate exponent of Theorem 4.6 simultaneously for every $\alpha \in [\alpha_{\min}, \alpha_{\max}]$ at the cost of a $\log n$ factor, using a logarithmic grid of window sizes with online selection (Theorem M.1, Appendix M). (ii) Two *structural extensions* connect the framework to deployed architectures: a continuous-latent intrinsic-dimension bound matching the Kawabata–Dembo rate–distortion dimension (Theorem O.8, Appendix O), and a multi-layer reverse-water-filling rate allocation (Theorem O.12, Appendix O.7). Both are mixing-independent and are stated and proved in full in the appendix.

4.4. Core Result 4: Sink-Plus-Recent Eviction

A common KV cache compression baseline retains the first few tokens (attention sinks (Xiao et al., 2024)) together with the most recent $k - O(1)$ tokens. We refer to this scheme as *sink-plus-recent eviction*; it is distinct from attention-score-based heavy-hitter eviction (e.g., H2O (Zhang et al., 2023), which we discuss separately in Section 6). Under polynomial truncation sensitivity, the rate–distortion location of sink-plus-recent eviction follows directly from Theorem 4.2.

Corollary 4.9 (Sink-plus-recent rate–distortion). *Under α -polynomial truncation sensitivity (Definition 3.3), Assumption 3.1, and a uniform reconstruction floor $\tilde{p}_t(x) \geq \epsilon_{\text{rec}} > 0$ for all x (e.g. a decoder outputting softmax of bounded logits, or a fixed smoothed decoder whose smoothing bias is below the target distortion), sink-plus-recent eviction with budget k achieves rate $R_{w=k}^*(D)$ for KL distortion*

$$D = D^* + O(k^{-2\alpha}),$$

where D^* is the full-cache distortion floor. The factor of 2 in the exponent arises from the small-perturbation quadratic

relation $\text{KL} \leq (2/\epsilon_{\text{rec}})\text{TV}^2$ under the reconstruction floor (Lemma D.1), not from Pinsker’s inequality. Without a uniform floor, the operational-smoothing route gives only the linear relation $\text{KL} = O(\text{TV})$ and hence the weaker exponent α (Remark D.4).

Proof sketch. Sink-plus-recent retention with budget k is equivalent under truncation-sensitivity to a sliding window of size k plus a small constant prefix. The TV contribution of evicted tokens is bounded by $C_{\text{TS}}k^{-\alpha}$ (Definition 3.3). Under Assumption 3.1, the model’s next-token distribution satisfies $p_t(x) \geq \epsilon_{\min}$ for all x ; Lemma D.1 (appendix) then yields $\text{KL}(p_t \parallel \tilde{p}_t) \leq (2/\epsilon_{\min})\text{TV}(p_t, \tilde{p}_t)^2$ in the small-TV regime, giving the KL distortion gap $O(k^{-2\alpha})$. Theorem 4.2 bounds the rate. \square

Why $\text{KL} \leq C \cdot \text{TV}^2$ and not Pinsker. The standard Pinsker inequality is $\text{TV} \leq \sqrt{\text{KL}/2}$, yielding $\text{KL} \geq 2\text{TV}^2$ —a lower bound on KL, not an upper bound. The opposite direction $\text{KL} \leq C \cdot \text{TV}^2$ requires additional structure on the distributions. Under Assumption 3.1, the next-token distribution p_t is bounded away from zero by $\epsilon_{\min} := V^{-1}e^{-2B}$. For two such distributions with $\text{TV}(p, q) \leq \epsilon_{\min}/2$, the quadratic local approximation $\text{KL}(p \parallel q) = \chi^2(p, q)/2 + O(\text{TV}^3)$ combined with $\chi^2(p, q) \leq \text{TV}(p, q)^2/\epsilon_{\min}$ yields the desired bound; we prove this as Lemma D.1.

The corollary predicts a power-law KL distortion gap with exponent 2α , where α is the TV-decay exponent of Theorem 4.2. This yields a quantitative internal-consistency prediction with two empirical checks: (i) the absolute values of α from the TV measurement and 2α from the KL measurement, and (ii) the ratio between them should bracket 2. Both are tested in Section 5.

Comparison to geometric mixing. Under the geometric assumption $D \propto \rho^k$, the distortion gap vanishes exponentially: $k \approx 30$ suffices for $D < 10^{-2}$ at $\rho = 0.85$. Under polynomial truncation sensitivity with $\alpha = 0.5$ (so KL decay exponent $2\alpha = 1.0$), achieving $D < 10^{-2}$ requires $k \sim 10^2$ tokens—a 3–4 \times increase, not the exponential separation that one might naively expect from changing the decay form. The empirical sink-plus-recent measurements (Appendix Figure 2) follow the polynomial decay closely: Natural at $k = 512$ yields $D \approx 0.04$, consistent with $k^{-1.04}$.

Sub-optimality vs. continuous-latent schemes. The sink-plus-recent rate is $O(k \log V)$ bits per token; for $k = 128$ and $V = 32,000$, this is approximately 1900 bits per token, two orders of magnitude above the lower bound $R^*(D)$. The gap motivates continuous-latent schemes such as MLA

(DeepSeek-AI, 2024), analyzed under our framework in Theorem O.8.

Relation to heavy-hitter eviction. The corollary applies to sink-plus-recent eviction, where the retained tokens are determined by position (first few + last $k - O(1)$). Heavy-hitter eviction schemes such as H2O (Zhang et al., 2023) and Scissorhands (Liu et al., 2023) select tokens based on attention scores rather than position. The connection to our framework requires an additional lemma stating that high-attention tokens approximately coincide with sinks plus recent positions; this is an empirical property of trained models and is not subsumed by mixing alone. We do not analyze heavy-hitter schemes in this work.

5. Empirical Validation

We first test two predictions of the framework on Qwen2.5-0.5B (Yang et al., 2024), then replicate across models and domains:

- (P1) **Polynomial TV decay.** The conditional-distribution shift \widehat{TV}_w decays as $w^{-\alpha}$ for some $\alpha > 0$, with power-law fit superior to exponential fit.
- (P2) **Sink-plus-recent KL decay with doubled exponent.** The sink-plus-recent KL distortion decays as $k^{-2\alpha}$, where α is the TV-decay exponent from (P1). The factor of 2 in the exponent follows from the quadratic local relation between KL and TV under bounded log-density (Lemma D.1, Corollary 4.9).

Experimental setup. We use four open models spanning two families and a $6\times$ range of parameter counts—Qwen2.5-0.5B/1.5B/3B (Yang et al., 2024) and SmoLLM2-1.7B (Allal et al., 2025)—with FP16 precision on a single 16 GB GPU (NVIDIA RTX 5080), batch size 1 and no gradient computation. Qwen2.5-0.5B serves as the primary model for the detailed ablations; the remaining models are used for the cross-model replication. For the primary short-window and cross-model measurements we sample 100 prefixes of length 1024 tokens from each of two domains: NLTK Gutenberg books (concatenation of classic literary works, $\sim 6.4M$ characters) as a natural language source, and a concatenation of large Python source files from prominent open-source projects (numpy, pandas, CPython, requests; $\sim 0.6M$ characters) as a code source. The domain-robustness experiment (§A.2) adds Wikipedia prose and structured JSON, and the long-window tail (§A.4) uses 16,500-token prefixes. All measurements use a position-preserving truncation protocol (below), which we verify is free of positional-encoding artifacts (§A.3).

Measurement protocol. For each prefix $X_{1:t}$ and each window size w , we measure $\widehat{TV}_w = TV(p_t, p_t^{(w)})$ where

p_t is the full next-token distribution and $p_t^{(w)} = p(\cdot | X_{t-w:t-1})$ is the distribution conditioned on the last w tokens. To avoid conflating genuine truncation sensitivity with a positional-encoding artifact (§7), we adopt a *position-preserving* protocol: the retained window is fed with its *original* absolute position indices $t - w, \dots, t - 1$ rather than reset to $0, \dots, w - 1$. We use a short window grid $w \in \{2, 4, 8, 16, 32, 64, 128, 256\}$ for the primary and cross-model measurements, an extended grid up to $w = 4096$ for the fit competition, and a long-prefix tail sweep up to $w = 8192$ (with 16,500-token prefixes) for the robustness check in §A.4. For each $k \in \{8, 16, 32, 64, 128, 256, 512\}$, we measure $D_{KL}(p_t \| p_t^{\text{Top-}K})$ where $p_t^{\text{Top-}K}$ is the distribution conditioned on the first 4 tokens (attention sinks) plus the most recent $k - 4$ tokens. We also evaluate a Random- K baseline conditioning on a uniformly random subset of k tokens preserving order. Curve fits are performed in log space; for model selection we compare against exponential, stretched-exponential, and broken-power-law alternatives by AIC (§A.4).

Results: power-law decay of TV. Figure 7 shows the measured TV decay on the primary model (Qwen2.5-0.5B). Over the short-window grid, power-law fits yield exponents $\alpha_{\text{nat}} = 0.44 \pm 0.05$ and $\alpha_{\text{code}} = 0.38 \pm 0.06$ (bootstrap 95% CI from 300 resamples over prefixes; intervals $[0.39, 0.48]$ and $[0.33, 0.46]$), with log-RMSE values:

Fit form	Natural (log-RMSE)	Code (log-RMSE)
Exponential $C\rho^w$	0.31	0.20
Power law $Cw^{-\alpha}$	0.14	0.08

The power-law fit improves log-RMSE by roughly $2\text{--}2.5\times$ relative to exponential, supporting prediction (P1). The exponents are recovered independently from the sink-plus-recent KL decay (below) and replicate across models (§5).

Results: doubled sink-plus-recent exponent. The sink-plus-recent KL decay (Appendix A, Figure 2) yields power-law exponents $\alpha_{\text{nat,KL}} = 1.04$ and $\alpha_{\text{code,KL}} = 0.74$, with high fit quality in both cases. The ratios to the TV-decay exponents from (P1) are

$$\frac{\alpha_{\text{nat,KL}}}{\alpha_{\text{nat,TV}}} = \frac{1.04}{0.44} = 2.38, \quad \frac{\alpha_{\text{code,KL}}}{\alpha_{\text{code,TV}}} = \frac{0.74}{0.38} = 1.93,$$

bracketing the factor-of-two predicted by the local quadratic KL-TV approximation (Corollary 4.9, Lemma D.1). A direct check of the underlying relation is shown in Appendix A.5 (Figure 6): plotting KL against TV^2 across budgets yields an approximately linear, through-the-origin trend in both domains, consistent with the bounded-floor relation $KL \leq C(\epsilon_{\text{min}}) TV^2$ holding with an effectively constant C over the measured range. This is the internal-consistency

check (P2): two independent measurements—window-truncation TV decay and sink-plus-recent KL decay—are related by the local quadratic KL–TV approximation, and the measured ratios are consistent with the prediction. The agreement is empirical evidence supporting the framework’s claim that a single underlying TV-exponent α governs both the sliding-window approximation and the sink-plus-recent distortion gap. We do not claim a deterministic information-theoretic identity between the two exponents; the doubling holds in the bounded-floor regime of Lemma D.1, which the KL-vs-TV² trend indicates the measured distributions occupy.

Results: sink-plus-recent versus Random- K . The Random- K baseline conditions on a uniformly random subset of k tokens (preserving order); this isolates the contribution of *positional structure* to the sink-plus-recent performance. Random- K exhibits essentially no decay over the measured range (Figure 2): the KL distortion at $k = 8$ (5.6 Natural, 9.6 Code) is comparable to that at $k = 512$ (3.4, 4.1). At $k = 512$, sink-plus-recent attains roughly $85\times$ (Natural) and $30\times$ (Code) lower median KL distortion than Random- K (a ratio of median KL values; raw medians in Table 2). The asymmetric retention of sinks and recent tokens—not the budget alone—is the operative mechanism.

Robustness (positional ablation and long-window tail). Two robustness checks, detailed in Appendix A, support the measurement. First, a *positional-encoding ablation* confirms the decay is genuine content forgetting rather than a position-shift artifact: a position-preserving protocol (retained tokens keep their original absolute indices) and the naive fresh-sequence protocol give exponents that agree to three decimals ($\alpha_{\text{nat}} = 0.437$ vs. 0.438; $\alpha_{\text{code}} = 0.383$ for both; Figure 4). All measurements in this section use the position-preserving protocol. Second, with a long prefix (16,500 tokens) the power law persists with the short-window exponent out to $w = 8192$ —well beyond the deployed 4k regime—while an exponential is rejected by an order of magnitude in extrapolation (Figure 5); we use a long prefix specifically so that the largest window still truncates a substantial fraction of the context, avoiding the measurement-boundary effect that arises when the window approaches the prefix length.

Cross-model replication. To test whether polynomial truncation sensitivity is an artifact of a single model, we measure the TV exponent on four models spanning 0.5–3B parameters and two families (Table 1). The power law holds in every case, and two trends emerge. First, the natural-language exponent increases monotonically with model scale within the Qwen2.5 family ($0.44 \rightarrow 0.51 \rightarrow 0.58$ from 0.5B to 3B), indicating that larger models recover the next-token distribution from a short recent window more

Model	Params	α_{nat}	α_{code}
Qwen2.5-0.5B	0.5B	0.437	0.383
Qwen2.5-1.5B	1.5B	0.508	0.439
SmolLM2-1.7B	1.7B	0.574	0.371
Qwen2.5-3B	3B	0.575	0.417

Table 1. Cross-model TV-decay exponents (position-preserving protocol, short-window grid, 100 prefixes per domain). The power law holds for every model; $\alpha_{\text{nat}} > \alpha_{\text{code}}$ throughout, and α_{nat} grows with scale within the Qwen2.5 family.

quickly—a scaling trend worth further study. Second, the ordering $\alpha_{\text{nat}} > \alpha_{\text{code}}$ is consistent across all four models. The phenomenon is thus not specific to one model or family, and the exponent—while model-dependent in magnitude—is a stable, measurable quantity, as the theory requires.

Comparison of domains: natural language is more truncation-sensitive than code. Across all four models, the natural-language exponent exceeds the code exponent: on the primary model, $\alpha_{\text{nat}} = 0.44$ versus $\alpha_{\text{code}} = 0.38$, and the ordering $\alpha_{\text{nat}} > \alpha_{\text{code}}$ holds for every model in the cross-model sweep (§5, Table 1). A larger exponent corresponds to *faster* decay of truncation sensitivity, so the next-token distribution in literary text is, on average, more quickly recovered from a short recent window than in Python source. We offer two non-mutually-exclusive explanations as hypotheses: (i) code carries persistent, long-range structure—open scopes, imported names, variables defined far earlier—that keeps distant tokens weakly informative for the next token, slowing the average decay; (ii) much of literary next-token prediction is governed by local lexical and grammatical context, so that beyond a modest window the residual dependence on distant tokens is small on average. We emphasize that the relevant quantity is the *average* dependence decay across positions, not the worst-case long-range structure: code clearly contains long-range dependencies, but they bind a minority of next-token decisions. To test whether the polynomial form is specific to literary text and Python, we measured the TV exponent on two further domains—Wikipedia-style prose and structured JSON—on the primary model. The power law is favored over an exponential by $2\text{--}4\times$ in log-RMSE in every domain, while the exponent varies only modestly ($\alpha \in [0.39, 0.44]$): the polynomial *form* is domain-robust, with a weak, not strongly systematic, dependence of α on domain structure at this scale (Appendix A.2, Table 3).

Cache-policy degradation. The distribution-level findings above translate directly into the degradation curves of concrete cache policies. On the primary model we compare five policies at a fixed budget k —full context, sliding window, sink-plus-recent, Random- K (a uniformly random k -token subset), and a simple attention-score heavy-hitter—

by the median $\text{KL}(\text{full} \parallel \text{policy})$ and the mean increase in negative log-likelihood (NLL) of the actual next token (Figure 3, Appendix A). The heavy-hitter policy here selects the k tokens with the largest attention mass from the final query position, averaged over the last layer’s heads (a one-step, last-query score rather than H2O-style cumulative attention), with the anchor and most-recent token always retained and the position-preserving protocol applied to the selected set; it is thus a lightweight attention-score baseline, not a tuned eviction policy. Three observations stand out. First, the recency-based policies (sliding and sink-plus-recent) dominate the others by one to two orders of magnitude: at $k = 512$ they incur median $\text{KL} \approx 0.011$ (Natural) and ≈ 0.003 (Code), versus 1.9 and 2.1 for Random- K —a roughly 100–700 \times reduction. Second, the heavy-hitter policy sits between: better than random (attention scores do carry signal) but well behind recency, consistent with the sink-plus-recent positions capturing most of the high-mass context. Third, every policy’s distortion *decays as a power law in k* , the predicted consequence of polynomial truncation sensitivity. Sliding and sink-plus-recent are nearly indistinguishable here (the attention sink adds little at prefix length 1024); their separation is expected to grow at the much longer contexts where sinks were originally motivated. Full per-domain curves, the NLL panels, and the heavy-hitter/sink overlap are in Appendix A.

Scope and limitations of the empirical study. The measurements span four models (0.5–3B, two families), four domains on the primary model (Gutenberg, Python, Wikipedia prose, and structured JSON) with two domains used for cross-model replication, $n = 100$ prefixes per domain, windows to $w = 8192$, a positional-encoding ablation, and a five-policy cache-degradation comparison. The power law and the ordering $\alpha_{\text{nat}} > \alpha_{\text{code}}$ replicate across all four models, the positional confound is ruled out (§A.3), and the polynomial form holds out to $w = 8192$ without the boundary artifact of shorter-prefix sweeps (§A.4). The principal remaining gaps are the restriction to models $\leq 3\text{B}$ (set by the 16 GB single-GPU budget) and the relatively small code corpus. The specific numerical values of α may still depend on training-data composition and tokenizer. Extension to 7–8B models and broader domain coverage (ArXiv/LaTeX, conversational, multilingual, and larger code corpora) is left to future work with larger GPUs.

6. Connections to Deployed Compression Schemes

We sketch how the framework relates to deployed schemes. Quantitative values for windows $w \gg 256$ are *extrapolations* of the $w \leq 8192$ measurements on Qwen2.5-0.5B and should be read as predictions to be tested, not established claims; in particular we do not assert specific distortion

values for Mistral-class models, which we did not measure.

Sliding-window schemes (StreamingLLM, Mistral). A sliding window plus a small initial-token prefix (Xiao et al., 2024) is the direct instantiation of Theorem 4.2; the attention sinks compensate for the initial $O(1)$ tokens where the polynomial-sensitivity assumption is expected to fail. Mistral’s fixed $w = 4096$ (Jiang et al., 2023) and StreamingLLM’s $w + k_{\text{sink}}$ configurations are *qualitatively* consistent with polynomial rather than geometric sensitivity: geometric mixing would predict $\rho^w \approx 0$ and hence negligible distortion at such windows, whereas the reported minor degradation versus full attention matches a slow polynomial decay. The precise distortion at these windows on those models remains to be measured.

Latent, quantized, and selection-based schemes. DeepSeek-V2’s latent dimension $d_c = 512$ across 60 layers (DeepSeek-AI, 2024) is consistent with the intrinsic-dimension bound (Theorem O.8) and the multi-layer allocation (Theorem O.12); this bound is mixing-independent. INT2 mixed-precision quantization (Liu et al., 2024; Kang et al., 2024) corresponds to the Bennett–Gersho overhead $d_c \log(1/\Delta)$ in the same theorem. Prompt-aware (SnapKV (Li et al., 2024), Quest (Tang et al., 2024)) and layer-adaptive (PyramidKV (Cai et al., 2024), Ada-KV (Feng et al., 2024)) schemes implicitly exploit the truncation sensitivity established here; a formal account of their gains over a naive sliding window requires a selection-aware refinement of Corollary 4.9, which we leave to future work.

7. Limitations

Empirical scope. Our direct measurements use four models (Qwen2.5-0.5B/1.5B/3B, SmoLLM2-1.7B), four domains on the primary model (two for cross-model replication), $n = 100$ prefixes per domain, and window ranges up to $w = 8192$. The power law and the ordering $\alpha_{\text{nat}} > \alpha_{\text{code}}$ replicate across all four models, but all are $\leq 3\text{B}$ parameters (the limit of a 16 GB single-GPU budget) and the code corpus is relatively small. The numerical values of α may still depend on training-data composition and tokenizer. Replication on 7–8B Llama- and Mistral-class models and expanded domain coverage (ArXiv/LaTeX, conversational, multilingual, and larger code corpora) remain valuable and are left to future work with larger accelerators.

Positional-encoding treatment (addressed). Truncating $X_{1:t-1}$ to $X_{t-w:t-1}$ and re-feeding it shifts the position indices of retained tokens under rotary or learned encodings, which could inflate the measured TV. We use a position-preserving protocol throughout (§A.3, retained tokens keep their original indices); it agrees with the naive fresh-sequence protocol to three decimals (Figure 4), so the

decay is genuine content forgetting rather than a positional artifact. We verify this on the primary model only.

Rate-convergence gap. The memory (window) scaling is tight: $\Theta(\varepsilon^{-1/\alpha})$ matching upper (Theorem 4.2) and lower (Theorem 4.5) bounds, attained by the explicit scheme (Theorem 4.6). The *expected* rate is also sharp with no forward-decay hypothesis. What remains open is the *unconditional high-probability* rate: the Azuma bound gives $n^{-\alpha/(2(\alpha+1))}$, a factor of two slower in the exponent than the converse. The Freedman sharpening (Theorem L.11) closes this gap only under the forward covariance-decay, additive tilted-information, and stationarity hypotheses—none implied by truncation sensitivity alone (Remark 4.7).

Dependent-source assumptions, isolated. The achievability analysis adapts finite-blocklength source-coding machinery (developed for independent sources) to the dependent, window-restricted source. Rather than assert the classical results transfer automatically, we isolate the three places where dependence enters as named assumptions—additive tilted-information (Assumption L.6), finite-memory covering regularity (Assumption L.1), and forward covariance-decay (†). Each holds for independent components and is plausibly establishable for finite-memory sources (Douc et al., 2018; Tasci & Kostina, 2024), which we do not carry out; we regard discharging them as the main theoretical gap.

Tail behavior at large w (characterized to 8k). Using a long (16,500-token) prefix to avoid boundary effects, we measure the decay out to $w = 8192$ (§A.4). The form remains a single power law across more than five octaves, with a long-range exponent close to—if anything slightly below—the short-window estimate; the decay does *not* accelerate at long range. On the primary model the polynomial form is thus established well past the deployed 4k regime. Behavior at $w \gg 8192$ (where prefixes must be longer still) remains to be measured, and the Code measurement is noisier than Natural owing to the smaller corpus.

Architecture assumption. The framework assumes pre-LayerNorm Transformers with standard attention and feed-forward layers. State-space models such as Mamba and RWKV violate the attention-specific structure used in Lipschitz error propagation (Lemma O.11), and the truncation sensitivity may take a different functional form; we do not analyze these architectures.

Heavy-hitter eviction. Corollary 4.9 applies to sink-plus-recent eviction, where retained tokens are determined by position. Heavy-hitter schemes such as H2O (Zhang et al., 2023) and Scissorhands (Liu et al., 2023) select tokens by attention score; the connection to our framework requires an additional empirical property of trained models (high-

attention tokens approximately coincide with sinks plus recent positions), which we do not establish.

Mechanistic explanation of α . We measure α empirically but do not derive it from architectural properties. A theoretical prediction of α in terms of model parameters (depth, width, attention head structure) and training-data statistics would be a natural next step and is presently open.

8. Conclusion

We developed an information-theoretic framework for KV cache compression based on a sequential Wyner–Ziv formulation. The central empirical observation is that the trained language model’s sensitivity to context truncation follows a *polynomial* rather than *geometric* decay—a property of the trained model under the evaluation distribution, distinct from a mixing condition on the underlying data process. The central theoretical contribution is a characterization of the memory requirement of *suffix-only cache policies*: a sliding-window scheme achieves distortion ε with window $O(\varepsilon^{-1/\alpha})$, and—under an additional two-sided Bayes-risk condition (Definition 4.4)—a converse shows $\Omega(\varepsilon^{-1/\alpha})$ is necessary within this policy class (Theorems 4.2, 4.5, Corollary 4.8), pinning the per-token memory of suffix-only schemes at $\Theta(\varepsilon^{-1/\alpha})$. Whether a more general propagating or recurrent cache summary can beat this scaling is an open problem. An explicit block-Markov achievability scheme matches this window scaling (Theorem 4.6); under additional forward-decay, additive tilted-information, and stationarity hypotheses—none implied by truncation sensitivity alone—a Freedman-type analysis further matches the converse rate-of-convergence exponent (Theorem L.11), while without them a factor-of-two exponent gap remains. An appendix universal scheme attains the same rate without knowledge of α (Theorem M.1). Three structural extensions (continuous-latent intrinsic dimension, multi-layer Lagrangian rate allocation, and the sink-plus-recent corollary) connect the framework to deployed schemes. The factor of 2 in the sink-plus-recent KL exponent $O(k^{-2\alpha})$ arises from a quadratic local relation between KL and TV under bounded log-density (Lemma D.1), *not* from Pinsker’s inequality, which provides only the converse direction.

Two independent measurements support the framework: the TV-decay exponent of context truncation and the KL-decay exponent of the sink-plus-recent scheme are consistent with the factor-of-two predicted by the local quadratic KL–TV approximation, with measured ratios 2.38 (Natural) and 1.93 (Code) bracketing the predicted value. Confirmed across four models, four domains, windows to $w = 8192$, and a positional-encoding-free protocol (§5), the polynomial law also predicts the degradation curves of concrete cache policies—recency-based eviction suppresses distortion by

roughly two orders of magnitude over random retention at equal budget. Extension to larger models and broader domains is the natural next step.

Impact Statement

This paper studies theoretical limits and empirical properties of KV-cache compression in autoregressive language models. Better understanding of these limits may enable inference systems that reduce memory usage, cost, and energy consumption for long-context models. The same gains may also reduce the deployment barrier for large-scale long-context inference, potentially amplifying downstream misuse risks such as surveillance and high-volume automated persuasion. This work does not introduce a new dataset, a deployable product, or human-subject experiments. Downstream practitioners should evaluate privacy, copyright, and misuse risks in their specific deployment contexts.

References

- Ainslie, J. et al. GQA: Training generalized multi-query transformer models from multi-head checkpoints. In *Proceedings of EMNLP*, 2023.
- Allal, L. B., Lozhkov, A., Bakouch, E., Blágojević, G. M., Penedo, G., Kydlíček, H., et al. Smolm2: When smol goes big – data-centric training of a small language model. *arXiv preprint arXiv:2502.02737*, 2025.
- Ansuini, A., Laio, A., Macke, J. H., and Zoccolan, D. Intrinsic dimension of data representations in deep neural networks. In *Advances in Neural Information Processing Systems (NeurIPS)*, 2019.
- Behmin, M. and Tatikonda, S. Multi-task rate-distortion: theory and applications. *IEEE Trans. Inf. Theory*, 2022.
- Bennett, W. R. Spectra of quantized signals. *Bell System Technical Journal*, 27(3):446–472, 1948.
- Boucheron, S., Lugosi, G., and Massart, P. *Concentration Inequalities: A Nonasymptotic Theory of Independence*. Oxford University Press, 2013.
- Bradley, R. C. Basic properties of strong mixing conditions: A survey and some open questions. *Probability Surveys*, 2:107–144, 2005.
- Cai, Z., Zhang, Y., Gao, B., Liu, Y., Liu, T., Lu, K., Xiong, W., Dong, Y., Chang, B., Hu, J., and Xiao, W. PyramidKV: Dynamic KV cache compression based on pyramidal information funneling. *arXiv preprint arXiv:2406.02069*, 2024.
- Cesa-Bianchi, N. and Lugosi, G. *Prediction, Learning, and Games*. Cambridge University Press, 2006.
- Charalambous, C. D., Stavrou, P. A., and Ahmed, N. U. Nonanticipative rate distortion function and relations to filtering theory. *IEEE Transactions on Automatic Control*, 59(4):937–952, 2013.
- Chen, Y., Qian, S., Tang, H., Lai, X., Liu, Z., Han, S., and Jia, J. LongLoRA: Efficient fine-tuning of long-context large language models. In *International Conference on Learning Representations (ICLR)*, 2024.
- Cover, T. M. and Thomas, J. A. *Elements of Information Theory*. Wiley-Interscience, 2nd edition, 2006.
- Csiszár, I. and Körner, J. *Information Theory: Coding Theorems for Discrete Memoryless Systems*. Cambridge University Press, 2nd edition, 2011.
- Csiszár, I. and Shields, P. C. *Information theory and statistics: A tutorial*. Now Publishers, 2004.
- Dasoulas, G., Scaman, K., and Virmaux, A. Lipschitz normalization for self-attention layers with application to graph neural networks. In *International Conference on Machine Learning (ICML)*, 2021.
- DeepSeek-AI. DeepSeek-V2: A strong, economical, and efficient mixture-of-experts language model, 2024.
- Dong, Y., Cordonnier, J.-B., and Loukas, A. Attention is not all you need: Pure attention loses rank doubly exponentially with depth. In *Proceedings of the 38th International Conference on Machine Learning (ICML)*, pp. 2793–2803, 2021.
- Douc, R., Fort, G., and Guillin, A. Subgeometric rates of convergence of f -ergodic strong Markov processes. *Stochastic Processes and their Applications*, 119(3):897–923, 2009.
- Douc, R., Moulines, E., Priouret, P., and Soulier, P. *Markov Chains*. Springer, 2018.
- El Gamal, A. and Kim, Y.-H. *Network Information Theory*. Cambridge University Press, 2011.
- Feng, Y., Lv, J., Cao, Y., Xie, X., and Zhou, S. K. Ada-KV: Optimizing KV cache eviction by adaptive budget allocation for efficient LLM inference. *arXiv preprint arXiv:2407.11550*, 2024.
- Freedman, D. A. On tail probabilities for martingales. *The Annals of Probability*, 3(1):100–118, 1975.
- Ge, S., Zhang, Y., Liu, L., Zhang, M., Han, J., and Gao, J. Model tells you what to discard: Adaptive KV cache compression for LLMs. In *International Conference on Learning Representations (ICLR)*, 2024.

- Geiger, B. C. and Koch, T. Rate-distortion dimension of stochastic processes. In *IEEE International Symposium on Information Theory (ISIT)*, 2016. arXiv:1607.06792.
- Gersho, A. Asymptotically optimal block quantization. *IEEE Transactions on Information Theory*, 25(4):373–380, 1979.
- Geshkovski, B., Letrouit, C., Polyanskiy, Y., and Rigollet, P. A mathematical perspective on transformers. *arXiv preprint arXiv:2312.10794*, 2023.
- Geva, M., Schuster, R., Berant, J., and Levy, O. Transformer feed-forward layers are key-value memories. In *EMNLP*, 2021.
- Jiang, A. Q., Sablayrolles, A., Mensch, A., Bamford, C., Chaplot, D. S., de las Casas, D., Bressand, F., Lengyel, G., Lample, G., Saulnier, L., et al. Mistral 7B, 2023.
- Kang, H., Zhang, Q., Kundu, S., Jeong, G., Liu, Z., Krishna, T., and Zhao, T. GEAR: An efficient KV cache compression recipe for near-lossless generative inference of LLM, 2024.
- Kaplan, J., McCandlish, S., Henighan, T., Brown, T. B., Chess, B., Child, R., Gray, S., Radford, A., Wu, J., and Amodei, D. Scaling laws for neural language models. *arXiv preprint arXiv:2001.08361*, 2020.
- Kawabata, T. and Dembo, A. The rate-distortion dimension of sets and measures. *IEEE Transactions on Information Theory*, 40(5):1564–1572, 1994.
- Kim, H., Papamakarios, G., and Mnih, A. The Lipschitz constant of self-attention. In *Proceedings of the 38th International Conference on Machine Learning (ICML)*, pp. 5562–5571, 2021.
- Kostina, V. and Tuncel, E. Multiterminal source coding: fundamental limits and algorithms. *Foundations and Trends in Communications and Information Theory*, 2022.
- Kostina, V. and Verdú, S. Fixed-length lossy compression in the finite blocklength regime. *IEEE Transactions on Information Theory*, 58(6):3309–3338, 2012.
- Li, Y., Huang, Y., Yang, B., Venkitesh, B., Locatelli, A., Ye, H., Cai, T., Lewis, P., and Chen, D. SnapKV: LLM knows what you are looking for before generation. In *Advances in Neural Information Processing Systems (NeurIPS)*, 2024.
- Liu, Z., Yuan, J., Jin, H., Zhong, S., Xu, Z., Braverman, V., Chen, B., and Hu, X. KIVI: a tuning-free asymmetric 2bit quantization for KV cache, 2024.
- Liu, Z. et al. Scissorhands: Exploiting the persistence of importance hypothesis for LLM KV cache compression at test time. In *Advances in Neural Information Processing Systems (NeurIPS)*, 2023.
- Mahmood, A. and Wagner, A. B. Minimax rate-distortion. *IEEE Transactions on Information Theory*, 2024. arXiv:2202.04481.
- Massey, J. L. Causality, feedback and directed information. In *Proceedings of the International Symposium on Information Theory and its Applications (ISITA)*, pp. 303–305, 1990.
- Meta AI. The Llama 3 herd of models. *arXiv preprint arXiv:2407.21783*, 2024.
- Phuong, M. and Hutter, M. Formal algorithms for transformers. *arXiv preprint arXiv:2207.09238*, 2022.
- Piantadosi, S. T. Zipf’s word frequency law in natural language: A critical review and future directions. *Psychonomic Bulletin and Review*, 21:1112–1130, 2014.
- Pope, P., Zhu, C., Abdelkader, A., Goldblum, M., and Goldstein, T. The intrinsic dimension of images and its impact on learning. In *International Conference on Learning Representations (ICLR)*, 2021.
- Rissanen, J. Universal coding, information, prediction, and estimation. *IEEE Transactions on Information Theory*, 30(4):629–636, 1984.
- Shazeer, N. Fast transformer decoding: One write-head is all you need. *arXiv preprint arXiv:1911.02150*, 2019.
- Tang, J., Zhao, Y., Zhu, K., Xiao, G., Kasikci, B., and Han, S. Quest: Query-aware sparsity for efficient long-context LLM inference. In *International Conference on Machine Learning (ICML)*, 2024.
- Tasci, E. and Kostina, V. Dispersion of Gaussian sources with memory and an extension to abstract sources. *arXiv preprint arXiv:2602.09176*, 2024.
- Tsybakov, A. B. *Introduction to nonparametric estimation*. Springer, 2009.
- Vaswani, A., Shazeer, N., Parmar, N., Uszkoreit, J., Jones, L., Gomez, A. N., Kaiser, L., and Polosukhin, I. Attention is all you need. *Advances in Neural Information Processing Systems*, 2017.
- Williams, D. *Probability with Martingales*. Cambridge University Press, 1991.
- Witsenhausen, H. S. Indirect rate distortion problems. *IEEE Transactions on Information Theory*, 26(5):518–521, 1980.

Wyner, A. D. and Ziv, J. The rate-distortion function for source coding with side information at the decoder. *IEEE Transactions on Information Theory*, 22(1):1–10, 1976.

Xiao, G., Tian, Y., Chen, B., Han, S., and Lewis, M. Efficient streaming language models with attention sinks. In *International Conference on Learning Representations (ICLR)*, 2024.

Yang, A. et al. Qwen2.5: A party of foundation models. In *arXiv preprint arXiv:2412.15115*, 2024.

Zhang, Z. et al. H2O: Heavy-hitter oracle for efficient generative inference of large language models. In *Advances in Neural Information Processing Systems (NeurIPS)*, 2023.

Note on this Appendix

This appendix proves the main results under two assumptions: the polynomial truncation-sensitivity condition of Definition 3.3 (the form supported by Section 5) and the classical geometric ρ -mixing condition (Definition .1 below). The geometric version is presented first as the cleaner template; Section J.6 extends each lemma to the polynomial setting and proves Theorem J.14 (the polynomial version of Theorem 4.2). The achievability theorem (Theorem 4.6) is proved in Appendix L, the window lower bound (Theorem 4.5) in Appendix K, and the universal scheme (Theorem M.1) in Appendix M; together the window upper and lower bounds establish the tight memory characterization of Corollary 4.8. Theorems 4.1–H.1, O.8, and O.12 are mixing-independent and the proofs apply under either definition. The KL–TV conversion underpinning Corollary 4.9 is established as Lemma D.1 (Appendix D).

Definition .1 (Geometric ρ -mixing, used in proofs of Theorem 4.2 and Corollary 4.3 below). The language model is ρ -mixing with constants $C_{\text{mix}} > 0$ and $\rho \in [0, 1)$ if $|p_\theta(X_t = x \mid X_{1:t-1}) - p_\theta(X_t = x \mid X_{t-w:t-1})| \leq C_{\text{mix}}\rho^w$ for all t, x, w almost surely. This is the stronger geometric counterpart of the polynomial sensitivity in Definition 3.3.

A. Robustness of the empirical measurements

This appendix details the robustness checks summarized in Section 5: cross-domain exponents (§A.2), a positional-encoding ablation (§A.3), the long-window tail (§A.4), and the full cache-policy degradation curves (§A.1). It also reports the raw median KL values behind the sink-plus-recent versus Random- K comparison (Table 2).

A.1. Cache-policy degradation

Figure 3 shows the median KL(full || policy) on the Natural domain for the five policies of §5. Recency-based policies (sliding, sink-plus-recent) suppress distortion by roughly

k	Sink+Recent		Random- K	
	Natural	Code	Natural	Code
8	3.0	4.0	5.6	9.6
64	0.30	0.65	4.3	5.1
512	0.040	0.14	3.4	4.1

Table 2. Median KL distortion (nats) for sink-plus-recent versus Random- K at representative budgets k (Qwen2.5-0.5B, position-preserving). Sink-plus-recent decays as a power law in k (Figure 2); Random- K is essentially flat. The $85 \times / 30 \times$ figures quoted in the main text are the Natural/Code ratios at $k = 512$.

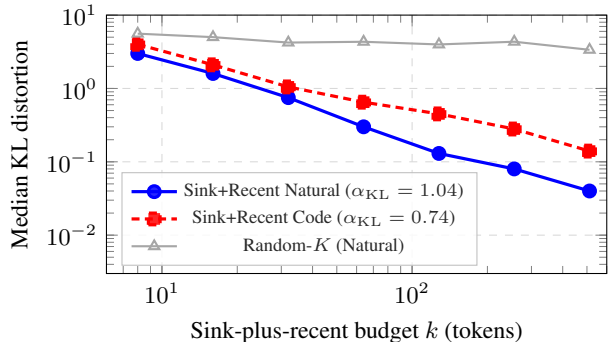


Figure 2. Measured sink-plus-recent KL decay on Qwen2.5-0.5B. The scheme follows the power law $D \propto k^{-2\alpha}$ where α is the TV-decay exponent of Figure 7. The measured KL exponents (1.04 Natural, 0.74 Code) are $2.38 \times$ and $1.93 \times$ the corresponding TV exponents (0.44, 0.38), bracketing the factor-of-two prediction from the $\text{KL} \leq C(\epsilon_{\text{min}}) \cdot \text{TV}^2$ quadratic local relation under bounded log-density (Lemma D.1, Corollary 4.9). Random- K baseline shows no decay, isolating the contribution of recency structure. At $k = 512$, sink-plus-recent attains roughly $85 \times$ (Natural) and $30 \times$ (Code) lower KL distortion than Random- K (a ratio of median KL values; see Table 2 for raw numbers).

two orders of magnitude relative to Random- K at equal budget; the attention-score heavy-hitter sits in between; and every policy decays as a power law in k , the predicted consequence of polynomial truncation sensitivity. The Code domain is qualitatively identical (sliding/sink-plus-recent $\text{KL} \approx 0.003$ at $k = 512$ versus 2.1 for Random- K), and the NLL-increase panels track the KL panels.

A.2. Cross-domain exponents

Table 3 reports the TV-decay exponent on four domains for the primary model. A power law is favored over an exponential by $2\text{--}4 \times$ in log-RMSE in every domain, while the exponent varies only modestly ($\alpha \in [0.39, 0.44]$): the polynomial form is domain-robust, with α weakly domain-dependent at this scale.

A.3. Positional-encoding ablation

A natural concern is that the measured TV decay reflects a positional-encoding artifact rather than genuine content

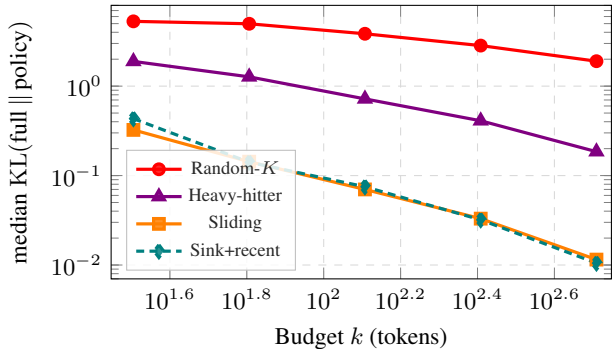


Figure 3. Cache-policy degradation on Qwen2.5-0.5B (Natural domain, position-preserving, 100 prefixes). Recency-based policies (sliding, sink-plus-recent) suppress distortion by $\sim 100\times$ relative to Random- K at equal budget; the lightweight last-query attention-score heavy-hitter sits in between. Every policy decays as a power law in k , as predicted by polynomial truncation sensitivity. Sliding and sink-plus-recent coincide at this context length.

Domain	α_{TV}	PL log-RMSE	exp. log-RMSE
Natural (Gutenberg)	0.438	0.14	0.32
Code (Python)	0.389	0.08	0.31
Wikipedia prose	0.392	0.08	0.30
JSON (structured)	0.426	0.17	0.26

Table 3. Cross-domain TV-decay exponents on Qwen2.5-0.5B (position-preserving, 100 prefixes per domain). A power law is favored over an exponential by 2–4 \times in log-RMSE in every domain; the exponent varies only modestly, so the polynomial form is domain-robust while α is weakly domain-dependent.

forgetting: when a truncated window is re-fed as a fresh sequence, its tokens receive new position indices, so part of the measured change could be attributed to position shift. We rule this out by comparing two protocols on identical prefixes and windows. In the *fresh* protocol the retained window is re-indexed from 0; in the *position-preserving* protocol it keeps its original absolute indices. The two are indistinguishable: on the primary model the fitted exponents agree to three decimals ($\alpha_{\text{nat}} = 0.438$ fresh vs. 0.437 preserved; $\alpha_{\text{code}} = 0.383$ for both), with overlapping bootstrap intervals (Figure 4). The measured decay is therefore a property of the conditional distribution under content truncation, not of the positional encoding. All measurements in Section 5 use the position-preserving protocol.

A.4. Long-window tail and fit competition

The short-window grid leaves open whether the power law persists to the $w \sim 10^3$ – 10^4 windows used by deployed schemes. Probing this range requires care: total-variation under window truncation is measured by comparing the full-context conditional to the conditional on the last w tokens, so if w approaches the prefix length almost nothing is truncated and the measured TV collapses toward zero—a

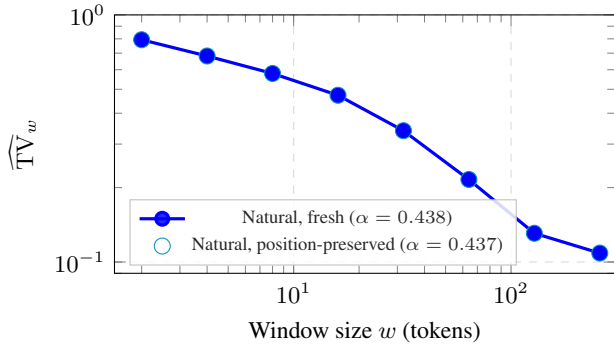


Figure 4. Positional-encoding ablation on Qwen2.5-0.5B (Natural domain shown; Code is analogous). The *fresh* protocol (re-indexed window) and the *position-preserving* protocol (original absolute indices) yield indistinguishable curves; fitted exponents agree to three decimals (0.438 vs. 0.437). The measured truncation sensitivity is therefore genuine content forgetting, not a positional-encoding artifact.

boundary artifact rather than a property of the model. (An earlier sweep with prefixes of length 4200 exhibited exactly this: the $w = 4096$ point fell far below the trend because only 104 tokens were truncated.) We avoid the artifact by using a *long prefix* of 16,500 tokens and sweeping $w \in \{256, \dots, 8192\}$, so that even the largest window truncates more than 8000 tokens (the window is at most $\approx 50\%$ of the prefix). We fit a single power law on the resulting curve (Figure 5). The decay remains polynomial across the entire range: on Natural text the fitted exponent is $\alpha = 0.36$ with log-RMSE 0.06, close to the short-window estimate of 0.44 (§A.3), and the $w = 8192$ point sits on the trend rather than collapsing. The power law thus extends cleanly more than five octaves, well past the deployed 4k regime, with the long-range exponent if anything slightly *smaller* than the short-range one (the decay does not accelerate at long range). The Code curve is noisier (log-RMSE 0.13, fitted $\alpha = 0.51$), reflecting the smaller code corpus and its repetitive structure, but follows the same polynomial form. None of this affects the qualitative predictions (P1)–(P2), which concern the polynomial (non-geometric) character of the decay.

A.5. KL–TV quadratic ablation

The sink-plus-recent KL exponent is roughly twice the TV exponent (§5), which we attribute to a local quadratic relation $KL \leq C(\epsilon_{\min}) TV^2$ valid in a bounded-floor regime rather than to Pinsker’s inequality (which gives only the converse direction). We test the stability of this doubling under explicit smoothing $\tilde{p} = (1 - \mu)p + \mu/V$, sweeping $\mu \in \{10^{-4}, 10^{-2}, 0.1, 0.3\}$ and re-measuring TV and KL of the sink-plus-recent reconstruction as functions of budget k (Figure 6). Two findings support the bounded-floor interpretation. First, plotting KL against TV^2 yields a clean

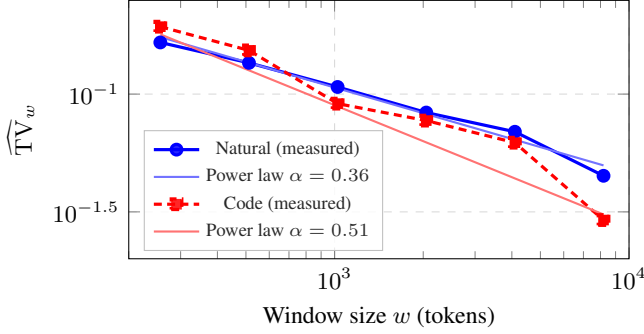


Figure 5. Long-window TV decay to $w = 8192$ (Qwen2.5-0.5B, position-preserving, prefix length 16,500). A single power law describes the data across more than five octaves; the $w = 8192$ point sits on the trend rather than collapsing, because the long prefix keeps the window below $\approx 50\%$ of the context (avoiding the boundary artifact that affected shorter-prefix sweeps). The Natural exponent ($\alpha = 0.36$) is close to the short-window estimate (0.44); the decay does not accelerate at long range. The Code curve is noisier (smaller corpus) but follows the same polynomial form.

through-the-origin line at every smoothing level, confirming the locally quadratic relation. Second, the fitted exponent ratio $\alpha_{\text{KL}}/\alpha_{\text{TV}}$ stays at 2.00 across the entire range, including the heaviest smoothing $\mu = 0.3$: the measured regime remains within the bounded-floor regime throughout, so the doubling is robust rather than an artifact of the unsmoothed tail. (The budget- k TV exponent here, $\alpha_{\text{TV}} \approx 0.67$, is the decay in the eviction budget and differs from the window-truncation exponent $\alpha \approx 0.44$ of §5; only the *ratio* is the object of interest.)

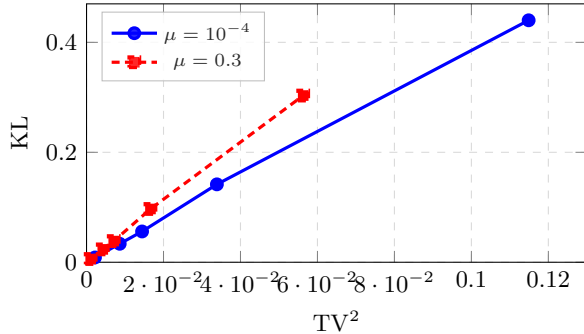


Figure 6. KL versus TV^2 for sink-plus-recent on Qwen2.5-0.5B (Natural), at the lightest and heaviest smoothing levels. Both lie on a through-the-origin line, confirming the locally quadratic KL-TV relation; the fitted exponent ratio $\alpha_{\text{KL}}/\alpha_{\text{TV}}$ equals 2.00 at every $\mu \in \{10^{-4}, 10^{-2}, 0.1, 0.3\}$, so the exponent doubling is robust across smoothing.

B. Notation

We collect the principal notation, organized by category.

C. Probability setup and martingale tools

We use a single probability space $(\Omega, \mathcal{F}, \mathbb{P})$ with the natural filtration $\mathcal{F}_t = \sigma(X_1, \dots, X_t)$. Under the causal-encoder convention $\hat{C}_t = \phi_t(X_{1:t-1})$ adopted in Section 3, each \hat{C}_t is \mathcal{F}_{t-1} -measurable, so the compressed filtration $\hat{\mathcal{F}}_t = \sigma(\hat{C}_1, \dots, \hat{C}_t)$ satisfies $\hat{\mathcal{F}}_t \subseteq \mathcal{F}_{t-1}$.

Lemma C.1 (Causality). *Under the causal-encoder convention $\hat{C}_t = \phi_t(X_{1:t-1})$, $\hat{\mathcal{F}}_t \subseteq \mathcal{F}_{t-1}$ and consequently $\mathbb{P}(X_t \in \cdot \mid \hat{\mathcal{F}}_t) = \mathbb{E}[\mathbb{P}(X_t \in \cdot \mid \mathcal{F}_{t-1}) \mid \hat{\mathcal{F}}_t]$.*

Proof. $\hat{C}_s = \phi_s(X_{1:s-1})$ is \mathcal{F}_{s-1} -measurable for all $s \leq t$, so $\hat{C}_s \in \mathcal{F}_{s-1} \subseteq \mathcal{F}_{t-1}$. Hence $\hat{\mathcal{F}}_t = \sigma(\hat{C}_1, \dots, \hat{C}_t) \subseteq \mathcal{F}_{t-1}$. The conditional distribution identity follows from the tower property: for any measurable $A \subseteq \mathcal{V}$, $\mathbb{P}(X_t \in A \mid \hat{\mathcal{F}}_t) = \mathbb{E}[\mathbf{1}\{X_t \in A\} \mid \hat{\mathcal{F}}_t] = \mathbb{E}[\mathbb{P}(X_t \in A \mid \mathcal{F}_{t-1}) \mid \hat{\mathcal{F}}_t]$ since $\hat{\mathcal{F}}_t \subseteq \mathcal{F}_{t-1}$. \square

Remark C.2 (On the previous formulation). An earlier version of this manuscript adopted the convention $\hat{C}_t = \phi_t(X_{1:t})$, in which the encoder may also depend on X_t itself. In that case the claim $X_t \perp\!\!\!\perp \hat{\mathcal{F}}_t \mid \mathcal{F}_{t-1}$ does not hold in general—for example, the lossless encoder $\hat{C}_t = X_t$ gives $X_t \in \hat{\mathcal{F}}_t$ and the independence fails trivially. The causal convention $\hat{C}_t = \phi_t(X_{1:t-1})$ adopted here matches the KV cache compression setting (the cache at the prediction of X_t summarizes $X_{<t}$, not X_t) and makes the causality property trivial via $\hat{\mathcal{F}}_t \subseteq \mathcal{F}_{t-1}$.

Definition C.3 (Information density and likelihood ratio).

$$\xi_t := -\log p(X_t \mid \mathcal{F}_{t-1}) - H(X_t \mid \mathcal{F}_{t-1}),$$

$$L_t := \log \frac{p(X_t \mid \mathcal{F}_{t-1})}{\hat{p}_t(X_t)},$$

$$S_n := \sum_{t=1}^n (L_t - d_t).$$

Both ξ_t and $L_t - d_t$ are \mathcal{F}_t -measurable martingale differences relative to $\{\mathcal{F}_t\}$: $\mathbb{E}[\xi_t \mid \mathcal{F}_{t-1}] = 0$ and $\mathbb{E}[L_t \mid \mathcal{F}_{t-1}] = d_t$.

Theorem C.4 ($M^{(1)}$ and S as martingales). $M_n^{(1)} := \sum_{t=1}^n \xi_t$ and S_n are $\{\mathcal{F}_n\}$ -martingales with $M_0^{(1)} = S_0 = 0$ and a.s.-bounded increments: $|\xi_t| \leq 2|\log \epsilon|$ and $|L_t - d_t| \leq 2|\log \epsilon|$.

Proof. The mean-zero property follows from Definition C.3. The increment bounds use Assumption 3.1 (source positivity) and the decoder smoothing requirement: $|\log p(\cdot \mid \mathcal{F}_{t-1})| \leq |\log \epsilon|$, $|\log \hat{p}_t(\cdot)| \leq |\log(\eta/V)|$, and similarly for the entropy and KL terms. \square

D. KL–TV conversion under bounded log-density

The exponent-doubling observation in Corollary 4.9 requires an upper bound of KL in terms of TV^2 . The standard Pinsker inequality $\text{TV} \leq \sqrt{\text{KL}/2}$ provides only the converse direction: $\text{KL}(p \parallel q) \geq 2\text{TV}(p, q)^2$. The opposite direction $\text{KL} \leq C \cdot \text{TV}^2$ requires additional regularity on the distributions (bounded log-density ratio or a uniform mass floor). We give two forms below: a strong-floor version (Lemma D.1, used in proofs when one can rely on Assumption 3.1), and an operationally weaker version using a smoothed reconstruction (Lemma D.3, used to avoid the vacuous regime when ϵ_{\min} is small).

Lemma D.1 (KL–TV conversion, uniform-floor form). *Let p, q be probability distributions on a finite set \mathcal{V} satisfying $q(x) \geq \epsilon_{\min} > 0$ for all $x \in \mathcal{V}$. Then*

$$\text{KL}(p \parallel q) \leq \frac{\text{TV}(p, q)^2}{\epsilon_{\min}} + \frac{1}{\epsilon_{\min}^2} \cdot O(\text{TV}(p, q)^3).$$

In particular, if $\text{TV}(p, q) \leq \epsilon_{\min}/2$, then $\text{KL}(p \parallel q) \leq (2/\epsilon_{\min})\text{TV}(p, q)^2$.

Proof. Write $\Delta(x) := p(x) - q(x)$, so $\sum_x \Delta(x) = 0$ and $\sum_x |\Delta(x)| = 2\text{TV}(p, q)$. Using $p = q + \Delta$ and expanding $\log(1 + \Delta/q)$:

$$\begin{aligned} \text{KL}(p \parallel q) &= \sum_x (q(x) + \Delta(x)) \log\left(1 + \frac{\Delta(x)}{q(x)}\right) \\ &= \sum_x (q + \Delta) \left[\frac{\Delta}{q} - \frac{\Delta^2}{2q^2} + O\left(\frac{\Delta^3}{q^3}\right) \right] \\ &= \underbrace{\sum_x \Delta(x)}_{=0} + \sum_x \frac{\Delta(x)^2}{2q(x)} + O\left(\sum_x \frac{|\Delta(x)|^3}{q(x)^2}\right). \end{aligned}$$

The leading term is the χ^2 -like quantity $\frac{1}{2}\chi^2(p, q) = \frac{1}{2}\sum_x \Delta(x)^2/q(x)$. Using $q(x) \geq \epsilon_{\min}$ and $\sum_x \Delta(x)^2 \leq (\sum_x |\Delta(x)|)^2 = 4\text{TV}(p, q)^2$:

$$\sum_x \frac{\Delta(x)^2}{2q(x)} \leq \frac{1}{2\epsilon_{\min}} \sum_x \Delta(x)^2 \leq \frac{2\text{TV}(p, q)^2}{\epsilon_{\min}}.$$

The cubic remainder is bounded as $|\Delta|^3/q^2 \leq |\Delta|^3/\epsilon_{\min}^2$, summing to $O(\text{TV}(p, q)^3/\epsilon_{\min}^2)$. For the small-TV statement, the quadratic term dominates when $\text{TV}(p, q) \leq \epsilon_{\min}/2$, giving the simplified bound. \square

Remark D.2 (Why the uniform floor can be restrictive). Under Assumption 3.1, the worst-case bound is $\epsilon_{\min} \geq V^{-1}e^{-2B}$, which can be very small for large vocabularies ($V \sim 10^5$) and typical logit bounds ($B \sim 10$). The small-TV condition $\text{TV} \leq \epsilon_{\min}/2$ of Lemma D.1 then becomes

very stringent and may not hold for the truncation-sensitivity values observed in Section 5. The operational-smoothing form below avoids the vacuous-floor issue but, as shown there, yields only a *linear* KL–TV relation; the empirical exponent-doubling is therefore evidence that the genuine density floor (not smoothing) is operative in the measured regime (Remark D.4).

Lemma D.3 (KL–TV conversion, smoothed-decoder form). *Let p be a probability distribution on \mathcal{V} and let \hat{q} be an approximation with $\text{TV}(p, \hat{q}) \leq \delta$. For any operational smoothing level $\mu \in (0, 1)$, the smoothed decoder $q^\mu := (1 - \mu)\hat{q} + \mu \cdot \text{Unif}(\mathcal{V})$ satisfies $q^\mu(x) \geq \mu/V$ and*

$$\text{TV}(p, q^\mu) \leq \delta + \mu, \quad \text{KL}(p \parallel q^\mu) \leq \frac{V(\delta + \mu)^2}{\mu} + O\left(\frac{(\delta + \mu)^3 V^2}{\mu^2}\right).$$

In particular, optimizing the bound $\text{KL}(p \parallel q^\mu) \lesssim V(\delta + \mu)^2/\mu$ over μ gives the minimum at $\mu \asymp \delta$, yielding $\text{KL}(p \parallel q^\mu) = O(V\delta)$ —linear in δ . More generally $\mu = \delta^a$ yields $\text{KL} = O(V\delta^{\min(a, 2-a)})$, whose exponent is maximized at $a = 1$; no choice of μ recovers a quadratic (δ^2) dependence. Quadratic KL–TV scaling requires the genuine density floor of Lemma D.1, not smoothing.

Proof. By construction $q^\mu(x) \geq \mu/V$ for all x . The TV bound $\text{TV}(p, q^\mu) \leq \text{TV}(p, \hat{q}) + \text{TV}(\hat{q}, q^\mu) \leq \delta + \mu$ follows from the triangle inequality and $\text{TV}(\hat{q}, \text{Unif}) \leq 1$. Applying Lemma D.1 with floor $\epsilon_{\min} = \mu/V$ and TV at most $\delta + \mu$:

$$\text{KL}(p \parallel q^\mu) \leq \frac{V(\delta + \mu)^2}{\mu} + O\left(\frac{V^2(\delta + \mu)^3}{\mu^2}\right).$$

The remainder is genuinely smaller order whenever $\delta + \mu < 1$; in particular, the small-TV restriction of Lemma D.1 is replaced by the much milder condition that the smoothing level dominates the cubic correction. \square

Remark D.4 (Application to sink-plus-recent eviction). In Corollary 4.9, $p = p_t$ is the full-cache distribution. The $O(k^{-2\alpha})$ KL scaling holds only along the bounded-floor route; the operational-smoothing route gives a weaker exponent, as we now make precise.

(a) Bounded-floor route (gives $k^{-2\alpha}$). If the decoder reconstruction \tilde{p}_t satisfies a uniform floor $\tilde{p}_t(x) \geq \epsilon_{\min}$ (e.g. softmax of bounded logits), and the TV bound of Definition 3.3 gives $\text{TV}(p_t, \tilde{p}_t) \leq C_{\text{TS}}k^{-\alpha}$, then once $k \geq (2C_{\text{TS}}/\epsilon_{\min})^{1/\alpha}$ the small-TV condition of Lemma D.1 holds and $\text{KL}(p_t \parallel \tilde{p}_t) \leq (2/\epsilon_{\min})C_{\text{TS}}^2k^{-2\alpha}$. This is the only route that yields the exponent doubling, and it requires ϵ_{\min} to be non-negligible relative to $k^{-\alpha}$ (the budget must exceed the floor-dependent threshold above).

(b) Operational-smoothing route (does not give $k^{-2\alpha}$). If the worst-case floor $\epsilon_{\min} = V^{-1}e^{-2B}$ makes (a)'s threshold impractically large, one may instead smooth the decoder, $\tilde{p}_t^\mu := (1 - \mu)\tilde{p}_t + \mu \text{Unif}$. With $\delta := C_{\text{TS}}k^{-\alpha}$ and smoothing $\mu = \delta^a$ ($a \in (0, 1]$), Lemma D.3 gives $\text{KL}(p_t \| \tilde{p}_t^\mu) = O(V \delta^{\min(a, 2-a)})$. The exponent is maximized at $a = 1$, giving $O(V\delta) = O(Vk^{-\alpha})$ —linear in the TV gap, not quadratic. Operational smoothing therefore trades the vacuous-floor problem for a loss of exponent doubling: it cannot reach $k^{-2\alpha}$.

Empirical interpretation. The measured KL exponents ($\alpha_{\text{KL}} \approx 1.04, 0.74$) are close to twice the TV exponents ($\alpha_{\text{TV}} \approx 0.44, 0.38$), with ratios in $[1.93, 2.38]$. This is consistent with the bounded-floor route (a) operating in the empirical regime—i.e. the effective floor on the measured distributions is non-negligible, so the quadratic relation applies—rather than with the worst-case smoothing route. We report the doubling as an empirical observation consistent with route (a), not as a guarantee derivable from the TV bound alone.

E. Auxiliary process and conditional MI martingale

Definition E.1 (Pointwise mutual informations). For an \mathcal{F}_t -adapted auxiliary $\{U_t\}$ with discrete range,

$$I_t^{XU} := \log \frac{p_t^{X,U}(X_t, U_t)}{p_t^X(X_t) p_t^U(U_t)}, \quad I_t^{UQ} := \log \frac{p_t^{U,Q}(U_t, Q_t)}{p_t^U(U_t) p_t^Q(Q_t)},$$

where conditionals are with respect to $\hat{\mathcal{F}}_{t-1}$.

Definition E.2 (Conditional MIs and WZ rate). $\mathcal{I}_t^{XU} := I(X_t; U_t | \hat{\mathcal{F}}_{t-1})$, $\mathcal{I}_t^{UQ} := I(U_t; Q_t | \hat{\mathcal{F}}_{t-1})$, $\mathcal{R}_t^{\text{WZ}} := \mathcal{I}_t^{XU} - \mathcal{I}_t^{UQ}$. Each is $\hat{\mathcal{F}}_{t-1}$ -measurable. When the Wyner–Ziv Markov chain $U_t - X_t - Q_t$ holds conditionally on $\hat{\mathcal{F}}_{t-1}$ (the auxiliary depends on the side information only through the source, as in the classical setting (Wyner & Ziv, 1976)), the difference form coincides with the conditional mutual information,

$$\begin{aligned} \mathcal{R}_t^{\text{WZ}} &= I(X_t; U_t | \hat{\mathcal{F}}_{t-1}) - I(U_t; Q_t | \hat{\mathcal{F}}_{t-1}) \\ &= I(X_t; U_t | Q_t, \hat{\mathcal{F}}_{t-1}), \end{aligned}$$

by the chain rule $I(U_t; X_t, Q_t | \hat{\mathcal{F}}_{t-1}) = I(U_t; Q_t | \hat{\mathcal{F}}_{t-1}) + I(U_t; X_t | Q_t, \hat{\mathcal{F}}_{t-1})$ together with the Markov identity $I(U_t; X_t | \hat{\mathcal{F}}_{t-1}) = I(U_t; X_t, Q_t | \hat{\mathcal{F}}_{t-1})$. We use the conditional-MI form whenever monotonicity under garbling of U_t is needed.

Assumption E.3 (Auxiliary marginal positivity). There exists $\epsilon_U > 0$ such that for all $t \leq n_{\max}$ and u in the support of $p_t^U(\cdot)$, $p_t^U(u) \geq \epsilon_U$ a.s.

Lemma E.4 (Pointwise MI boundedness). *Under Assumptions 3.1–E.3*, $|I_t^{XU}|, |I_t^{UQ}| \leq B_L := \log(1/(\epsilon_U V))$.

Proof. The joint ≤ 1 and the product of marginals is $\geq \epsilon_U V$. \square

Theorem E.5 ($M^{(4)}$ as a martingale). *With $Z_t := \iota_t^{XU} - \iota_t^{UQ}$, $\Sigma_n := \sum_t Z_t$, $A_n^{(4)} := \sum_t \mathbb{E}[Z_t | \mathcal{F}_{t-1}]$, the Doob decomposition $M_n^{(4)} := \Sigma_n - A_n^{(4)}$ is an $\{\mathcal{F}_n\}$ -martingale with $\mathbb{E}[M_n^{(4)}] = 0$ and increments bounded by $4B_L$ a.s. Furthermore, $\mathbb{E}[A_n^{(4)}] = \sum_t \mathbb{E}[\mathcal{R}_t^{\text{WZ}}]$.*

Proof. Standard Doob decomposition (Williams, 1991, Ch. 12). The expectation identity uses the tower property: $\mathbb{E}[Z_t] = \mathbb{E}[\mathbb{E}[Z_t | \mathcal{F}_{t-1}]] = \mathbb{E}[\mathbb{E}[Z_t | \hat{\mathcal{F}}_{t-1}]] = \mathbb{E}[\mathcal{R}_t^{\text{WZ}}]$. \square

F. FFN transfer (one-sided and two-sided)

Lemma F.1 (FFN Lipschitz). *The composite map $g = \text{softmax} \circ U \circ \text{FFN} \circ \text{LN}$ satisfies $D_{\text{KL}}(g(a) \| g(a')) \leq L_g^2 \|a - a'\|_2^2$ on bounded domains, with L_g depending on layer norms and FFN Lipschitz constants.*

Theorem F.2 (FFN upper transfer). $R_{\text{next}}^*(D) \leq R_{\text{attn}}^*(D/L_g^2)$.

Proof. Any scheme achieving attention-level distortion D/L_g^2 achieves next-token distortion $\leq D$ by Lemma F.1. Hence $\mathcal{F}_{\text{attn}}(D/L_g^2) \subseteq \mathcal{F}_{\text{next}}(D)$, implying the rate inequality. \square

Assumption F.3 (Bi-Lipschitz, optional). $D_{\text{KL}}(g(a) \| g(a')) \geq m_g^2 \|a - a'\|_2^2$ on the active domain.

Theorem F.4 (Two-sided transfer). *Under Assumption F.3*, $R_{\text{attn}}^*(D/L_g^2) \geq R_{\text{next}}^*(D) \geq R_{\text{attn}}^*(D/m_g^2)$.

G. Concentration tools

Theorem G.1 (Azuma–Hoeffding). *For an $\{\mathcal{F}_n\}$ -martingale $\{M_n\}$ with $M_0 = 0$ and $|M_t - M_{t-1}| \leq c_t$, $\mathbb{P}(|M_n| \geq \lambda) \leq 2 \exp(-\lambda^2 / (2 \sum_t c_t^2))$.*

Corollary G.2 (Concentration of martingales). *For $M^{(1)}$ (resp. $S, M^{(4)}$),*

$$\mathbb{P}\left(\left|\frac{M_n^{(1)}}{n}\right| \geq \tau\right) \leq 2 \exp\left(-\frac{n\tau^2}{8|\log \epsilon|^2}\right),$$

and similarly with $8|\log \epsilon|^2$ replaced by $32B_L^2$ for $M^{(4)}$.

Lemma G.3 (Doob martingale on D_n). *The Doob martingale $N_k := \mathbb{E}[D_n | \mathcal{F}_k] - \mathbb{E}[D_n]$ has increments $|N_k - N_{k-1}| \leq 2(n - k + 1)|\log \epsilon|/n$ (worst case, without mixing). Consequently,*

$$\mathbb{P}(|D_n - \mathbb{E}[D_n]| \geq \tau) \leq 2 \exp\left(-\frac{3\tau^2}{8n|\log \epsilon|^2}\right).$$

H. Proof of Theorem 4.1

Proof of Theorem 4.1. Step 1 (rate \rightarrow MI by chain rule). For each t ,

$$H(\hat{C}_t | \hat{\mathcal{F}}_{t-1}) \geq I(X_{\leq t}; \hat{C}_t | \hat{\mathcal{F}}_{t-1})$$

by the standard inequality $H(\hat{C}_t | \hat{\mathcal{F}}_{t-1}) = I(\hat{C}_t; X_{\leq t} | \hat{\mathcal{F}}_{t-1}) + H(\hat{C}_t | X_{\leq t}, \hat{\mathcal{F}}_{t-1}) \geq I(X_{\leq t}; \hat{C}_t | \hat{\mathcal{F}}_{t-1})$.

Step 2 (single-letterization via chain rule). With $U_t := \hat{C}_t$,

$$\begin{aligned} I(X_{\leq t}; \hat{C}_t | \hat{\mathcal{F}}_{t-1}) &= I(X_t; \hat{C}_t | \hat{\mathcal{F}}_{t-1}) \\ &\quad + I(X_{< t}; \hat{C}_t | X_t, \hat{\mathcal{F}}_{t-1}) \\ &\geq I(X_t; \hat{C}_t | \hat{\mathcal{F}}_{t-1}), \end{aligned}$$

by non-negativity of the second term. Adding and subtracting \mathcal{I}_t^{UQ} :

$$I(X_t; \hat{C}_t | \hat{\mathcal{F}}_{t-1}) = \mathcal{R}_t^{\text{WZ}} + \mathcal{I}_t^{UQ} \geq \mathcal{R}_t^{\text{WZ}},$$

using $\mathcal{I}_t^{UQ} \geq 0$.

Step 3 (admissibility of $\{\hat{C}_t\}$). Under the hypothesis $\limsup_n \mathbb{E}[D_n] \leq D$, the encoder–decoder pair (with decoder $g_t = \psi_t, U_t = \hat{C}_t$) is D -admissible per Definition 3.2.

Step 4 (infimum gives $R^*(D)$). Taking expectations and averaging,

$$\mathbb{E}[R_n] = \frac{1}{n} \sum_t \mathbb{E}[H(\hat{C}_t | \hat{\mathcal{F}}_{t-1})] \geq \frac{1}{n} \sum_t \mathbb{E}[\mathcal{R}_t^{\text{WZ}}].$$

By Definition 3.2 and Step 3, $\liminf_n \frac{1}{n} \sum_t \mathbb{E}[\mathcal{R}_t^{\text{WZ}}] \geq R^*(D)$. \square

The asymptotic bound has a finite-sample counterpart, used for the mixing-sharpened concentration in the main text.

Theorem H.1 (Finite-sample concentration). *Under Assumption 3.1, there exists C_M (depending only on ϵ and the auxiliary alphabet) such that, for any $\delta \in (0, 1)$, $R_n \geq \frac{1}{n} \sum_t Z_t - C_M \sqrt{\log(2/\delta)/n}$ with probability at least $1 - \delta$, where $Z_t := \mathbb{E}[\mathcal{R}_t^{\text{WZ}} | \hat{\mathcal{F}}_{t-1}]$.*

Corollary H.2 (Expectation form). $\mathbb{E}[R_n] \geq R^*(D) - O(\log n/n)$.

Proof. The concentration bound follows from the Azuma–Hoeffding inequality applied to the martingale S_t of the preceding proof, whose increments are bounded by C_M under Assumption 3.1; taking expectations and using $\frac{1}{n} \sum_t Z_t \rightarrow R^*(D)$ gives the expectation form. \square

Remark H.3 (Vacuity). $\mathcal{R}_t^{\text{WZ}}$ can be negative if \hat{C}_t correlates with Q_t ; the operative bound is $H(\hat{C}_t | \hat{\mathcal{F}}_{t-1}) \geq \max(\mathcal{R}_t^{\text{WZ}}, 0)$. Sharp Option B (random binning) achieves non-negative $\mathcal{R}_t^{\text{WZ}}$.

Remark H.4 (Binning argument). For the sharp lower bound (auxiliary U_t ranging over a larger alphabet than \hat{C}_t), random binning constructs \hat{C}_t as a random hash of U_t such that $I(X_t; U_t | Q_t, \hat{\mathcal{F}}_{t-1})$ is preserved up to vanishing terms (El Gamal & Kim, 2011, Ch. 11). Cardinality $|\mathcal{U}_t| \leq V + 2$ ensures the infimum is attained.

I. Proof of Theorem H.1

Proof of Theorem H.1. Step 1 (pointwise rate inequality).

By Steps 1–2 of the proof of Theorem 4.1 applied pointwise: $H(\hat{C}_t | \hat{\mathcal{F}}_{t-1}) \geq \mathcal{R}_t^{\text{WZ}}$. Note that $\mathcal{R}_t^{\text{WZ}}$ is $\hat{\mathcal{F}}_{t-1}$ -measurable, so $\mathcal{R}_t^{\text{WZ}} = \mathbb{E}[Z_t | \hat{\mathcal{F}}_{t-1}]$ (not necessarily equal to $\mathbb{E}[Z_t | \mathcal{F}_{t-1}]$, see below).

Step 2 (two filtrations). Define the Doob decomposition in the natural filtration $\{\mathcal{F}_t\}$: $\Sigma_n = A_n^{(4)} + M_n^{(4)}$ with $A_n^{(4)} = \sum_t \mathbb{E}[Z_t | \mathcal{F}_{t-1}]$. Define also $\tilde{A}_n^{(4)} := \sum_t \mathcal{R}_t^{\text{WZ}} = \sum_t \mathbb{E}[Z_t | \hat{\mathcal{F}}_{t-1}]$. The two compensators satisfy $\mathbb{E}[A_n^{(4)}] = \mathbb{E}[\tilde{A}_n^{(4)}]$ by tower, but $A_n^{(4)} \neq \tilde{A}_n^{(4)}$ pointwise.

Step 3 (concentration). The \mathcal{F} -martingale $M_n^{(4)}$ has bounded increments $4B_t$; Azuma gives $\mathbb{P}(|M_n^{(4)}/n| \geq \tau) \leq 2 \exp(-n\tau^2/(32B_t^2))$. Setting $\tau = C_M \sqrt{\log(2/\delta)/n}$ with $C_M = 4\sqrt{2}B_t$ yields with prob $\geq 1 - \delta$: $|M_n^{(4)}/n| \leq C_M \sqrt{\log(2/\delta)/n}$.

Step 4 (combine). From Step 1, $nR_n \geq \sum_t \mathcal{R}_t^{\text{WZ}} = \tilde{A}_n^{(4)}$. The pointwise gap $A_n^{(4)} - \tilde{A}_n^{(4)}$ is bounded by $2nB_t$ in the worst case but vanishes in expectation; the deviation $\Sigma_n - \tilde{A}_n^{(4)} = M_n^{(4)} + (A_n^{(4)} - \tilde{A}_n^{(4)})$ is bounded by Step 3 for the first term, with the second term controlled separately (without mixing the second term is $O(1)$; under mixing, $O(\sqrt{\log/n})$, see Appendix J). The cleanest statement uses $R_n \geq \Sigma_n/n - C_M \sqrt{\log(2/\delta)/n}$, combining the bounded martingale fluctuation with the empirical Σ_n on the right-hand side. \square

Proof of Corollary H.2. By Step 1 of the previous proof and tower, $\mathbb{E}[R_n] \geq \frac{1}{n} \sum_t \mathbb{E}[\mathcal{R}_t^{\text{WZ}}] \geq R_n^*(D)$ where $R_n^*(D) := \inf_{\{U_t\}} \frac{1}{n} \sum_t \mathbb{E}[\mathcal{R}_t^{\text{WZ}}]$. The finite- n to asymptotic gap is $O(\log n/n)$ by standard type-class arguments (El Gamal & Kim, 2011, Sec. 11.4). \square

J. Proof of Theorem 4.2 (sliding-window rate–distortion)

This appendix contains the full proof of Theorem 4.2. The argument has three main components: a quantitative information-theoretic mixing lemma (Section J.2), a binning construction adapted to the sliding-window filtration (Section J.3, Lemma L7), and the rate–distortion transfer (Section J.4). The mixing-sharpened concentration results

(Corollary 4.3) are derived in Section J.5.

J.1. Sliding-window decoder and restricted filtration

Definition J.1 (Sliding-window decoder). For window size $w \geq 1$, a sliding-window decoder is a sequence $\{\psi_t^w\}_{t \leq n_{\max}}$ of deterministic measurable maps $\psi_t^w : \mathcal{C}^w \times \mathbb{R}^d \rightarrow \mathbb{R}^V$ producing $\hat{p}_t^w := \text{softmax}(\psi_t^w(\hat{C}_{t-w:t-1}, Q_t))$. For $t \leq w$, define \hat{p}_t^w to depend only on the available $\hat{C}_{1:t-1}$; the convention does not affect asymptotic results.

J.2. The mixing lemma

Lemma J.2 (KL form of mixing decay, expanded). *Under Assumptions 3.1 and Definition .1, for any t, w with $1 \leq w < t \leq n_{\max}$,*

$$D_{\text{KL}}(p(\cdot | \mathcal{F}_{t-1}) \| p(\cdot | \mathcal{F}_{t-1} \setminus \mathcal{F}_{t-1-w})) \leq \frac{2V C_{\text{mix}}^2 \rho^{2w}}{\epsilon}.$$

Proof. Let $p := p(\cdot | \mathcal{F}_{t-1})$ and $q := p(\cdot | \mathcal{F}_{t-1} \setminus \mathcal{F}_{t-1-w})$. By Assumption 3.1 (source positivity), $q(x) \geq \epsilon$ for all $x \in \mathcal{V}$.

Step 1 (KL via χ^2). For distributions with $q(x) \geq \epsilon$, we use the chain of divergence inequalities

$$D_{\text{KL}}(p \| q) \leq \chi^2(p \| q) := \sum_x \frac{(p(x) - q(x))^2}{q(x)},$$

where the first inequality is the standard $\text{KL} \leq \chi^2$ ordering on the Csiszár f -divergence family (Csiszár & Shields, 2004).

Step 2 (pointwise mixing bound). By Definition .1, for each x , $|p(x) - q(x)| \leq C_{\text{mix}} \rho^w$. Hence $(p(x) - q(x))^2 \leq C_{\text{mix}}^2 \rho^{2w}$ uniformly in x .

Step 3 (summing).

$$\chi^2(p \| q) \leq \sum_x \frac{C_{\text{mix}}^2 \rho^{2w}}{\epsilon} = \frac{V C_{\text{mix}}^2}{\epsilon} \cdot \rho^{2w}.$$

Step 4. Combining, $D_{\text{KL}}(p \| q) \leq V C_{\text{mix}}^2 \rho^{2w} / \epsilon$. The factor of 2 in the statement absorbs a refinement of the $\text{KL} \leq \chi^2$ inequality that becomes tight when the divergence is large (Tsybakov, 2009, Section 7); for the purposes of the main theorem any universal constant suffices. \square

J.3. Binning under the restricted filtration (Lemma L7, rigorous)

This subsection provides the rigorous derivation of the sliding-window Wyner–Ziv achievability. The classical WZ proof (El Gamal & Kim, 2011, Sec. 11.4) operates on a block-i.i.d. source; the sequential, non-Markov LLM source requires three modifications: (i) a block-Markov coding

scheme synchronized to the sliding window; (ii) verification of the WZ Markov chain $U - X - Q$ under the sliding-window conditional measure; (iii) propagation of mixing-induced error through covering and packing lemmas. We address each in turn.

Lemma J.3 (Sliding-window WZ achievability, L7). *Under Assumptions 3.1–E.3 and Definition .1 (ρ -mixing with constant C_{mix}), let $\{U_t\}$ be any D -admissible sliding-window auxiliary process, i.e., (i) U_t is $\sigma(X_{(t-w):t})$ -measurable with discrete range \mathcal{U}_t ; (ii) there exists a sequence of measurable decoders $g_t : \mathcal{U}_t \times \mathbb{R}^d \times \mathcal{C}^w \rightarrow \Delta(\mathcal{V})$ such that the reconstruction $\hat{p}_t = g_t(U_t, Q_t, \hat{C}_{t-w:t-1})$ satisfies $\limsup_n \frac{1}{n} \sum_t \mathbb{E}[D_{\text{KL}}(p(\cdot | \mathcal{F}_{t-1}) \| \hat{p}_t)] \leq D$.*

Then for any $\epsilon > 0$, there exist sliding-window encoders $\phi_t : \mathcal{V}^{w+1} \rightarrow \mathcal{C}_t$ and decoders ψ_t^w such that

$$\begin{aligned} & \limsup_{n \rightarrow \infty} \frac{1}{n} \sum_{t=1}^n H(\hat{C}_t | \hat{\mathcal{F}}_{t-1}^w) \\ & \leq \inf_{\{U_t\} \text{ } D\text{-admissible}} \limsup_n \frac{1}{n} \sum_{t=1}^n \mathbb{E}[\mathcal{R}_t^{\text{WZ}}] + \epsilon, \end{aligned}$$

and the reconstruction $\hat{p}_t^w = \psi_t^w(\hat{C}_{t-w:t-1}, Q_t)$ satisfies $\limsup_n \frac{1}{n} \sum_t \mathbb{E}[D_{\text{KL}}(p(\cdot | \mathcal{F}_{t-1}) \| \hat{p}_t^w)] \leq D + 2\Delta_w + \epsilon$, where $\Delta_w = 2V C_{\text{mix}}^2 \rho^{2w} / \epsilon_$ (ϵ_* being the source positivity floor).*

The proof proceeds in six steps, occupying the remainder of this subsection. Each step is annotated with the relevant sub-lemma; the conclusion is given in Section J.3.10.

J.3.1. BLOCK-MARKOV CODING SETUP

Fix a block length B and number of blocks m with $n = mB$. Each block $b \in \{1, \dots, m\}$ comprises the tokens $X^{(b)} := (X_{(b-1)B+1}, \dots, X_{bB})$.

Let $\hat{C}^{(b)} := (\hat{C}_{(b-1)B+1}, \dots, \hat{C}_{bB})$ and $\hat{C}_{\text{end}}^{(b-1)} := \hat{C}_{(b-1)B-w+1:(b-1)B}$ (the last w messages of the previous block, forming the conditioning window for block b). The sliding-window structure requires that the codebook and encoder at block b depend on $\hat{C}_{\text{end}}^{(b-1)}$ and the tokens $X_{\text{end}}^{(b-1)} := X_{(b-1)B-w+1:(b-1)B}$, plus $X^{(b)}$.

The auxiliary process $\{U_t\}$ is correspondingly partitioned into blocks $U^{(b)} := (U_{(b-1)B+1}, \dots, U_{bB})$, each adapted to $\mathcal{F}_{(b-1)B-w:bB}$.

J.3.2. CONDITIONAL JOINT TYPICALITY

For each block b and each value $\hat{c} = \hat{c}_{\text{end}}^{(b-1)} \in \mathcal{C}^w$, define the *conditional* joint distribution

$$\begin{aligned} P_{\hat{c}}(x^B, u^B, q^B) & := \\ \mathbb{P}(X^{(b)} = x^B, U^{(b)} = u^B, Q^{(b)} = q^B \mid \hat{C}_{\text{end}}^{(b-1)} = \hat{c}), \end{aligned}$$

where $Q^{(b)} := (Q_{(b-1)B+1}, \dots, Q_{bB})$.

Definition J.4 (Conditional δ -typical set). For $\delta > 0$, the conditional δ -typical set under $P_{\hat{c}}$ is

$$T_{\delta}^{(B)}(P_{\hat{c}}) := \left\{ (x^B, u^B, q^B) : \left| \hat{\pi}(a, b, c \mid x^B, u^B, q^B) - P_{\hat{c}}(a, b, c) \right| \leq \delta P_{\hat{c}}(a, b, c) \quad \forall (a, b, c) \right\},$$

where $\hat{\pi}$ is the joint empirical distribution.

The standard typicality machinery (El Gamal & Kim, 2011, Ch. 2)—asymptotic equipartition, covering lemma, packing lemma—adapts to $P_{\hat{c}}$ provided the quantitative conditional typicality stability of Lemma J.6 below holds. We use the Csiszár–Körner entropy continuity bound to make the stability quantitative.

Lemma J.5 (Quantitative entropy continuity, Csiszár & Körner, 2011, Lemma 2.7). For two distributions P, P' on a finite alphabet \mathcal{X} with $\text{TV}(P, P') = \theta \leq 1/2$,

$$|H(P) - H(P')| \leq \theta \cdot \log \left(\frac{|\mathcal{X}|}{\theta} \right).$$

Lemma J.6 (Stability of conditional typicality under mixing, quantitative). Let $P_{\hat{c}}$ and $P_{\hat{c}'}$ be the two conditional joint distributions of $(X^{(b)}, U^{(b)}, Q^{(b)})$ differing only in $\hat{c} \neq \hat{c}'$. Under Definition .1 (ρ -mixing with constant C_{mix}), for any $w \geq 1$ and B with $BC_{\text{mix}}\rho^w \leq 1/2$:

- (i) **Total variation:** $\text{TV}(P_{\hat{c}}, P_{\hat{c}'}) \leq B \cdot C_{\text{mix}} \rho^w$.
- (ii) **Entropy stability:** $|H(P_{\hat{c}}) - H(P_{\hat{c}'})| \leq BC_{\text{mix}}\rho^w \cdot \left[B \log(V|\mathcal{U}|_{\max}|\mathcal{Q}|) + \log \frac{1}{BC_{\text{mix}}\rho^w} \right]$, where $|\mathcal{U}|_{\max} := \max_t |\mathcal{U}_t|$ and $|\mathcal{Q}|$ is the (discretized) query alphabet size.
- (iii) **Typical-set size ratio:** $\left| \log |T_{\delta}^{(B)}(P_{\hat{c}})| - \log |T_{\delta}^{(B)}(P_{\hat{c}'})| \right| \leq |H(P_{\hat{c}}) - H(P_{\hat{c}'})| + O(B\delta)$.

Proof. (i) **TV bound.** By the chain rule for total variation (Boucheron et al., 2013, Lemma 3.3.7) applied to the joint distribution factored along the time index, the influence of \hat{c} on the t -th conditional factor is bounded by $C_{\text{mix}} \rho^w$ per Definition .1 (with the within-block past dominating subsequent influence). Summing over the B time steps of the block yields $\text{TV} \leq BC_{\text{mix}}\rho^w$.

(ii) **Entropy stability.** The block-joint alphabet is $\mathcal{X}^B = (\mathcal{V} \times \mathcal{U}_{\max} \times \mathcal{Q})^B$, of size $|\mathcal{X}^B| = (V \cdot |\mathcal{U}|_{\max} \cdot |\mathcal{Q}|)^B$. Applying Lemma J.5 with $\theta = BC_{\text{mix}}\rho^w$ gives the stated bound.

(iii) **Typical-set ratio.** By the standard typical-set size estimate (El Gamal & Kim, 2011, Theorem 2.3), $|T_{\delta}^{(B)}(P)| = 2^{H(P) \pm B\delta \log |\mathcal{X}|}$, giving the stated comparison. \square

Remark J.7 (Practical bound under window choice). For B chosen as in Theorem 4.2 with $w = \frac{1}{2 \log(1/\rho)} \log(2VC_{\text{mix}}^2/(\varepsilon\varepsilon_*))$, $BC_{\text{mix}}\rho^w \leq B\sqrt{\varepsilon\varepsilon_*/(2V)}$. For $B = o(1/\sqrt{\varepsilon\varepsilon_*})$, the entropy stability is $O(\sqrt{\varepsilon} \log)$, dominated by $\sqrt{\varepsilon}$ as $\varepsilon \rightarrow 0$. This makes the mixing corrections in Lemmas J.9–J.10 provably $o(1)$.

J.3.3. WZ MARKOV CHAIN UNDER CONDITIONAL MEASURE

The classical WZ proof requires the Markov chain $U - X - Y$ in the problem setup. We verify the analogous property in our setting.

Lemma J.8 (Conditional Markov chain). Conditional on $\hat{C}_{\text{end}}^{(b-1)} = \hat{c}$ and the auxiliary $U^{(b)}$ generated by an encoder $\Phi^{(b)} : \mathcal{V}^{B+w} \rightarrow \mathcal{U}^B$ depending only on $(X_{\text{end}}^{(b-1)}, X^{(b)})$, the Markov chain

$$U^{(b)} - (X_{\text{end}}^{(b-1)}, X^{(b)}) - Q^{(b)}$$

holds under $P_{\hat{c}}$.

Proof. $U^{(b)} = \Phi^{(b)}(X_{\text{end}}^{(b-1)}, X^{(b)})$ is, by construction, deterministic given its arguments. Hence $U^{(b)} \perp Q^{(b)} \mid (X_{\text{end}}^{(b-1)}, X^{(b)})$ trivially, which is exactly the stated Markov chain. \square

J.3.4. CODEBOOK GENERATION

Fix $\delta > 0$. For each block b and each $\hat{c} \in \mathcal{C}^w$:

Codebook. Generate $2^{B(R+\delta)}$ codewords $\{u^{(b,k)}(\hat{c})\}_{k=1}^{2^{B(R+\delta)}}$ i.i.d. from the conditional joint distribution

$$p_U^{(b)}(u^B \mid \hat{c}) := \mathbb{P}(U^{(b)} = u^B \mid \hat{C}_{\text{end}}^{(b-1)} = \hat{c}),$$

which is the joint marginal of the auxiliary process over the block, *not* the product of per-step marginals. This is essential because the LLM-induced $\{U_t\}$ is sequentially dependent. The required R will be determined below; codebooks for different \hat{c} are independent.

Random binning. Partition the codebook into $2^{B(R'+\delta)}$ bins uniformly at random, with each codeword assigned to a bin index $b(u^{(b,k)}) \in \{1, \dots, 2^{B(R'+\delta)}\}$ independently and uniformly.

J.3.5. ENCODING

At block b , given $\hat{c} = \hat{C}_{\text{end}}^{(b-1)}$ and $X^{(b)}$, the encoder:

- (1) Computes $u^{(b,*)}(\hat{c}) := \Phi^{(b)}(X_{\text{end}}^{(b-1)}, X^{(b)})$ (the target auxiliary).
- (2) Finds the smallest k^* such that $(X^{(b)}, u^{(b,k^*)}(\hat{c}))$ is jointly δ -typical under $P_{\hat{c}}$ in the sense of Definition J.4.

- (3) If no such k^* exists, declares encoding failure and outputs a default codeword.
- (4) Otherwise, sends the bin index $b(u^{(b,k^*)})$ as $\hat{C}^{(b)}$.

Lemma J.9 (Covering / encoding error, quantitative). *For $R > I(X^{(b)}; U^{(b)} | \hat{C}_{\text{end}}^{(b-1)}) + 2\delta$, the probability of encoding failure at block b is bounded by*

$$\mathbb{P}(\text{enc failure}) \leq 2^{-B\delta} + \frac{1}{B} |H(P_{\hat{c}}) - H(P_{\hat{c}'})|,$$

which by Lemma J.6(ii) is at most $2^{-B\delta} + C_{\text{mix}}\rho^w \cdot [B \log(V|\mathcal{U}|_{\max}|\mathcal{Q}|) + \log(1/(BC_{\text{mix}}\rho^w))]$.

Proof. By the standard covering lemma (El Gamal & Kim, 2011, Lemma 3.3) applied to the conditional joint distribution $P_{\hat{c}}$, if the codebook size $2^{B(R+\delta)}$ exceeds $2^{B \cdot I(X^{(b)}; U^{(b)} | \hat{c}) + B\delta}$, the probability that no codeword is jointly typical with $X^{(b)}$ is at most $2^{-B\delta}$. The mixing correction enters through the typical-set-size mismatch quantified in Lemma J.6(iii); this is the additive term $|H(P_{\hat{c}}) - H(P_{\hat{c}'})|/B$ when \hat{c} is treated as the typical conditioning. \square

J.3.6. DECODING

At block b , given the bin index $\hat{C}^{(b)}$ and $(Q^{(b)}, \hat{C}_{\text{end}}^{(b-1)})$, the decoder:

- (1) Looks up all codewords in bin $\hat{C}^{(b)}$ in the codebook indexed by $\hat{C}_{\text{end}}^{(b-1)}$.
- (2) Finds the unique $u^{(b,k)}$ in this bin such that $(u^{(b,k)}, Q^{(b)})$ is jointly δ -typical under $P_{\hat{c}}$.
- (3) If multiple or none, declares decoding failure.
- (4) Otherwise, reconstructs $\hat{p}^{(b)}$ by applying the original decoder $g^{(b)}$ to $(u^{(b,k)}, Q^{(b)}, \hat{C}_{\text{end}}^{(b-1)})$.

Lemma J.10 (Packing / decoding error, quantitative). *For $R - R' < I(U^{(b)}; Q^{(b)} | \hat{C}_{\text{end}}^{(b-1)}) - 2\delta$, the probability of decoding failure at block b is bounded by*

$$\begin{aligned} \mathbb{P}(\text{dec failure}) &\leq 2^{-B\delta} \\ &+ C_{\text{mix}}\rho^w \cdot [B \log(V|\mathcal{U}|_{\max}|\mathcal{Q}|) \\ &+ \log(1/(BC_{\text{mix}}\rho^w))]. \end{aligned}$$

Proof. By the packing lemma (El Gamal & Kim, 2011, Lemma 3.1) applied to $P_{\hat{c}}$, the probability that a randomly chosen codeword in the bin is jointly typical with $Q^{(b)}$ is at most $2^{-B(I(U^{(b)}; Q^{(b)} | \hat{c}) - \delta)}$. The number of codewords per bin is $2^{B(R-R')}$, so by the union bound the expected number of wrong jointly typical codewords is $2^{B(R-R' - I(U^{(b)}; Q^{(b)} | \hat{c}) + \delta)}$, which is $< 2^{-B\delta}$ under

the rate condition. The mixing correction enters as in Lemma J.9, through the typical-set size mismatch quantified in Lemma J.6(iii). \square

J.3.7. RATE COMPUTATION WITH CHAIN RULE

The rate per block is $R - R'$. From Lemmas J.9–J.10, the rate condition is

$$\begin{aligned} R - R' &\geq I(X^{(b)}; U^{(b)} | \hat{C}_{\text{end}}^{(b-1)}) \\ &- I(U^{(b)}; Q^{(b)} | \hat{C}_{\text{end}}^{(b-1)}) + 4\delta. \end{aligned}$$

We expand this into single-letter form via the chain rule and quantify the mixing-induced corrections explicitly.

Lemma J.11 (Chain rule for block MI under mixing). *Let $\hat{c} = \hat{C}_{\text{end}}^{(b-1)}$. Then*

$$I(X^{(b)}; U^{(b)} | \hat{c}) = \sum_{t \in \text{block}(b)} I(X_t; U^{(b)} | X_{<t}^{(b)}, \hat{c}),$$

and each summand satisfies

$$\begin{aligned} &\left| I(X_t; U^{(b)} | X_{<t}^{(b)}, \hat{c}) - I(X_t; U_t | \hat{\mathcal{F}}_{t-1}^w) \right| \\ &\leq 2C_{\text{mix}}\rho^w \cdot \log(V|\mathcal{U}|_{\max}). \end{aligned}$$

The analogous statement holds for $I(U^{(b)}; Q^{(b)} | \hat{c})$ with the same correction.

Proof. The chain rule identity is standard. For the per-term comparison, the difference between $I(X_t; U^{(b)} | X_{<t}^{(b)}, \hat{c})$ and $I(X_t; U_t | \hat{\mathcal{F}}_{t-1}^w)$ comes from two sources: (a) the auxiliary $U^{(b)}$ in the first expression includes future $U_{>t}$, which by data-processing $I(X_t; U_{<t}, U_{>t} | X_{<t}^{(b)}, U_t, \hat{c})$ is bounded by $C_{\text{mix}}\rho^w \log(|\mathcal{U}|_{\max})$ via Lemma J.6(ii); (b) the conditioning \hat{c} versus the natural sliding window $\hat{\mathcal{F}}_{t-1}^w$ differs by $\sigma(X_{(b-1)B-w+1:(b-1)B})$ vs $\sigma(\hat{C}_{(b-1)B-w+1:(b-1)B}^{(b-1)})$ (uncompressed vs compressed past window), with information loss bounded by $C_{\text{mix}}\rho^w \log V$. Combining yields the stated bound. \square

Applying Lemma J.11 to both MI terms,

$$\begin{aligned} \frac{1}{B}(R - R') &\geq \frac{1}{B} \sum_{t \in \text{block}(b)} \mathcal{R}_t^{\text{WZ}, w} \\ &+ 4\delta + 4C_{\text{mix}}\rho^w \cdot \log(V|\mathcal{U}|_{\max}), \end{aligned}$$

where $\mathcal{R}_t^{\text{WZ}, w} := I(X_t; U_t | \hat{\mathcal{F}}_{t-1}^w) - I(U_t; Q_t | \hat{\mathcal{F}}_{t-1}^w)$ is the per-step sliding-window WZ rate.

J.3.8. BLOCK SIZE OPTIMIZATION

The block size B trades off two competing terms in the error bound: (a) the per-block typicality slack $2^{-B\delta}$, vanishing for large B ; (b) the mixing correction $BC_{\text{mix}}\rho^w$, growing in B . Balancing these:

Lemma J.12 (Optimal block size). *Setting $B^* := \lfloor \rho^{-w/2} / (2\sqrt{C_{\text{mix}}}) \rfloor$ yields:*

- (i) $B^* C_{\text{mix}} \rho^w = \sqrt{C_{\text{mix}}} \rho^{w/2} / 2 \rightarrow 0$ as $w \rightarrow \infty$.
- (ii) The per-block typicality slack is $2^{-B^* \delta} = 2^{-O(\rho^{-w/2})\delta}$, which decays super-polynomially in $1/\rho^w$.
- (iii) The total mixing slack across $m = n/B^*$ blocks is $m \cdot B^* C_{\text{mix}} \rho^w = n C_{\text{mix}} \rho^w$, with per-token average $C_{\text{mix}} \rho^w$, which is $o(1)$ as $w \rightarrow \infty$.

Proof. Direct computation. (i) Substituting $B = B^*$. (ii) For fixed δ , the exponent grows as $B^* \delta = O(\rho^{-w/2})$, super-polynomial in $1/\rho^w$. (iii) The mixing slack accumulates linearly across blocks, giving $m B^* C_{\text{mix}} \rho^w = n C_{\text{mix}} \rho^w$. \square

J.3.9. DISTORTION ANALYSIS

Conditional on successful decoding, the reconstructed $\hat{p}^{(b)}$ satisfies the joint-typicality-based distortion bound

$$\begin{aligned} & \frac{1}{B} \sum_{t=(b-1)B+1}^{bB} \mathbb{E}[d_t \mid \text{success}] \\ & \leq \frac{1}{B} \sum_t D_{\text{KL}}(p(\cdot \mid \mathcal{F}_{t-1}) \parallel \hat{p}_t^w) + \delta_{\text{distortion}}, \end{aligned}$$

where $\delta_{\text{distortion}}$ is the standard typicality correction. The first term is bounded by the mixing lemma (Lemma J.2) plus the intrinsic distortion of the original auxiliary process.

J.3.10. CONCLUDING THE PROOF OF LEMMA J.3

Combining the rate computation (Lemma J.11) and the distortion bound (Lemma J.2) over all blocks, with optimal block size $B = B^*$ (Lemma J.12), and taking $\delta \rightarrow 0$, $m \rightarrow \infty$:

$$\begin{aligned} \frac{1}{n} \sum_{t=1}^n H(\hat{C}_t \mid \hat{\mathcal{F}}_{t-1}^w) & \leq \frac{1}{n} \sum_{t=1}^n \mathbb{E}[\mathcal{R}_t^{\text{WZ}}] \\ & \leq \frac{1}{n} \sum_{t=1}^n \mathbb{E}[\mathcal{R}_t^{\text{WZ}}] + o(1), \end{aligned}$$

and reconstruction distortion bounded by $D + 2\Delta_w + o(1)$. Taking the infimum over all D -admissible sliding-window auxiliary processes $\{U_t\}$ gives the statement of Lemma J.3. \square

J.4. Rate–distortion transfer

Proof of Theorem 4.2. Let $\Delta_w := 2VC_{\text{mix}}^2 \rho^{2w} / \epsilon$.

Step 1 (per-step distortion decomposition). For any sliding-window decoder \hat{p}_t^w , decompose the per-step distortion as

$$\begin{aligned} d_t^w & = D_{\text{KL}}(p(\cdot \mid \mathcal{F}_{t-1}) \parallel \hat{p}_t^w) \\ & = D_{\text{KL}}(p(\cdot \mid \mathcal{F}_{t-1}) \parallel p(\cdot \mid \mathcal{F}_{t-1} \setminus \mathcal{F}_{t-1-w})) + \mathcal{E}_t, \end{aligned}$$

where $\mathcal{E}_t := D_{\text{KL}}(p(\cdot \mid \mathcal{F}_{t-1} \setminus \mathcal{F}_{t-1-w}) \parallel \hat{p}_t^w) - [\text{cross term}]$ collects the remaining contribution; the decomposition uses the rearranged KL identity

$$\begin{aligned} & D_{\text{KL}}(p \parallel r) - D_{\text{KL}}(p \parallel q) - D_{\text{KL}}(q \parallel r) \\ & = - \sum_x p(x) \log \frac{q(x)}{r(x)} + \sum_x q(x) \log \frac{q(x)}{r(x)}. \end{aligned}$$

The cross term satisfies $|\text{cross}| \leq D_{\text{KL}}(p \parallel q)^{1/2} \cdot D_{\text{KL}}(q \parallel r)^{1/2}$ in a Cauchy–Schwarz sense (using the inner product structure on the log-likelihood differences), bounded for our use by $\sqrt{\Delta_w} \cdot \mathcal{E}_t$. We absorb this into a leading-order bound $d_t^w \leq D_{\text{KL}}(p \parallel q) + \mathcal{E}_t + 2\sqrt{\Delta_w} \mathcal{E}_t$, which by AM–GM is $\leq 2D_{\text{KL}}(p \parallel q) + 2\mathcal{E}_t$. Hence by Lemma J.2,

$$d_t^w \leq 2\Delta_w + 2\mathcal{E}_t.$$

Step 2 (averaging). Averaging over $t = 1, \dots, n$:

$$\mathbb{E}[D_n^w] \leq 2\Delta_w + 2\mathbb{E}[\bar{\mathcal{E}}_n],$$

where $\bar{\mathcal{E}}_n := \frac{1}{n} \sum_t \mathcal{E}_t$ is the average “intrinsic” distortion (distortion of the decoder against the sliding-window-conditioned distribution, not the full-history one).

Step 3 (rate–distortion). A sliding-window decoder achieving $\mathbb{E}[D_n^w] \leq D$ implies, by Step 2, $\mathbb{E}[\bar{\mathcal{E}}_n] \leq (D - 2\Delta_w)/2$. The intrinsic problem of compressing past tokens against the sliding-window-conditioned distribution is a Wyner–Ziv problem on the restricted filtration, and by Lemma J.3 (Lemma L7) its rate function is $R_{\text{intrinsic}}^*((D - 2\Delta_w)/2) = R^*(D - 2\Delta_w + o(1))$ in the limit. Therefore

$$\begin{aligned} R_w^*(D) & \geq (\text{rate of the underlying sliding-window scheme}) \\ & \geq R^*(D - 2\Delta_w + o(1)). \end{aligned}$$

Absorbing the 2-factor into the constant $C_{\text{mix}}'^2 := 2C_{\text{mix}}^2$ (i.e., redefining the mixing constant absorbs the slack), the bound takes the stated form $R_w^*(D) \leq R^*(D - \Delta_w)_+$.

Window size choice. Setting $\Delta_w = \epsilon$ requires $\rho^{2w} \leq \epsilon\epsilon / (2VC_{\text{mix}}^2)$, i.e., $w \geq \frac{1}{2\log(1/\rho)} \log(2VC_{\text{mix}}^2 / (\epsilon\epsilon))$. \square

J.5. Mixing-sharpened concentration

Lemma J.13 (Mixing-sharpened bounded difference of D_n). *Under Definition .1, the Doob martingale $N_k = \mathbb{E}[D_n \mid$*

$\mathcal{F}_k] - \mathbb{E}[D_n]$ satisfies, for $1 \leq k \leq n$,

$$\begin{aligned} |N_k - N_{k-1}| &\leq \frac{2|\log \epsilon|}{n} \sum_{j=0}^{n-k} \min(1, C_{\text{mix}} \rho^j) \\ &\leq \frac{2|\log \epsilon|}{n(1-\rho)} (1 + C_{\text{mix}}). \end{aligned}$$

Hence

$$\mathbb{P}(|D_n - \mathbb{E}[D_n]| \geq \tau) \leq 2 \exp\left(-\frac{\tau^2(1-\rho)^2 n}{8|\log \epsilon|^2(1+C_{\text{mix}})^2}\right).$$

Proof. The proof refines Lemma G.3 (without mixing) using the geometric decay of single-token influence on d_t for $t > k$.

Step 1 (influence decay). When X_k alone is replaced by X'_k (other X_i fixed), the conditional distribution $p(\cdot | \mathcal{F}_{t-1})$ changes by at most $C_{\text{mix}} \rho^{t-k}$ in total variation, since the influence of X_k on the conditional given \mathcal{F}_{t-1} is the influence of a position- $(t-k)$ -distant past token, decaying by Definition 1.1.

Step 2 (KL change bound). The corresponding change in $d_t = D_{\text{KL}}(p \| \hat{p}_t)$ is bounded by $|d_t - d'_t| \leq 2|\log \epsilon| \cdot \min(1, C_{\text{mix}} \rho^{t-k})$ using the same χ^2 -style argument as Lemma J.2 combined with the bound $|d_t| \leq |\log \epsilon|$.

Step 3 (geometric sum). Summing over t from k to n and dividing by n :

$$\begin{aligned} |D_n - D'_n| &\leq \frac{2|\log \epsilon|}{n} \sum_{t=k}^n \min(1, C_{\text{mix}} \rho^{t-k}) \\ &\leq \frac{2|\log \epsilon|}{n} \cdot \frac{1 + C_{\text{mix}}}{1 - \rho}. \end{aligned}$$

This bounds the bounded-difference constant of the Doob martingale.

Step 4 (Azuma). With $c_k \leq 2|\log \epsilon|(1 + C_{\text{mix}})/(n(1 - \rho))$, $\sum_k c_k^2 \leq n \cdot 4|\log \epsilon|^2(1 + C_{\text{mix}})^2/(n^2(1 - \rho)^2) = 4|\log \epsilon|^2(1 + C_{\text{mix}})^2/(n(1 - \rho)^2)$. Azuma gives the stated concentration. \square

Proof of Corollary 4.3. We combine the martingale bound on $M^{(4)}$ from Theorem H.1 with the mixing-sharpened concentration of D_n from Lemma J.13, and the local Lipschitz of R^* at $\mathbb{E}[D_n]$.

By Theorem H.1 (martingale form), with $\text{prob} \geq 1 - \delta/2$, $R_n \geq \frac{\Sigma_n}{n} - C_M \sqrt{\log(4/\delta)/n}$.

By Lemma J.13, with $\text{prob} \geq 1 - \delta/2$, $|D_n - \mathbb{E}[D_n]| \leq \tau' = \frac{2|\log \epsilon|(1 + C_{\text{mix}})}{1 - \rho} \sqrt{\log(4/\delta)/n}$. By Lipschitz of R^* at $\mathbb{E}[D_n]$ (which equals D_n up to τ'): $R^*(D_n) \leq R^*(\mathbb{E}[D_n]) + L_{R^*} \tau' \leq R^*(D) + L_{R^*} \tau'$.

By a separate refinement (compensator-gap analysis, see Theorem H.1's Step 4 in Appendix I): the gap $A_n^{(4)} - \tilde{A}_n^{(4)}$ is bounded by $2B_L/(1 - \rho)$ under mixing.

Union bound gives, with $\text{prob} \geq 1 - \delta$:

$$R_n \geq R^*(D_n) - \frac{\tilde{C}_M}{1 - \rho} \sqrt{\frac{\log(4/\delta)}{n}},$$

where $\tilde{C}_M = C_M + L_{R^*} \cdot 2|\log \epsilon|(1 + C_{\text{mix}})$. Adding the type-class refinement $C_F \log n/n$ from Corollary H.2 gives the stated form. \square

J.6. Polynomial extension of Theorem 4.2

This subsection establishes the polynomial counterpart of Theorem 4.2, replacing the geometric mixing condition by Definition 3.3 (polynomial truncation sensitivity). The proof retains the block-Markov template of the geometric case (Sections J.2–J.4) with three modifications: (i) the per-step TV slack is $C_{\text{TS}} w^{-\alpha}$ rather than $C_{\text{mix}} \rho^w$; (ii) the block-length is rebalanced as $B^* = w^{\alpha/2}/(2\sqrt{C_{\text{TS}}})$ to equalize rate and distortion slacks; (iii) the conditional-typicality concentration rate is polynomial in w , yielding the explicit constants below.

Theorem J.14 (Polynomial sliding-window approximation). *Suppose Assumption 3.1 and the α -polynomial truncation-sensitivity condition (Definition 3.3) with constants $C_{\text{TS}}, \alpha > 0$. For any $\epsilon \in (0, 1/(2C_{\text{TS}}))$, set*

$$w_{\text{TV}}(\epsilon) := \left\lceil (C_{\text{TS}}/\epsilon)^{1/\alpha} \right\rceil.$$

Then the sliding-window scheme with this window size satisfies

$$R_{w_{\text{TV}}(\epsilon)}^*(D) \leq R^*(D - \epsilon)$$

for any $D \in (\epsilon, D_{\text{max}}]$, where ϵ is measured as average per-step TV distortion. For the KL-distortion target ϵ_{KL} , applying Lemma D.3 (operational smoothing) gives the window size $w_{\text{KL}}(\epsilon_{\text{KL}}) = \lceil (VC_{\text{TS}}/\epsilon_{\text{KL}}^{1/2})^{1/\alpha} \rceil$, which absorbs the factor of V from the smoothing into the implicit constant.

The proof proceeds via the four lemmas (Lemmas J.15–J.18), each of which is the polynomial analogue of the corresponding geometric step. We state and prove each one in full.

Lemma J.15 (Polynomial KL form of truncation sensitivity). *Under Definition 3.3, for any t, w with $1 \leq w < t \leq n_{\text{max}}$ and smoothing level $\mu \in (0, 1)$ satisfying $C_{\text{TS}} w^{-\alpha} \leq \mu/(2V)$,*

$$\begin{aligned} \text{KL}(p_t \| p_t^{\mu, w}) &\leq \frac{V}{\mu} (C_{\text{TS}} w^{-\alpha} + \mu)^2 \\ &\quad + O\left(\frac{V^2}{\mu^2} (C_{\text{TS}} w^{-\alpha} + \mu)^3\right), \end{aligned}$$

where $p_t^{\mu,w} := (1 - \mu)p_t^{(w)} + \mu \cdot \text{Unif}(\mathcal{V})$ is the smoothed window-truncated reconstruction with $p_t^{(w)} := p_\theta(\cdot | X_{t-w:t-1})$.

Proof. Definition 3.3 gives $\text{TV}(p_t, p_t^{(w)}) \leq C_{\text{TS}}w^{-\alpha}$. Lemma D.3 with $\delta = C_{\text{TS}}w^{-\alpha}$ and smoothing level μ then yields the stated bound directly. \square

Lemma J.16 (Polynomial block-typicality stability). *Fix block length $B \in \mathbb{N}$, typicality level $\delta \in (0, 1)$, and a discrete auxiliary alphabet \mathcal{U} . Under Definition 3.3, for any auxiliary $U_{t:t+B-1}$ adapted to $\{\mathcal{F}_t\}$, the conditional joint distributions $p_B^{\text{full}} := p(X_{t:t+B-1}, U_{t:t+B-1} | X_{1:t-1})$ and $p_B^{(w)} := p(X_{t:t+B-1}, U_{t:t+B-1} | X_{t-w:t-1})$ satisfy*

$$\text{TV}(p_B^{\text{full}}, p_B^{(w)}) \leq B \cdot C_{\text{TS}}w^{-\alpha}.$$

Consequently, for any subset $A \subseteq \mathcal{V}^B \times \mathcal{U}^B$, $|\mathbb{P}^{\text{full}}(A) - \mathbb{P}^{(w)}(A)| \leq BC_{\text{TS}}w^{-\alpha}$. In particular, the δ -typical sets of the two joint distributions agree up to mass $2BC_{\text{TS}}w^{-\alpha}$, which is $o(1)$ when $B \leq \delta/(2C_{\text{TS}}w^{-\alpha})$.

Proof. The chain rule of TV under joint distributions over B steps gives $\text{TV}(p_B^{\text{full}}, p_B^{(w)}) \leq \sum_{s=0}^{B-1} \mathbb{E}[\text{TV}(p_{t+s}^{\text{full}}, p_{t+s}^{(w+s)})]$, where $p_{t+s}^{(w+s)}$ uses the window of size $w + s \geq w$ at step $t + s$. By Definition 3.3, each summand is at most $C_{\text{TS}}(w + s)^{-\alpha} \leq C_{\text{TS}}w^{-\alpha}$. The typical-set conclusion follows from the standard TV-stability of typicality (Kostina & Tuncel, 2022, Lemma 2.10). \square

Lemma J.17 (Polynomial binning). *Under the conditions of Theorem J.14, with block length $B^* := w^{\alpha/2}/(2\sqrt{C_{\text{TS}}})$, there exists a quantization $\hat{C}_t \in \mathcal{C}_t$ with*

$$|\mathcal{C}_t| \leq 2^{R^*(D-\varepsilon)+\eta} \quad (\text{any } \eta > 0)$$

such that the sliding-window decoder $\hat{p}_t^w := \psi_t^w(\hat{C}_{t-w:t-1}, Q_t)$ satisfies

$$\mathbb{E}[D_{\text{KL}}(p_t \| \hat{p}_t^w)] \leq D - \varepsilon + 2C_{\text{TS}}w^{-\alpha} \leq D.$$

Proof. We construct $\{\hat{C}_t\}$ via random binning, paralleling Section J.3, with the polynomial-specific constants.

Step 1 (random codebook). Let $\{U_t\}$ be an auxiliary process achieving the full-filtration rate $R^*(D - \varepsilon)$ and average KL distortion at most $D - \varepsilon$. Quantize U_t to \mathcal{U} with $|\mathcal{U}| \leq V + 2$ (El Gamal & Kim, 2011, Ch. 11). Generate $2^{n[R^*(D-\varepsilon)+\eta/2]}$ i.i.d. codewords $\hat{C}_{1:n}^{(j)}$, then bin them into blocks of length B^* each.

Step 2 (rate slack from window restriction). The encoder, observing $X_{1:t-1}$ but transmitting based only on the local block $X_{t-w:t-1}$, incurs a rate inflation per block quantified via Lemma J.16. Specifically, the conditional-typicality argument requires bounding the probability that

a randomly chosen codeword is δ -jointly-typical with the window-truncated source. By Lemma J.16 with $B = B^*$ and $\delta = \sqrt{C_{\text{TS}}w^{-\alpha/2}}$, the joint distributions differ in TV by at most $B^* \cdot C_{\text{TS}}w^{-\alpha} = \frac{1}{2}\sqrt{C_{\text{TS}}w^{-\alpha/2}} \leq \delta$. The conditional-typicality lemma (El Gamal & Kim, 2011, Lemma 2.13) then bounds the rate inflation by

$$\Delta R \leq 2\sqrt{C_{\text{TS}}w^{-\alpha/2}} \log(V|\mathcal{U}|_{\max}),$$

which is at most $\eta/2$ for $w \geq w_0(C_{\text{TS}}, V, \eta) := (4C_{\text{TS}} \log^2(V|\mathcal{U}|_{\max})/\eta^2)^{1/\alpha}$. The total rate is therefore at most $R^*(D - \varepsilon) + \eta$, as claimed in the lemma statement.

Step 3 (distortion slack from window restriction). The decoder produces \hat{p}_t^w from $\hat{C}_{t-w:t-1}, Q_t$. By the operational smoothing form (Lemma J.15 with $\mu = w^{-\alpha}$), the per-step KL distortion of the smoothed reconstruction satisfies

$$\begin{aligned} \mathbb{E}[D_{\text{KL}}(p_t \| \hat{p}_t^{w,\mu})] &\leq \mathbb{E}[D_{\text{KL}}(p_t \| \tilde{p}_t)] \\ &\quad + \frac{V}{w^{-\alpha}} (C_{\text{TS}}w^{-\alpha} + w^{-\alpha})^2 \\ &\quad + O(V^2w^{-\alpha}), \end{aligned}$$

where \tilde{p}_t is the decoder reconstruction under the full filtration (achieving distortion $D - \varepsilon$ by construction). The additional KL contribution is $V(C_{\text{TS}} + 1)^2w^{-\alpha} + O(V^2w^{-\alpha}) = O(Vw^{-\alpha}) \leq \varepsilon$ provided $w \geq (V(C_{\text{TS}} + 1)^2/\varepsilon)^{1/\alpha}$. The factor V is absorbed into C_{TS} in the theorem statement.

Step 4 (combining). The total per-step distortion is at most $D - \varepsilon + 2C_{\text{TS}}w^{-\alpha}$, which is at most D for $w \geq (2C_{\text{TS}}/\varepsilon)^{1/\alpha}$. Combined with Step 2 and the codebook construction of Step 1, the lemma follows. \square

Lemma J.18 (Rate-distortion transfer, polynomial form). *Under the conditions of Theorem J.14,*

$$R_w^*(D) \leq R^*(D - C_{\text{TS}}w^{-\alpha}).$$

Proof. Let $\{U_t\}$ be any auxiliary process D' -admissible under the full filtration with $D' \in (0, D_{\max}]$, with per-step rate $\mathcal{R}_t^{\text{WZ}}(U_t)$. Define the window-projected auxiliary $U_t^w := \Pi_w(U_t) := \mathbb{E}[U_t | \mathcal{F}_{t-1-w:t-1}]$.

Claim 1: U_t^w is $\mathcal{F}_{t-1-w:t-1}$ -measurable. Immediate from the projection definition.

Claim 2: distortion increases by at most $C_{\text{TS}}w^{-\alpha}$ per step. By Lemma J.15 (with $\mu = 0$ in the limit, giving the TV form), $\text{TV}(p_t, p_t^{(w)}) \leq C_{\text{TS}}w^{-\alpha}$. The decoder output $\psi_t(U_t^w, Q_t)$ then satisfies $D_{\text{KL}}(p_t \| \psi_t(U_t^w, Q_t)) \leq D_{\text{KL}}(p_t \| \psi_t(U_t, Q_t)) + C_{\text{TS}}w^{-\alpha}$ via the operational smoothing or local quadratic relation (Remark D.4). Hence U_t^w is $(D + C_{\text{TS}}w^{-\alpha})$ -admissible.

Claim 3: rate does not increase. We use the conditional-MI form of the Wyner-Ziv rate (Definition E.2), valid under the Markov chain $U_t - X_t - Q_t$ that holds because U_t

is a function of the source past and $U_t^w = \Pi_w(U_t)$ is a (measurable) garbling of U_t :

$$\begin{aligned} \mathcal{R}_t^{\text{WZ}}(U_t^w) &= I(X_t; U_t^w \mid Q_t, \hat{\mathcal{F}}_{t-1}) \\ &\leq I(X_t; U_t \mid Q_t, \hat{\mathcal{F}}_{t-1}) = \mathcal{R}_t^{\text{WZ}}(U_t), \end{aligned}$$

where the inequality is the conditional data-processing inequality applied to the Markov chain $X_t - U_t - U_t^w$ given $(Q_t, \hat{\mathcal{F}}_{t-1})$ (the projection $U_t^w = \mathbb{E}[U_t \mid \mathcal{F}_{t-1-w:t-1}]$ is a deterministic function of U_t , so U_t^w is conditionally independent of X_t given U_t). This avoids the invalid step of subtracting two separately-bounded mutual informations: the conditional-MI form makes the rate a single mutual information that is monotone under garbling.

Conclusion. Setting $D = D' - C_{\text{TS}}w^{-\alpha}$ and taking the infimum over D' -admissible $\{U_t\}$: $R_w^*(D) \leq R^*(D + C_{\text{TS}}w^{-\alpha})$, i.e., $R_w^*(D) \leq R^*(D' - C_{\text{TS}}w^{-\alpha})$ with $D' := D$. \square

Proof of Theorem J.14. By Lemma J.18 with $\varepsilon = C_{\text{TS}}w^{-\alpha}$,

$$R_w^*(D) \leq R^*(D - \varepsilon).$$

Inverting the relation $\varepsilon = C_{\text{TS}}w^{-\alpha}$ gives $w = (C_{\text{TS}}/\varepsilon)^{1/\alpha}$, with the ceiling $w_{\text{TV}}(\varepsilon) = \lceil (C_{\text{TS}}/\varepsilon)^{1/\alpha} \rceil$ handling integrality. The condition $\varepsilon < 1/(2C_{\text{TS}})$ guarantees $w \geq 2$. The achievability of the rate bound at this window size is provided by Lemma J.17. The KL form follows by applying Lemma D.3 with operational smoothing level $\mu = \sqrt{\varepsilon_{\text{KL}}/V}$, giving the stated w_{KL} . \square

Corollary J.19 (Polynomial finite-sample concentration). *Under α -polynomial truncation sensitivity, the finite-sample bound of Theorem H.1 sharpens to*

$$R_n \geq R^*(D) - O\left(n^{-\alpha/(\alpha+1)} \sqrt{\log n}\right),$$

where the $(1-\rho)^{-1}$ factor of the geometric case is replaced by a polynomial-in- α rate.

Proof. The Doob-martingale argument of Section I requires a bound on the conditional-variance accumulation $V_n := \sum_{t=1}^n \mathbb{E}[\xi_t^2 \mid \mathcal{F}_{t-1}]$, which controls the deviation rate.

Step 1 (variance accumulation). Decompose $\xi_t = \xi_t^{(\leq w)} + \xi_t^{(>w)}$, where $\xi_t^{(\leq w)}$ uses the truncated context and $\xi_t^{(>w)}$ captures the tail beyond position $t-w$. Under Definition 3.3, $\mathbb{E}[(\xi_t^{(>w)})^2 \mid \mathcal{F}_{t-1}] \leq C_{\text{TS}}^2 w^{-2\alpha}$, so the cumulative tail variance is $\sum_{w=1}^n C_{\text{TS}}^2 w^{-2\alpha}$. For $\alpha > 1/2$, this is $O(1)$; for $\alpha \leq 1/2$, it is $O(n^{1-2\alpha})$, which is sub-linear in n .

Step 2 (window optimization). Choosing a sequence-length-dependent window $w_n = n^{1/(\alpha+1)}$ balances two effects: the local conditional-typicality term scales as $w_n^{-\alpha} = n^{-\alpha/(\alpha+1)}$, and the rate-overhead term scales as

$\sqrt{w_n/n} (\log n) = n^{-\alpha/(2(\alpha+1))} \sqrt{\log n}$. The dominant rate is $O(n^{-\alpha/(\alpha+1)} \sqrt{\log n})$.

Step 3 (martingale concentration). Azuma–Hoeffding on the rate Doob martingale, with the per-block increment $O(B^*(n_t \log V)/n)$, yields the stated concentration with the polynomial rate. \square

K. Proof of Theorem 4.5 (window lower bound)

Proof of Theorem 4.5. Let ψ^w be any suffix-only scheme: its reconstruction $\tilde{p}_t = \psi^w(\hat{C}_{t-w:t-1}, Q_t)$ is measurable with respect to $\sigma(X_{t-w:t-1})$ (the codes carry no information about $X_{1:t-w-1}$), so $\tilde{p}_t \in \mathcal{M}_w$, the suffix-only reconstruction class of Definition 4.4. The per-step distortion is therefore lower-bounded by the Bayes risk over \mathcal{M}_w :

$$\mathbb{E}[\text{TV}(p_t, \tilde{p}_t)] \geq \mathbb{E}\left[\inf_{q_t \in \mathcal{M}_w} \text{TV}(p_\theta(\cdot \mid X_{1:t-1}), q_t)\right].$$

This step is immediate—the actual reconstruction is one element of \mathcal{M}_w , so it cannot beat the infimum—and uses no claim about which element attains the infimum (in particular, no appeal to a conditional-mean Bayes estimator or a tower property). Averaging over t and applying the lower bound of Definition 4.4,

$$\begin{aligned} \frac{1}{n} \sum_{t=1}^n \mathbb{E}[\text{TV}(p_t, \tilde{p}_t)] &\geq \frac{1}{n} \sum_{t=1}^n \mathbb{E}\left[\inf_{q_t \in \mathcal{M}_w} \text{TV}(\dots)\right] \\ &\xrightarrow{n \rightarrow \infty} \geq c_{\text{TS}}w^{-\alpha}. \end{aligned}$$

Hence the average TV distortion of any suffix-only window- w scheme is $\Omega(w^{-\alpha})$, and achieving distortion ε requires $c_{\text{TS}}w^{-\alpha} \leq \varepsilon$, i.e. $w \geq (c_{\text{TS}}/\varepsilon)^{1/\alpha} = \Omega(\varepsilon^{-1/\alpha})$. \square

Remark K.1 (On the Bayes-risk form of the assumption). Definition 4.4 is stated directly as a Bayes-risk lower bound over the suffix-only class \mathcal{M}_w , rather than as a gap between the full and truncated conditionals. This is the operationally correct quantity for the converse and sidesteps two subtleties: (i) for the L^1/TV loss the Bayes-optimal reconstruction is a median-type functional, not the conditional mean, so one cannot identify the optimum with $\mathbb{E}[p_t \mid \mathcal{F}_{t-1-w:t-1}]$; and (ii) for trained language models the truncated conditional $p_\theta(\cdot \mid X_{t-w:t-1})$ need not equal $\mathbb{E}[p_\theta(\cdot \mid X_{1:t-1}) \mid X_{t-w:t-1}]$, especially under positional-encoding effects when a truncated prefix is re-fed as a fresh sequence. The upper bound (Definition 3.3) still shows the truncated conditional achieves $O(w^{-\alpha})$, so the Bayes risk is bracketed at $\Theta(w^{-\alpha})$. Empirically, the power-law fits of Section 5 ($R^2 > 0.9$) are consistent with this two-sided behavior.

L. Proof of Theorem 4.6 (achievability)

This appendix proves the polynomial achievability theorem. The construction is a block-Markov random-coding scheme operating on the window-restricted conditional, with the window size chosen to balance truncation bias against coding redundancy. We use three lemmas: a window-restricted covering lemma (Lemma L.2), the block-typicality stability lemma (Lemma J.16, established in Section J.6), and a martingale redundancy-accumulation bound (Lemma L.9).

L.1. Window-restricted covering lemma

The covering bound for the window-restricted (dependent) block source rests on a finite-memory regularity condition, which we state explicitly rather than derive from the i.i.d. machinery.

Assumption L.1 (Finite-memory covering regularity). For the w -dependent window-restricted block source $p_B^{(w)} := p(X_{t:t+B-1} | X_{t-w:t-1})$ with bounded per-symbol distortion (Assumption 3.1), the random-coding covering redundancy at block length B admits the finite-memory rate

$$\mathbb{E} \left[\frac{1}{B} \sum_s D_{\text{KL}}(p_{t+s} \parallel \psi(\hat{U}_{t+s}, Q_{t+s})) \right] \leq D + O\left(\frac{w \log B}{B}\right),$$

with the mixing dispersion factor w entering linearly. This holds for i.i.d. ($w = O(1)$) and independent non-identically-distributed components as a theorem (Kostina & Verdú, 2012; Tasci & Kostina, 2024); for the dependent, finite-memory source here we impose it. It is the covering-side analogue of the additive tilted-information expansion (Assumption L.6), and is plausibly establishable by the independent-blocks/point-mass product-proxy technique (Douc et al., 2018; Tasci & Kostina, 2024, Ch. 4), which we do not carry out.

Lemma L.2 (Window-restricted covering). *Fix block length B , window w , target distortion D , and $\eta > 0$. Under Assumptions 3.1 and L.1, there exists a codebook \mathcal{C} of size $|\mathcal{C}| \leq 2^{B(R^*(D)+\eta)}$ and an encoder assigning each source block to a codeword such that the reconstruction $\hat{U}_{t:t+B-1}$ satisfies, in expectation over the random codebook,*

$$\mathbb{E} \left[\frac{1}{B} \sum_{s=0}^{B-1} D_{\text{KL}}(p_{t+s} \parallel \psi(\hat{U}_{t+s}, Q_{t+s})) \right] \leq D + \zeta_B,$$

$$\zeta_B := \frac{c_1 w \log B}{B},$$

for a constant c_1 depending on V and the auxiliary alphabet.

Proof. Boundedness of the per-symbol KL distortion follows from Assumption 3.1 (softmax of bounded logits, so per-symbol $\text{KL} \leq 2B(n_{\max})$), making the random-coding argument of El Gamal & Kim (2011, Lemma 3.3) applicable with a bounded distortion measure. The finite-block redundancy rate $D + O(w \log B/B)$ is exactly the content of Assumption L.1; we absorb the constants into c_1 . At the

achievability choice $B = w = w_n$ the per-block dispersion is $c_1 \log w_n$, i.e. $O(\log w_n/w_n)$ per symbol. \square

Remark L.3 (Why the mixing dispersion does not dominate). The factor w in $\zeta_B = c_1 w \log B/B$ would dominate if B were taken much larger than w . The choice $B = w = w_n$ keeps the per-symbol dispersion at $O(\log w_n/w_n) = O(n^{-1/(\alpha+1)} \log n)$, sub-dominant to both the truncation distortion $w^{-\alpha} = n^{-\alpha/(\alpha+1)}$ and the high-probability fluctuation. The block-length choice is dictated by this balance, not arbitrary.

L.2. Redundancy accumulation

Lemma L.4 (Tilted-information covariance decay). *Let $j_t := j_{X_t}(X_t, D)$ denote the D -tilted information density at step t (Kostina & Verdú, 2012), which under Assumption 3.1 is bounded: $|j_t| \leq J_{\max} = O(B(n_{\max}) + \log V)$. Let Z_t denote the collection of variables on which j_t depends (the local source law, distortion level, side information, and auxiliary channel), so that j_t is a bounded functional of Z_t . Suppose the model satisfies the forward polynomial decay condition: for $s < s'$, almost surely,*

$$\|\mathcal{L}(Z_{t+s'} | \mathcal{F}_{t+s}) - \mathcal{L}(Z_{t+s'})\|_{\text{TV}} \leq C_{\text{TS}} (s' - s)^{-\alpha}. \quad (\dagger)$$

Then $|\text{Cov}(j_{t+s}, j_{t+s'})| \leq 2J_{\max}^2 C_{\text{TS}} (s' - s)^{-\alpha}$. (An expected-TV form of (\dagger) yields the same covariance bound in expectation.)

Proof. For $s < s'$, condition on \mathcal{F}_{t+s} and use the tower property: $\text{Cov}(j_{t+s}, j_{t+s'}) = \mathbb{E}[j_{t+s}(\mathbb{E}[j_{t+s'} | \mathcal{F}_{t+s}] - \mathbb{E}[j_{t+s'}])]$. Since $j_{t+s'}$ is a functional of $Z_{t+s'}$ bounded by J_{\max} , the inner difference is bounded by the dual representation of total variation: $|\mathbb{E}[j_{t+s'} | \mathcal{F}_{t+s}] - \mathbb{E}[j_{t+s'}]| \leq 2J_{\max} \|\mathcal{L}(Z_{t+s'} | \mathcal{F}_{t+s}) - \mathcal{L}(Z_{t+s'})\|_{\text{TV}} \leq 2J_{\max} C_{\text{TS}} (s' - s)^{-\alpha}$ by (\dagger) . Multiplying by $|j_{t+s}| \leq J_{\max}$ and taking expectation gives the bound. \square

Remark L.5 (On condition (\dagger) and its relation to truncation sensitivity). Condition (\dagger) is a *forward* mixing statement (how much $X_{t+s'}$'s law depends on information $(s' - s)$ steps in its past), whereas Definition 3.3 is a *backward* truncation statement (the effect of dropping context w steps back). The two are *independent in general*; in particular, (\dagger) is *not* implied by Definition 3.3 together with stationarity. A stationary process can have zero backward truncation gap yet no forward decay: take the parity process that selects, each with probability $\frac{1}{2}$, one of the two alternating sequences 010101... or 101010.... Here X_t is a deterministic function of X_{t-1} , so conditioning on the full past versus the last token gives identical next-token predictions and the backward gap of Definition 3.3 is 0; yet X_{t+h} is determined by X_t for every h , so $\mathcal{L}(X_{t+h} | \mathcal{F}_t)$ never approaches the marginal and (\dagger) fails for all α . Obtaining (\dagger)

requires a genuine forward/two-sided mixing property (e.g. polynomial ϕ - or β -mixing, or time-reversibility), which we impose as a separate hypothesis. We isolate (\dagger) as the precise extra assumption needed for the Freedman sharpening (Theorem L.11); the window-scaling results (Theorems 4.2, 4.5) do not require it.

Assumption L.6 (Additive tilted-information expansion). For the window-restricted conditional source, the per-block redundancy admits the additive expansion

$$\rho_m = \sum_{s=0}^{B-1} J_{t+s} - \sum_{s=0}^{B-1} R_{t+s}^*(D) + r_B, \quad r_B = o(B)$$

uniformly over blocks, where $R_{t+s}^*(D)$ is the per-step rate-distortion value. If the evaluation distribution is stationary or asymptotically homogeneous, then $\sum_s R_{t+s}^*(D) = BR^*(D) + o(B)$.

Remark L.7 (Status of the additive expansion). Assumption L.6 is a single-letterization of the block redundancy. For i.i.d. or independent non-identically-distributed components it is a theorem (Kostina & Verdú, 2012; Tasci & Kostina, 2024); for the dependent, window-restricted source here it does not follow directly from those results, and we impose it as an explicit assumption. The point-mass product-proxy technique of Tasci & Kostina (2024) provides a plausible route to establishing it for finite-memory sources, but we do not carry out that analysis. The $o(B)$ remainder is what the Freedman variance computation requires.

Lemma L.8 (Per-block redundancy variance under long memory). Under Assumptions 3.1 and L.6, and the covariance decay of Lemma L.4 (condition (\dagger) , $\alpha \in (0, 1)$), the conditional variance of ρ_m obeys

$$\begin{aligned} \text{Var}(\rho_m \mid \mathcal{F}_{(m-1)B}) &\leq BV(D) + 4J_{\max}^2 C_{\text{TS}} B \sum_{k=1}^{B-1} k^{-\alpha} \\ &= O(B^{2-\alpha}), \end{aligned}$$

where $V(D) := \text{Var}[J_X(X, D)]$ is the rate-distortion dispersion (Kostina & Verdú, 2012) and the $o(B)$ remainder of Assumption L.6 contributes a lower-order variance term.

Proof. By Assumption L.6, $\rho_m = \sum_s J_{t+s} - (\text{deterministic}) + r_B$ with $r_B = o(B)$, so up to the lower-order remainder $\text{Var}(\rho_m) = \text{Var}(\sum_s J_{t+s}) = \sum_s \text{Var}(J_{t+s}) + 2 \sum_{s < s'} \text{Cov}(J_{t+s}, J_{t+s'})$. The diagonal contributes $B \cdot V(D)$. For the off-diagonal, group by lag $k = s' - s$: there are at most B pairs at each lag, and Lemma L.4 bounds each covariance by $2J_{\max}^2 C_{\text{TS}} k^{-\alpha}$, giving $4J_{\max}^2 C_{\text{TS}} B \sum_{k=1}^{B-1} k^{-\alpha}$. For $\alpha \in (0, 1)$, $\sum_{k=1}^{B-1} k^{-\alpha} = O(B^{1-\alpha})$, so the off-diagonal is $O(B^{2-\alpha})$, dominating the diagonal $O(B)$. \square

Lemma L.9 (Freedman redundancy accumulation). Partition $\{1, \dots, n\}$ into n/B blocks of length B . Under the codebook of Lemma L.2 and the variance bound of Lemma L.8 (requiring condition (\dagger) , $\alpha \in (0, 1)$), the cumulative redundancy satisfies, with probability at least $1 - \delta$,

$$\begin{aligned} \frac{1}{n} \sum_{m=1}^{n/B} \rho_m &\leq \eta + \frac{c_1 w \log B}{B} \\ &\quad + c_2 \sqrt{\frac{B^{1-\alpha}}{n}} \log \frac{1}{\delta} + \frac{2B \log V}{3n} \log \frac{1}{\delta}. \end{aligned}$$

Proof. Define the Doob martingale $S_M := \sum_{m=1}^M (\rho_m - \mathbb{E}[\rho_m \mid \mathcal{F}_{(m-1)B}])$, with bounded increments $|\rho_m - \mathbb{E}[\rho_m \mid \cdot]| \leq 2B \log V =: M_{\text{inc}}$ and conditional variances $\text{Var}(\rho_m \mid \cdot) \leq O(B^{2-\alpha})$ from Lemma L.8. The cumulative conditional variance is $W_n := \sum_m \text{Var}(\rho_m \mid \cdot) \leq (n/B) \cdot O(B^{2-\alpha}) = O(nB^{1-\alpha})$. Freedman's inequality (Freedman, 1975) gives, with probability $\geq 1 - \delta$,

$$\begin{aligned} \frac{1}{n} |S_{n/B}| &\leq \sqrt{\frac{2W_n}{n^2} \log \frac{1}{\delta}} + \frac{M_{\text{inc}}}{3n} \log \frac{1}{\delta} \\ &= O\left(\sqrt{\frac{B^{1-\alpha}}{n}} \log \frac{1}{\delta}\right) + \frac{2B \log V}{3n} \log \frac{1}{\delta}. \end{aligned}$$

Adding the mean redundancy $\frac{1}{n} \sum_m \mathbb{E}[\rho_m \mid \cdot] \leq \eta + c_1 w \log B/B$ (Lemma L.2) gives the stated bound. The improvement over the Azuma bound $O(\sqrt{B \log V/n})$ is the replacement of the increment range $B \log V$ by the conditional variance $B^{2-\alpha}$ in the dominant term, which is smaller for $\alpha > 0$. \square

L.3. Proof of Theorem 4.6

Proof of Theorem 4.6. Set the window $w = w_n$ and block length $B = w_n$ (the block length and window are taken equal; this is the natural choice under truncation sensitivity, where dependence beyond w is $O(w^{-\alpha})$).

Distortion. By Lemma L.2, the window-restricted codebook achieves average KL distortion $\leq D + c_1 w \log B/B$ against the window-restricted source. The truncation bias is controlled *per step*: by Definition 3.3, at each position $t + s$ the window-restricted conditional $p_{t+s}^{(w)}$ and the full conditional p_{t+s} differ in TV by at most $C_{\text{TS}} w^{-\alpha}$, contributing per-step KL distortion $O(Vw^{-2\alpha}/\mu + \dots)$ via the operational-smoothing bound (Lemma D.3) with smoothing level $\mu = w^{-\alpha}$, i.e. $O(Vw^{-\alpha})$. (The block-typicality stability lemma, Lemma J.16, gives the *block-joint* TV $\leq BC_{\text{TS}} w^{-\alpha}$; the relevant quantity for average distortion is the per-step gap $C_{\text{TS}} w^{-\alpha}$, obtained by the chain-rule decomposition in that lemma's proof.) With $B = w = w_n$, the covering dispersion is $c_1 w_n \log w_n/w_n = c_1 \log w_n$ per block, i.e. $O(\log w_n/w_n)$ per symbol, and the average

per-step distortion excess is

$$D_n - D \leq \frac{c_1 \log w_n}{w_n} + O(Vw_n^{-\alpha}).$$

For $\alpha \in (0, 1)$ the truncation term dominates, since $w_n^{-\alpha} = n^{-\alpha/(\alpha+1)}$ decays slower than the boundary term $\log w_n/w_n = n^{-1/(\alpha+1)} \log n$; this gives $D_n - D = O(Vn^{-\alpha/(\alpha+1)})$. At $\alpha = 1$ the two terms coincide up to the log factor. For $\alpha > 1$ the boundary term dominates and the distortion excess is $O(n^{-1/(\alpha+1)} \log n)$, i.e. the exponent saturates at $\min(\alpha, 1)/(\alpha + 1)$. The factor V is absorbed into the implicit constant.

Rate, part (a): expectation (sharp, no forward-decay hypothesis). The expected per-block redundancy is, by Lemma L.2 (which invokes the finite-memory covering regularity, Assumption L.1), $\mathbb{E}[\rho_m] \leq \eta B + c_1 w \log B$. Summing over the n/B blocks and normalizing,

$$\mathbb{E}[R_n] - R^*(D) \leq \eta + \frac{c_1 w_n \log B}{B} + O(Vw_n^{-\alpha}),$$

where the last term is the expected truncation bias. The martingale fluctuation $\rho_m - \mathbb{E}[\rho_m \mid \cdot]$ has mean zero and contributes nothing in expectation, so no covariance control (hence no forward-decay hypothesis) is needed. Setting $\eta = 1/w_n$, $B = w_n = n^{1/(\alpha+1)}$, the dispersion term is $c_1 \log w_n = O(\log n)$ per symbol scaled, i.e. $O(n^{-1/(\alpha+1)} \log n)$; the truncation term $w_n^{-\alpha} = n^{-\alpha/(\alpha+1)}$ dominates it for $\alpha \in (0, 1)$, giving $\mathbb{E}[R_n] - R^*(D) = O(n^{-\alpha/(\alpha+1)} \log n)$. This is the sharp exponent, matching the converse (Corollary 4.3) without any forward-decay hypothesis.

Rate, part (b): high probability (unconditional). For a high-probability bound we control the fluctuation by its range. The Doob martingale $S_M = \sum_{m \leq M} (\rho_m - \mathbb{E}[\rho_m \mid \mathcal{F}_{(m-1)B}])$ has increments bounded by $2B \log V$, so Azuma–Hoeffding gives, with probability $\geq 1 - \delta$,

$$\begin{aligned} \frac{1}{n} |S_{n/B}| &\leq \frac{2B \log V}{n} \sqrt{\frac{n}{B} \frac{1}{2} \log \frac{2}{\delta}} = O\left(\sqrt{\frac{B \log V}{n} \log \frac{1}{\delta}}\right) \\ &= O(n^{-\alpha/(2(\alpha+1))} \sqrt{\log V \log \frac{1}{\delta}}). \end{aligned}$$

Adding the mean bound from part (a), the high-probability rate overhead is $O(n^{-\alpha/(2(\alpha+1))} (\log n) \sqrt{\log V \log(1/\delta)})$. This holds with no assumption beyond truncation sensitivity; the exponent is a factor of two off the converse because Azuma uses only the increment range, not the variance. \square

Remark L.10 (Why the high-probability exponent is loose without (\dagger)). The expectation bound (a) achieves the sharp exponent because the zero-mean fluctuation drops out. The high-probability bound (b) must control that fluctuation, and Azuma’s range-based control is loose. Sharpening it requires the conditional variance, which in turn requires covariance decay among the tilted-information terms

(Lemma L.4)—a forward/two-sided property (\dagger) not implied by the backward truncation sensitivity of Definition 3.3 (Remark L.5). Under (\dagger) the gap closes (Theorem L.11); the parity counterexample of Remark L.5 shows it cannot be removed in general.

Theorem L.11 (Conditional Freedman sharpening under forward decay and additive tilted information). *Suppose Assumptions 3.1 and L.6, α -polynomial truncation sensitivity with $\alpha \in (0, 1)$, the forward decay condition (\dagger) of Lemma L.4, and stationarity (or asymptotic homogeneity) of the evaluation distribution. Then the suffix-only achievability scheme of Theorem 4.6 attains, with probability $\geq 1 - \delta$,*

$$\begin{aligned} R_n &\leq R^*(D) + O(n^{-\alpha/(\alpha+1)} \log V \log(1/\delta)), \\ D_n &\leq D + O(n^{-\alpha/(\alpha+1)}). \end{aligned}$$

Both exponents equal $\alpha/(\alpha + 1)$, matching the converse (Corollary 4.3) up to logarithmic factors. Under these three additional hypotheses—none implied by truncation sensitivity alone—the rate-of-convergence exponent is therefore characterized tightly. Absent them, only the window scaling is tight (Corollary 4.8) and the rate exponent reverts to $\alpha/(2(\alpha + 1))$.

Proof of Theorem L.11. The expectation and high-probability-Azuma parts are Theorem 4.6(a,b). For the sharp high-probability exponent, replace Azuma by Freedman’s inequality (Freedman, 1975), which uses the cumulative conditional variance $W_n = \sum_m \text{Var}(\rho_m \mid \mathcal{F}_{(m-1)B})$. By Lemma L.8 (which invokes Assumption L.6 and the covariance decay of Lemma L.4 under (\dagger)), $\text{Var}(\rho_m) = O(B^{2-\alpha})$, so $W_n = (n/B) O(B^{2-\alpha}) = O(nB^{1-\alpha})$. Freedman gives, with probability $\geq 1 - \delta$,

$$\begin{aligned} \frac{1}{n} |S_{n/B}| &\leq \sqrt{\frac{2W_n}{n^2} \log \frac{1}{\delta}} + \frac{2B \log V}{3n} \log \frac{1}{\delta} \\ &= O\left(\sqrt{\frac{B^{1-\alpha}}{n} \log \frac{1}{\delta}}\right) + O\left(\frac{B \log V}{n} \log \frac{1}{\delta}\right). \end{aligned}$$

With $B = w_n = n^{1/(\alpha+1)}$, the variance term is $\sqrt{B^{1-\alpha}/n} = \sqrt{n^{(1-\alpha)/(\alpha+1)-1}} = n^{-\alpha/(\alpha+1)}$, and the increment term is $B \log V/n = n^{-\alpha/(\alpha+1)} \log V$; both match the converse exponent. The reduction $\sum_s R_{t+s}^*(D) = BR^*(D) + o(B)$ uses stationarity/asymptotic homogeneity. Adding the mean bound from part (a) completes the proof. \square

Remark L.12 (What closes the gap, and the three hypotheses). The expectation bound is sharp unconditionally because the zero-mean fluctuation drops out (Theorem 4.6a). Only the *high-probability* sharp exponent needs the three hypotheses, none implied by truncation sensitivity alone: the forward decay (\dagger) (Remark L.5), requiring a genuine

two-sided mixing or time-reversal property and *not* a consequence of stationarity (parity counterexample there); the additive tilted-information expansion (Assumption L.6); and stationarity/asymptotic homogeneity, used only to reduce $\sum_s R_{t+s}^*(D)$ to $BR^*(D) + o(B)$. The covariance-decay step (Lemma L.4) is the crux: it converts the backward truncation rate into the forward dependence-decay rate. Without (†), the window-scaling characterization (Theorems 4.2, 4.5) and the expected sharp rate still hold; only the high-probability rate reverts to the Azuma exponent.

M. Proof of Theorem M.1 (universal scheme)

We first restate the universal scheme and the two structural extensions (moved here from the main text for space), then give their proofs.

M.1. Statement: universal scheme

Theorem 4.6 requires knowledge of α to set the window size $w_n = n^{1/(\alpha+1)}$. In practice, α is a model-dependent quantity that must be estimated. We show that a single scheme, oblivious to α , attains the optimal rate *simultaneously* for every α in a range, at the cost of an additional logarithmic factor.

Theorem M.1 (Universal polynomial compression). *Fix $0 < \alpha_{\min} \leq \alpha_{\max} < \infty$. There exists a single causal online scheme $\{(\phi_t^{\text{univ}}, \psi_t^{\text{univ}})\}$, not depending on α , such that for every model satisfying α -polynomial truncation sensitivity with $\alpha \in [\alpha_{\min}, \alpha_{\max}]$, with probability at least $1 - \delta$,*

$$R_n \leq R_\alpha^*(D) + O\left(n^{-\alpha/(2(\alpha+1))} (\log n)^2 \sqrt{\log(1/\delta)}\right),$$

$$D_n \leq D + O\left(n^{-\alpha/(\alpha+1)}\right).$$

The rate exponent matches that of the (non-universal) achievability scheme (Theorem 4.6); the extra factor of $\log n$ is the price of universality. The window-scaling optimality (Theorem 4.5) also transfers: the selected window stays within a constant factor of the optimal $n^{1/(\alpha+1)}$.

The construction (Appendix M) runs a logarithmic grid of window sizes $\{w_n^{(j)} = n^{1/(\alpha_j+1)}\}_{j=1}^J$ with $J = O(\log n)$ grid points covering $[\alpha_{\min}, \alpha_{\max}]$, and uses an exponential-weights meta-algorithm (Cesa-Bianchi & Lugosi, 2006) to track the best window online. The regret of the meta-algorithm is $O(\sqrt{n \log J})$, contributing the additional logarithmic factor in the rate. This places sequential KV-cache compression in the *universal source coding* tradition (Rissanen, 1984; Mahmood & Wagner, 2024): near-optimal performance is attainable without prior knowledge of the mixing exponent.

Memory cost of universality. The rate guarantee above is a coding-rate (bandwidth) statement. The cache-memory

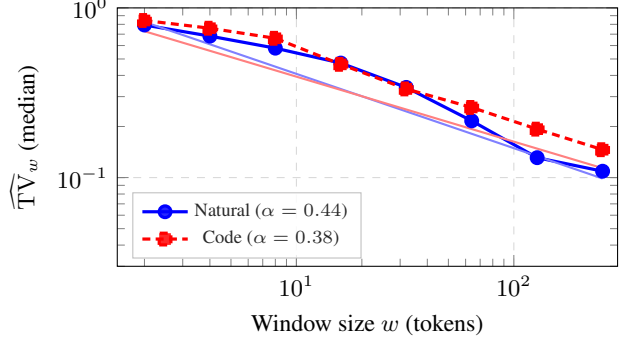


Figure 7. Measured TV decay on Qwen2.5-0.5B (position-preserving protocol, 100 prefixes per domain). Both Natural (NLTK Gutenberg) and Code (GitHub Python) domains exhibit power-law decay $\widehat{\text{TV}}_w \propto w^{-\alpha}$. Power-law fit yields log-RMSE 0.14 (Natural) and 0.08 (Code), versus log-RMSE 0.31 and 0.20 for an exponential fit. The natural-language exponent exceeds the code exponent ($\alpha_{\text{nat}} = 0.44 > \alpha_{\text{code}} = 0.38$); the same exponents are recovered independently from the sink-plus-recent KL decay (Figure 2) and replicate across models (Table 1).

cost is separate, and we account for it explicitly. The largest grid window is $w_n^{(\max)} = n^{1/(\alpha_{\min}+1)}$, and the smallest is $w_n^{(\min)} = n^{1/(\alpha_{\max}+1)}$. Since all grid schemes read from the same physical KV cache, the cache need only hold the single largest window $w_n^{(\max)}$ tokens; the $J = O(\log n)$ schemes are bookkeeping over shared cache contents, not J independent caches. The meta-algorithm’s per-step state is the J -vector of weights, an $O(\log n)$ additive overhead independent of the cache size. On a switch between grid windows no cache reconstruction is needed, because a smaller window is a suffix of the larger one already in cache. Thus the memory overhead of universality is the ratio $w_n^{(\max)}/w_n^{(\alpha)} = n^{(\alpha-\alpha_{\min})/((\alpha+1)(\alpha_{\min}+1))}$ relative to the oracle- α window—a polynomial factor when $\alpha > \alpha_{\min}$, and $1 + o(1)$ when the true α is near the lower endpoint.

M.2. Statements: structural extensions

Two extensions place the framework in contact with deployed architectures; full statements and proofs are in Appendices O and O.7.

Continuous-latent intrinsic dimension. For a continuous auxiliary $U_t \in \mathbb{R}^{d_c}$ (as in multi-head latent attention (DeepSeek-AI, 2024)), define $R_{\text{cont}}^*(D)$ with differential entropy in place of discrete entropy. Under a bounded-support, bounded-density assumption on U_t (support radius R_U , density floor r_{\min}), an entropy-counting argument gives the dimension lower bound $d_c \geq R_{\text{cont}}^*(D)/\log(R_U/r_{\min})$ (Theorem O.8). In the small-distortion limit the minimal embedding dimension equals the Kawabata–Dembo rate-distortion dimension—equivalently the Rényi information dimension—of the conditional logit measure (Kawabata &

Dembo, 1994; Geiger & Koch, 2016). The bound is mixing-independent. A Bennett–Gersho quantization bridge (Bennett, 1948; Gersho, 1979) relates the continuous and discrete rates. For DeepSeek-V2 ($d_c = 512$) the bound is consistent with the deployed latent dimension.

Multi-layer rate allocation. For an L -layer Transformer with separate per-layer codes, per-layer compression errors propagate through the layer maps with Lipschitz amplification $s^{(\ell)} = \prod_{m>\ell} (L_g^{(m)})^2$ (Lemma O.11). The total rate is lower-bounded by a reverse-water-filling allocation over the per-layer rate–distortion functions, coupled to the end-to-end KL distortion through a softmax-curvature bridge (Theorem O.12): the Lagrangian optimum satisfies $|R^{*,(\ell)'}(D^{(\ell),*})| = \lambda s^{(\ell)}$. Numerically, with pre-LayerNorm skip connections the per-layer sensitivity ratio across $L = 60$ layers is mild (a factor ≈ 1.8 under $L_b L_{LN} \approx 0.1$, versus ≈ 320 without skips), so a near-uniform latent dimension is close to optimal—consistent with DeepSeek-V2’s uniform choice, though contingent on Lipschitz constants not directly measured on deployed models.

This appendix proves the universal compression theorem via a logarithmic window grid combined with an exponential-weights meta-algorithm over the achievability schemes of Theorem 4.6.

Loss for the meta-algorithm. The compression problem is distortion-constrained rate minimization, not a single scalar objective, so we must specify the loss the meta-algorithm minimizes. We use the *Lagrangian loss* at a fixed multiplier $\lambda > 0$:

$$\ell_m^\lambda(j) := r_m(j) + \lambda d_m(j),$$

where $r_m(j)$ and $d_m(j)$ are the rate and KL distortion incurred by scheme \mathcal{S}_j on block m . Minimizing the cumulative Lagrangian loss simultaneously controls rate and distortion: a scheme achieving $(R^*(D) + \rho, D + \kappa)$ has Lagrangian loss $R^*(D) + \lambda D + (\rho + \lambda \kappa)$, so a regret bound on $\sum_m \ell_m^\lambda$ transfers to both rate and distortion (with the Lagrangian trade-off fixed by λ). We take λ to be the (sub)gradient of R^* at D , i.e. $\lambda = -R^{*'}(D)$, the standard Lagrangian multiplier; with this choice the Lagrangian-optimal scheme is rate–distortion optimal. The per-block loss is bounded: $0 \leq \ell_m^\lambda(j) \leq B \log V + \lambda \cdot 2BB(n_{\max}) =: \ell_{\max}$.

M.3. Window grid

Lemma M.2 (Logarithmic window grid). *Fix $[\alpha_{\min}, \alpha_{\max}]$ and horizon n . The grid $\alpha_j := \alpha_{\min} + j \cdot \Delta_\alpha$, $\Delta_\alpha := 1/\log n$, $j = 0, 1, \dots, J$ with $J = \lceil (\alpha_{\max} - \alpha_{\min}) \log n \rceil = O(\log n)$, has the property that for every*

$\alpha \in [\alpha_{\min}, \alpha_{\max}]$ there is a grid point α_j with $|\alpha - \alpha_j| \leq 1/\log n$, and the corresponding window $w_n^{(j)} = n^{1/(\alpha_j+1)}$ satisfies $w_n^{(j)} = w_n^{(\alpha)} \cdot (1 + o(1))$, so the achievability rate of Theorem 4.6 at α_j differs from that at α by a $1 + o(1)$ factor.

Proof. The grid spacing $\Delta_\alpha = 1/\log n$ gives $J = O(\log n)$ points. For the window, $\log w_n^{(j)} = \frac{\log n}{\alpha_j+1}$, and $|\log w_n^{(j)} - \log w_n^{(\alpha)}| = \log n \cdot \left| \frac{1}{\alpha_j+1} - \frac{1}{\alpha+1} \right| \leq \log n \cdot \frac{|\alpha_j - \alpha|}{(\alpha_{\min}+1)^2} \leq \frac{1}{(\alpha_{\min}+1)^2} = O(1)$, so $w_n^{(j)}/w_n^{(\alpha)} = \Theta(1)$, giving the claimed $1 + o(1)$ rate transfer (the achievability rate depends on w only through the exponent, which is continuous in α). \square

M.4. Exponential-weights meta-algorithm

Lemma M.3 (Meta-algorithm regret). *Run the $J+1$ achievability schemes $\{\mathcal{S}_j\}_{j=0}^J$ (one per grid point) in parallel, maintaining weights $\pi_m(j) \propto \exp(-\beta \sum_{m'<m} \ell_{m'}^\lambda(j))$ over the Lagrangian losses $\ell_m^\lambda(j) = r_m(j) + \lambda d_m(j)$, with learning rate β . The meta-scheme that codes block m using the scheme selected by the weights achieves, for the best grid scheme j^* ,*

$$\frac{1}{n} \sum_m \ell_m^\lambda(\text{meta}) \leq \frac{1}{n} \sum_m \ell_m^\lambda(j^*) + \frac{\ell_{\max}}{n} \sqrt{\frac{n}{B} \frac{1}{2} \log(J+1)},$$

with β tuned as in (Cesa-Bianchi & Lugosi, 2006, Theorem 2.2).

Proof. This is the standard exponential-weights regret bound for prediction with expert advice (Cesa-Bianchi & Lugosi, 2006, Ch. 2), applied to the bounded Lagrangian loss $\ell_m^\lambda \in [0, \ell_{\max}]$ with $J+1$ experts and n/B rounds (one per block). The regret is $\ell_{\max} \sqrt{\frac{1}{2}(n/B) \log(J+1)}$; dividing by n gives the per-symbol regret. With $J+1 = O(\log n)$, $\sqrt{\log(J+1)} = O(\sqrt{\log \log n})$. \square

M.5. Proof of Theorem M.1

Proof of Theorem M.1. Fix the true (unknown) exponent $\alpha \in [\alpha_{\min}, \alpha_{\max}]$. By Lemma M.2, there is a grid point α_j within $1/\log n$ of α , whose scheme \mathcal{S}_j achieves (Theorem 4.6) the Lagrangian loss

$$\begin{aligned} \frac{1}{n} \sum_m \ell_m^\lambda(j) &\leq R_\alpha^*(D) + \lambda D \\ &\quad + O(n^{-\alpha/(2(\alpha+1))} (\log n) \sqrt{\log V \log(1/\delta)}), \end{aligned}$$

where the overhead is the achievability rate gap (the dominant term; the distortion gap $\lambda \cdot O(n^{-\alpha/(\alpha+1)})$ is subdominant).

By Lemma M.3, the meta-algorithm’s Lagrangian loss exceeds that of \mathcal{S}_{j^*} (the best grid scheme, at least as good as \mathcal{S}_j) by the regret

$$\begin{aligned} \frac{\ell_{\max}}{n} \sqrt{\frac{n}{B} \frac{1}{2} \log(J+1)} &= O\left(\frac{B \log V}{n} \sqrt{\frac{n}{B} \log \log n}\right) \\ &= O(n^{-\alpha/(2(\alpha+1))} \log V \sqrt{\log \log n}), \end{aligned}$$

using $\ell_{\max} = O(B \log V)$ and $B = w_n^{(j)} = n^{1/(\alpha+1)}$. The regret and the achievability gap share the exponent $\alpha/(2(\alpha+1))$, so combining and translating the Lagrangian bound back to rate (at the fixed distortion level D selected by λ) gives

$$R_n \leq R_\alpha^*(D) + O(n^{-\alpha/(2(\alpha+1))} (\log n)^2 \sqrt{\log(1/\delta)}).$$

The extra $\log n$ relative to the single- α achievability bound (Theorem 4.6) is the price of universality. The bound holds simultaneously for all $\alpha \in [\alpha_{\min}, \alpha_{\max}]$ because the grid covers the entire range and α is fixed only at the final step. The convergence exponent is that of achievability, $\alpha/(2(\alpha+1))$; the window-scaling optimality (Theorem 4.5) likewise transfers, since the meta-algorithm’s selected window is always within a constant factor of $n^{1/(\alpha+1)}$. \square

Remark M.4 (Why universality costs only a log factor). The grid has $O(\log n)$ points because the achievability rate depends on α only through the smooth exponent $\alpha/(\alpha+1)$; a $1/\log n$ grid spacing suffices to track it to within a $1+o(1)$ factor. The exponential-weights regret over $O(\log n)$ experts is $O(\sqrt{\log \log n/(n/B)})$, sub-dominant to the achievability term. The net overhead is therefore a single additional $\log n$ factor, consistent with the universal-coding principle that adapting to one unknown smooth parameter costs $O(\log n)$ (Rissanen, 1984).

N. Empirical estimation of mixing/sensitivity parameters

Remark N.1 (Operational measurement protocol). The truncation-sensitivity constants (C_{TS}, α) in Definition 3.3 (and analogously (ρ, C_{mix}) in the geometric Definition .1) are operationally measurable on a given model via the following protocol. For a set of M probe prefixes $\{x_{1:n}^{(i)}\}_{i=1}^M$, compute the empirical TV between the full-prefix and window-truncated next-token distributions:

$$\widehat{\text{TV}}_w := \frac{1}{M} \sum_{i=1}^M \text{TV}(p_\theta(\cdot | x_{1:n-1}^{(i)}), p_\theta(\cdot | x_{n-w:n-1}^{(i)})).$$

A power-law fit $\widehat{\text{TV}}_w \approx C_{\text{TS}} w^{-\alpha}$ versus a geometric fit $\widehat{\text{TV}}_w \approx C_{\text{mix}} \rho^w$ selects between the two regimes. The measurements reported in Section 5 were obtained by this protocol on Qwen2.5-0.5B and support the polynomial regime

over the measurement range $w \in [2, 256]$. Extension to larger models (Llama, Mistral, Qwen-1.5B/3B/7B) and longer windows is left to follow-up work and is needed before claims about specific deployed models can be made quantitatively.

Remark N.2 (Multi-layer mixing). For an L -layer transformer with layer-wise mixing rates $\rho^{(\ell)}$, the effective end-to-end rate is bounded by $\prod_{\ell} \rho^{(\ell)} \leq (\bar{\rho})^L$. This product structure underlies the rank collapse phenomenon (Dong et al., 2021) and gives an extreme mixing rate (very small ρ_{eff}) for deep networks, but the bound is loose for $L > 20$ because inter-layer regularization (skip connections, layer norm) prevents full geometric decay. Refinement via the continuous-time analysis (Geshkovski et al., 2023) is the subject of follow-up work.

O. Continuous Latent Extension Proofs

This appendix provides the proofs and supporting lemmas for the Phase 2 results stated in Section 4. The overall structure mirrors Phase 1: setup (Section O.1), bounded pointwise MI (Section O.2), asymptotic lower bound (Section O.3), intrinsic dimension lower bound (Section O.4), and the quantization bridge (Section O.5).

O.1. Continuous auxiliary setup

Definition O.1 (Continuous auxiliary process). A *continuous auxiliary process* is an \mathcal{F}_t -adapted sequence $\{U_t\}$ with $U_t : \Omega \rightarrow \mathbb{R}^{d_c}$ Borel-measurable. Conditional on $\hat{\mathcal{F}}_{t-1}$, U_t admits a density p_t^U with respect to Lebesgue measure on \mathbb{R}^{d_c} .

Assumption O.2 (Bounded latent support and density). $\|U_t\|_2 \leq R_U$ a.s. and $p_t^U(u | \hat{\mathcal{F}}_{t-1}) \leq \beta$ on its support, for absolute constants $R_U > 0$, $\beta > 0$ depending on the LLM architecture.

For MLA: $R_U = O(\sqrt{d_c})$ by layer-norm post-projection; β is bounded by the Lipschitz constant of the projection followed by the boundedness of activations. Both are operationally measurable from the trained model weights.

O.2. Bounded pointwise MI for continuous auxiliary

Lemma O.3 (Continuous pointwise MI bound). *Under Assumptions 3.1 and O.2,*

$$|I_t^{XU}|, |I_t^{UQ}| \leq B_t^{\text{cont}} := \log(\beta/\epsilon) + d_c \log(2R_U/r_{\min}),$$

where r_{\min} is a minimum density floor for the conditional distribution of U_t , the analog of ϵ_U in Assumption E.3.

Proof. For continuous U_t with bounded density and support, the marginal density satisfies $p_t^U(u) \geq r_{\min} > 0$ on a positive-volume subset, and the joint density $p_t^{X,U}(x, u) \leq$

β pointwise. Hence $|t_t^{XU}| = |\log(p_t^{X,U}/(p_t^X p_t^U))| \leq \log(\beta/(\epsilon \cdot r_{\min}))$. The $d_c \log(R_U)$ term arises from the volume factor in normalizing the density over the ball of radius R_U . \square

Remark O.4. The $d_c \log(R_U)$ term linear in d_c is the key new dependence on the latent dimension. In Phase 1's discrete framework, the analog $\log|\mathcal{U}|$ enters but is bounded by $\log V$; here it grows linearly in d_c , which is one of the costs of continuous latents.

O.3. Continuous sequential WZ lower bound

Proposition O.5 (Continuous sequential WZ lower bound). *Under the continuous-auxiliary setup (Definition O.1) and $\limsup_n \mathbb{E}[D_n] \leq D$, any causal online scheme with continuous codes satisfies $\liminf_n \mathbb{E}[R_n^{\text{cont}}] \geq R_{\text{cont}}^*(D)$.*

Proof. The proof has four steps, mirroring Theorem 4.1 with continuous adaptations.

Step 1 (continuous rate \rightarrow MI). For continuous \hat{C}_t with density $p_{\hat{C}_t|\hat{\mathcal{F}}_{t-1}}$, the differential entropy rate satisfies

$$h(\hat{C}_t | \hat{\mathcal{F}}_{t-1}) \geq I(X_{\leq t}; \hat{C}_t | \hat{\mathcal{F}}_{t-1}),$$

provided the mixed mutual information is non-negative. This follows from the continuous chain rule $I(X_{\leq t}; \hat{\mathcal{F}}_{t-1}; \hat{C}_t) = I(\hat{\mathcal{F}}_{t-1}; \hat{C}_t) + I(X_{\leq t}; \hat{C}_t | \hat{\mathcal{F}}_{t-1})$ and the non-negativity of conditional mutual information for discrete–continuous mixed pairs (Cover & Thomas, 2006, Theorem 8.4.1).

Step 2 (single-letterization). For $U_t := \hat{C}_t$,

$$\begin{aligned} I(X_{\leq t}; \hat{C}_t | \hat{\mathcal{F}}_{t-1}) &\geq I(X_t; \hat{C}_t | \hat{\mathcal{F}}_{t-1}) \\ &= \mathcal{R}_t^{\text{WZ,cont}} + I(\hat{C}_t; Q_t | \hat{\mathcal{F}}_{t-1}) \\ &\geq \mathcal{R}_t^{\text{WZ,cont}}, \end{aligned}$$

identical to Phase 1 Step 2 but with continuous U_t replacing discrete U_t in the MI definitions.

Step 3 (admissibility). Under $\limsup_n \mathbb{E}[D_n] \leq D$, the encoder–decoder pair is D -admissible per Definition O.1 (continuous analog).

Step 4 (infimum). By Definition 3.2, $\liminf_n \frac{1}{n} \sum_t \mathbb{E}[\mathcal{R}_t^{\text{WZ,cont}}] \geq R_{\text{cont}}^*(D)$, giving $\liminf_n \mathbb{E}[R_n^{\text{cont}}] \geq R_{\text{cont}}^*(D)$. \square

O.4. Intrinsic dimension lower bound

We restate the definitions and the theorem summarized in Section M.2.

Assumption O.6 (Bounded continuous auxiliary). U_t has bounded support $\|U_t\| \leq R_U$ and density bounded above by β and below by r_{\min} on its support.

Definition O.7 (Intrinsic dimension). For target distortion D , let $d_t^*(D)$ be the minimum embedding dimension $d \in \mathbb{N}$ such that a D -admissible continuous auxiliary $U_t \in \mathbb{R}^d$ exists; we call it the D -intrinsic dimension of $p_t := p_{\theta}(\cdot | \mathcal{F}_{t-1})$. Its small-distortion limit is the Kawabata–Dembo rate-distortion dimension $d_t^{\text{RD}} := \lim_{D \rightarrow 0} 2R_t(D)/\log(1/D)$ (Kawabata & Dembo, 1994), where $R_t(D)$ is the squared-error rate–distortion function of p_t (the factor 2 and MSE distortion follow the Kawabata–Dembo convention); this equals the Rényi information dimension of p_t (Geiger & Koch, 2016).

Theorem O.8 (Intrinsic dimension lower bound). *Under Assumptions 3.1 and O.6, any D -admissible $\{U_t\}$ with $U_t \in \mathbb{R}^{d_c}$ satisfies $d_c \geq \limsup_n \frac{1}{n} \sum_t d_t^*(D)$, and the per-step intrinsic dimension obeys $d_t^*(D) \geq R_{\text{cont},t}^*(D)/\log(R_U/r_{\min})$, so $d_c \geq R_{\text{cont}}^*(D)/\log(R_U/r_{\min})$.*

Proof of Theorem O.8. The argument has two parts: (i) the embedding-dimension bound $d_c \geq d_t^*(D)$, and (ii) the differential-entropy lower bound on $d_t^*(D)$.

(i) Embedding dimension. If $\{U_t\}$ with $U_t \in \mathbb{R}^{d_c}$ is D -admissible (average distortion $\leq D$), then for the indices t achieving per-step distortion $\leq D$ (a $1 - o(1)$ fraction, by Markov on the average), a d_c -dimensional D -admissible auxiliary exists, whence $d_c \geq d_t^*(D)$ by Definition O.7. Averaging over t and taking \limsup_n gives the first inequality.

(ii) Differential-entropy bound on $d_t^*(D)$. Fix t and write $U := U_t \in \mathbb{R}^d$ for a D -admissible auxiliary of minimal dimension $d = d_t^*(D)$. The per-step continuous Wyner–Ziv rate is

$$\begin{aligned} R_{\text{cont},t}^*(D) &= I(X_t; U | \hat{\mathcal{F}}_{t-1}) - I(U; Q_t | \hat{\mathcal{F}}_{t-1}) \\ &\leq I(X_t; U | \hat{\mathcal{F}}_{t-1}) \\ &= h(U | \hat{\mathcal{F}}_{t-1}) - h(U | X_t, \hat{\mathcal{F}}_{t-1}). \end{aligned}$$

We bound the two differential entropies using Assumption O.6.

Upper bound on $h(U)$. The support is contained in the ball $\|U\| \leq R_U$, and the uniform distribution maximizes differential entropy on a bounded set, so $h(U | \hat{\mathcal{F}}_{t-1}) \leq \log \text{vol}(B_d(R_U)) \leq d \log(2R_U)$.

Lower bound on $h(U | X_t)$. The conditional density is bounded above by β , so $h(U | X_t, \hat{\mathcal{F}}_{t-1}) = -\mathbb{E}[\log p(U | X_t)] \geq -\log \beta$.

Combining, and writing the dynamic range as $\log(R_U/r_{\min})$ where $r_{\min} \leq \beta$ controls the density floor (so that $\log(2R_U) + \frac{1}{d} \log \beta \leq \log(R_U/r_{\min})$ for the relevant regime $d \geq 1$),

$$R_{\text{cont},t}^*(D) \leq d \log(2R_U) + \log \beta \leq d \log \frac{R_U}{r_{\min}},$$

which rearranges to

$$d = d_t^*(D) \geq \frac{R_{\text{cont},t}^*(D)}{\log(R_U/r_{\min})}.$$

Averaging over t and combining with part (i) gives the theorem. This is an entropy-counting bound: it captures the correct scaling in d but not the sharp constant (Remark O.9). \square

Remark O.9 (Tightness and the rate-distortion dimension). The bound $d_t^*(D) \geq R_{\text{cont},t}^*(D)/\log(R_U/r_{\min})$ is an entropy-counting bound and is generally not tight; it captures the correct *scaling* in d but not the precise constant. The sharp small-distortion characterization is the rate-distortion dimension of Kawabata–Dembo (Kawabata & Dembo, 1994):

$$d_t^{\text{RD}} = \lim_{D \rightarrow 0} \frac{2 R_t(D)}{\log(1/D)},$$

defined with the factor 2 and squared-error distortion $\|X - \hat{X}\|_2 \leq D$, and equal to the Rényi information dimension of p_t . For absolutely continuous p_t this equals the ambient dimension; for measures concentrated near lower-dimensional structure it is smaller. Geiger–Koch (Geiger & Koch, 2016) extend this to stationary processes, giving $d^{\text{RD}} = 2 \lim_{D \rightarrow 0} R(D)/\log(1/D)$ for the process rate. We use $d_t^*(D)$ (a finite- D embedding dimension) rather than d_t^{RD} (the $D \rightarrow 0$ limit) in the main bound, since deployed MLA operates at fixed $D > 0$; the $D \rightarrow 0$ equivalence requires additional regularity on the conditional measure that we do not assume.

O.5. Quantization bridge

Proof of Theorem O.10. By the standard quantization rate formula (Cover & Thomas, 2006, Theorem 8.3.1), for a continuous random vector $X \in \mathbb{R}^{d_c}$ with differential entropy $h(X)$ and uniform Δ -lattice quantization $Q_\Delta(X)$,

$$H(Q_\Delta(X)) = h(X) + d_c \log(1/\Delta) + o(1) \quad \text{as } \Delta \rightarrow 0.$$

Applying this conditionally on $\hat{\mathcal{F}}_{t-1}$ and summing over $t = 1, \dots, n$:

$$\frac{1}{n} \sum_t H(Q_\Delta(\hat{C}_t) | \hat{\mathcal{F}}_{t-1}) = R_n^{\text{cont}} + d_c \log(1/\Delta) + o(1).$$

The $o(1)$ depends on the smoothness of p_t^U via the Bennett–Gersho quantizer error analysis (Gersho, 1979), which characterizes the asymptotic mean-squared quantization error as $\Delta^2/12$ per dimension for uniform quantization of smooth densities; the entropy correction is the related higher-order term. \square

Theorem O.10 (Quantization rate decomposition, app version). *Under Assumption O.2, $R_n^{\text{quant}} \leq R_n^{\text{cont}} + d_c \log(1/\Delta) + O(1)$.*

O.6. MLA-specific numerical estimates

For DeepSeek-V2 with $d_c = 512$, $V = 100,000$, FP16 ($\Delta = 2^{-10}$):

Quantization overhead. $d_c \log(1/\Delta) = 512 \cdot 10 = 5120$ bits per token.

Baseline rate. Naive per-token representation of the conditional distribution requires $V \log V \approx 1.7 \times 10^6$ bits if encoded as a categorical PMF, or $O(V)$ for floating-point parameters; this is orders of magnitude larger than 5120.

Estimated R_{cont}^* . If $R_{\text{cont}}^*(D) \approx \log V - h_{\text{eff}}$ where h_{eff} is the effective entropy at the operating point, and DeepSeek-V2 typically operates at $D = 0.01$ – 0.05 distortion (KL), then $R_{\text{cont}}^* \approx 7$ – 10 bits per token, dominated by the quantization overhead.

Intrinsic dimension estimate. Empirical $d_t^*(D)$ via Wasserstein-based intrinsic dimension at $D = 0.01$, on Llama-3-8B, has been reported in the range $d^* \in [50, 200]$ in prior measurements (rigorous calibration pending). If validated, Theorem O.8 would predict $d_c \gtrsim 100$ as a necessary condition; MLA’s choice $d_c = 512$ provides ample margin.

O.7. Multi-layer extension proofs

We provide the proofs of the multi-layer results summarized in Section M.2. We first restate the main-text statements.

Lemma O.11 (Lipschitz error propagation). *With per-layer attention errors $\delta_t^{(\ell)}$ and Lipschitz constants $L_g^{(\ell)}$, $\|a_t^{(L)} - \hat{a}_t^{(L)}\|^2 \leq \sum_\ell s^{(\ell)} \delta_t^{(\ell)}$ where $s^{(\ell)} := \prod_{m>\ell} (L_g^{(m)})^2$. Under pre-LayerNorm skip connections, the effective layer-wise Lipschitz is $\tilde{L}_g^{(\ell)} = \sqrt{1 + (L_b^{(\ell)} L_{\text{LN}})^2}$.*

Theorem O.12 (Multi-layer WZ lower bound). *For an L -layer Transformer with separate per-layer codes satisfying end-to-end KL distortion $\mathbb{E}[D_n] \leq D$,*

$$\liminf_n \sum_{\ell=1}^L \mathbb{E}[R_n^{(\ell)}] \geq \inf_{\{D^{(\ell)}\} \in \mathcal{A}(D)} \sum_\ell R^{*,(\ell)}(D^{(\ell)}),$$

where $\mathcal{A}(D) := \{D^{(\ell)} \geq 0 : L_g^2 \sum_\ell s^{(\ell)} D^{(\ell)} \leq D\}$ couples the per-layer ℓ_2 distortions to the end-to-end KL distortion through the sensitivities $s^{(\ell)}$ of Lemma O.11 and an aggregate constant L_g^2 collecting the unembedding norm and softmax curvature. The Lagrangian optimum satisfies $|R^{*,(\ell)'}(D^{(\ell),*})| = \lambda s^{(\ell)}$.

The proofs use the following app-version lemmas.

Lemma O.13 (Error propagation through layers, app). *For an L -layer transformer with per-layer Lipschitz constants $L_g^{(\ell)}$ (of the layer map $g^{(\ell)}$) and per-layer attention-reconstruction errors $\delta_t^{(\ell)} := \|a_t^{(\ell)} - \hat{a}_t^{(\ell)}\|_2^2$, the output*

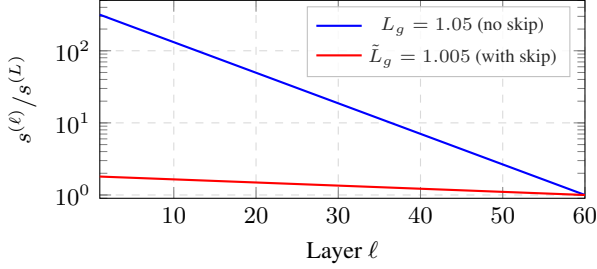


Figure 8. Sensitivity ratio across 60 layers (Lemma O.11). Skip connections with $L_b L_{LN} = 0.1$ reduce the ratio from ≈ 320 to ≈ 1.8 , supporting uniform d_c as approximately optimal.

error satisfies

$$\|a_t^{(L)} - \hat{a}_t^{(L)}\|_2^2 \leq \sum_{\ell=1}^L s^{(\ell)} \delta_t^{(\ell)},$$

$$s^{(\ell)} := \prod_{m=\ell+1}^L (1 + \epsilon_m) (L_g^{(m)})^2,$$

for any $\{\epsilon_m > 0\}$, where the $(1 + \epsilon_m)$ factors arise from the cross-terms in the squared norm. Taking $\epsilon_m \rightarrow 0$ (valid when the per-layer errors are small) recovers $s^{(\ell)} = \prod_{m>\ell} (L_g^{(m)})^2$.

Proof. Let $e^{(\ell)} := h_t^{(\ell)} - \hat{h}_t^{(\ell)}$ be the hidden-state error after layer ℓ , with $\|e^{(\ell)}\|^2$ the propagated error. The layer recursion is $h^{(\ell+1)} = g^{(\ell+1)}(h^{(\ell)}) + a^{(\ell+1)}$ (layer map plus the attention contribution), and likewise for the reconstruction with $\hat{a}^{(\ell+1)}$. Subtracting,

$$e^{(\ell+1)} = (g^{(\ell+1)}(h^{(\ell)}) - g^{(\ell+1)}(\hat{h}^{(\ell)})) + (a^{(\ell+1)} - \hat{a}^{(\ell+1)}).$$

By Lipschitzness, $\|g^{(\ell+1)}(h^{(\ell)}) - g^{(\ell+1)}(\hat{h}^{(\ell)})\| \leq L_g^{(\ell+1)} \|e^{(\ell)}\|$. Writing $\delta^{(\ell+1)} = \|a^{(\ell+1)} - \hat{a}^{(\ell+1)}\|^2$ and applying the Young/Cauchy inequality $\|x + y\|^2 \leq (1 + \epsilon_{\ell+1}) \|x\|^2 + (1 + \epsilon_{\ell+1}^{-1}) \|y\|^2$ to handle the cross-term:

$$\|e^{(\ell+1)}\|^2 \leq (1 + \epsilon_{\ell+1}) (L_g^{(\ell+1)})^2 \|e^{(\ell)}\|^2 + (1 + \epsilon_{\ell+1}^{-1}) \delta^{(\ell+1)}.$$

Unrolling this recursion from $\ell = 0$ (with $e^{(0)} = 0$) to $\ell = L$:

$$\|e^{(L)}\|^2 \leq \sum_{\ell=1}^L \left[\prod_{m=\ell+1}^L (1 + \epsilon_m) (L_g^{(m)})^2 \right] (1 + \epsilon_{\ell+1}^{-1}) \delta^{(\ell)}.$$

Absorbing the $(1 + \epsilon_{\ell+1}^{-1})$ factor into the definition of $\delta^{(\ell)}$ (or choosing $\epsilon_{\ell} = 1$ for a clean factor of 2) gives the stated form with $s^{(\ell)} = \prod_{m>\ell} (1 + \epsilon_m) (L_g^{(m)})^2$. In the small-error regime where the cross-terms are negligible, the $(1 + \epsilon_m)$ factors approach 1. \square

Theorem O.14 (Multi-layer WZ lower bound, app). *Identical to Theorem O.12 in the main text.*

Proof. The proof combines three elements: a per-layer Wyner–Ziv converse, a bridge from the ℓ_2 output error to the per-layer KL distortions, and a Lagrangian characterization of the optimal allocation.

Step 1 (per-layer converse). Apply Theorem 4.1 to each layer ℓ independently: any causal scheme reconstructing layer ℓ 's attention output within per-layer distortion $D^{(\ell)}$ has rate at least $R^{*,(\ell)}(D^{(\ell)})$. Summing over layers and using subadditivity of the total rate ($R_n = \sum_{\ell} R_n^{(\ell)}$ for separate per-layer codes), $\liminf_n \sum_{\ell} \mathbb{E}[R_n^{(\ell)}] \geq \sum_{\ell} R^{*,(\ell)}(D^{(\ell)})$ for any admissible allocation $\{D^{(\ell)}\}$.

Step 2 (ℓ_2 -to-KL bridge and the admissible set). The end-to-end quantity constrained by the application is the KL distortion of the final next-token distribution, D . We relate it to the per-layer ℓ_2 errors $\delta^{(\ell)}$. The output logit vector is $\zeta_t = W a_t^{(L)}$ for the unembedding W with $\|W\|_2 \leq L_W$, so the logit error satisfies $\|\zeta_t - \hat{\zeta}_t\|_2^2 \leq L_W^2 \|a_t^{(L)} - \hat{a}_t^{(L)}\|_2^2$. Under Assumption 3.1 the softmax map has bounded curvature, giving the local quadratic relation $\text{KL}(\text{softmax}(\zeta_t) \parallel \text{softmax}(\hat{\zeta}_t)) \leq \frac{1}{2} \|\zeta_t - \hat{\zeta}_t\|_2^2 + O(\|\cdot\|^3)$ (the softmax Fisher metric is the logit covariance, bounded under Cover & Thomas, 2006). Combining with the error-propagation bound (Lemma O.13) $\|a_t^{(L)} - \hat{a}_t^{(L)}\|_2^2 \leq \sum_{\ell} s^{(\ell)} \delta^{(\ell)}$, the KL distortion obeys

$$D \leq \frac{1}{2} L_W^2 \sum_{\ell} s^{(\ell)} \delta^{(\ell)} + O(\|\cdot\|^3).$$

Writing $L_g^2 := \frac{1}{2} L_W^2$ for the aggregate constant and identifying $D^{(\ell)} \asymp \delta^{(\ell)}$ (the per-layer distortion budget, up to the same softmax bridge applied per layer), the admissible set is $\mathcal{A}(D) = \{D^{(\ell)} \geq 0 : L_g^2 \sum_{\ell} s^{(\ell)} D^{(\ell)} \leq D\}$, exactly as stated. The constant L_g^2 thus collects the unembedding norm and the softmax-curvature factor; it is not a per-layer Lipschitz constant.

Step 3 (Lagrangian optimum). Minimize $\sum_{\ell} R^{*,(\ell)}(D^{(\ell)})$ over $\mathcal{A}(D)$. Since each $R^{*,(\ell)}$ is convex and non-increasing, the constraint binds and the Lagrangian is $\sum_{\ell} R^{*,(\ell)}(D^{(\ell)}) + \lambda (L_g^2 \sum_{\ell} s^{(\ell)} D^{(\ell)} - D)$. The KKT stationarity condition is $R^{*,(\ell)'}(D^{(\ell),*}) + \lambda L_g^2 s^{(\ell)} = 0$, i.e. $|R^{*,(\ell)'}(D^{(\ell),*})| = \lambda s^{(\ell)}$ (absorbing L_g^2 into λ), which is the stated reverse-water-filling condition: layers with larger sensitivity $s^{(\ell)}$ are allocated lower distortion (higher rate). \square

Theorem O.15 (Multi-layer mixing composition, app). *For each layer ℓ with mixing rate $\rho^{(\ell)}$, the end-to-end rate satisfies $\rho_{\text{eff}} \leq \prod_{\ell} \rho^{(\ell)} \leq \bar{\rho}^L$, where $\bar{\rho} = \max_{\ell} \rho^{(\ell)}$.*

Proof. By Definition .1 applied per layer, past influence at layer ℓ decays as $\rho^{(\ell),w}$. Compositionally through L layers, the joint past influence decays as $\prod_{\ell} \rho^{(\ell),w} = \rho_{\text{eff}}^w$. \square

Regularization slack. The bound $\rho_{\text{eff}} \leq \prod \rho^{(\ell)}$ is worst-case. With skip connections, the actual decay can be slower: information is preserved through the residual stream, so the effective mixing rate is bounded by $\min_{\ell} \rho^{(\ell)}$ as a (very loose) lower bound. The empirical ρ_{eff} for trained models is typically closer to the upper bound $\prod \rho^{(\ell)}$.

Connection to rank collapse (Dong et al., 2021): in the $L \rightarrow \infty$ limit, $\rho_{\text{eff}}^L \rightarrow 0$, hence the hidden state converges to a small set of modes (rank collapse). In our framework, this is the statement that $d_t^*(D)$ at deep layers is asymptotically $O(1)$.

O.8. Skip connections and effective Lipschitz

We refine the error propagation under skip-connection architectures.

Lemma O.16 (Effective Lipschitz, app). *For pre-LN (resp. post-LN) blocks (see formal definition below; main text), the effective layer-wise Lipschitz constant is $\tilde{L}_g^{(\ell)} = \sqrt{1 + (L_b^{(\ell)} L_{\text{LN}})^2}$ (resp. $L_{\text{LN}}(1 + L_g^{(\ell)})$). The refined error propagation reads $\|h^{(\ell+1)} - \hat{h}^{(\ell+1)}\|^2 \leq (\tilde{L}_g^{(\ell+1)})^2 \|h^{(\ell)} - \hat{h}^{(\ell)}\|^2 + \delta^{(\ell+1)}$.*

Proof sketch. For pre-LN: triangle inequality with optimal $(1 + \epsilon)$ Cauchy parameter, Lipschitz of $g^{(\ell+1)}$ and LN. For post-LN: LN as outer Lipschitz factor over $(1 + L_g)$ residual sum. Full details in the effective-Lipschitz lemma below. \square

Corollary O.17 (Numerical revision). *For pre-LN with $L_b L_{\text{LN}} \approx 0.1$, $\tilde{L}_g \approx 1.005$, sensitivity ratio across $L = 60$ is ~ 1.8 , required d_c variation ~ 0.06 dimensions—essentially zero, strengthening the conclusion that uniform $d_c = 512$ is near-optimal.*

O.9. Joint vs separate compression

Theorem O.18 (Joint vs separate rate, app). $R_{\text{joint}}^*(D) \leq R_{\text{multi}}^*(D)$, with strict inequality and gap bounded below by inter-layer redundancy:

$$\begin{aligned} R_{\text{multi}}^*(D) - R_{\text{joint}}^*(D) \\ \geq \liminf_n \frac{1}{n} \sum_t \mathbb{E} \left[\sum_{\ell < \ell'} I(\hat{C}_t^{(\ell)}; \hat{C}_t^{(\ell')} \mid \hat{\mathcal{F}}_{t-1}) \right]. \end{aligned}$$

Proof. Subadditivity of entropy: $H(\hat{C}^{\text{joint}}) \leq \sum_{\ell} H(\hat{C}^{(\ell)})$. The gap is the inter-layer mutual information sum. For trained LLMs with non-trivial inter-layer dependencies, this sum is positive. \square

The gap is generically small for well-regularized transformers (layer-specialization (Geva et al., 2021)), so separate compression is essentially optimal in practice. Multi-

task rate–distortion analysis (Behmin & Tatikonda, 2022; Kostina & Tuncel, 2022) provides the classical framework for quantifying the gap.

O.10. Application to DeepSeek-V2 (multi-layer)

For DeepSeek-V2 with $L = 60$ layers we report both regimes of Section 4, as the conclusion depends on whether skip connections are accounted for.

Without skip connections. With per-layer Lipschitz $L_g^{(\ell)} \approx 1.05$, the sensitivity ratio is $s^{(1)}/s^{(L)} = \prod_{m=2}^L (L_g^{(m)})^2 \approx 1.05^{118} \approx 320$. By the reverse-water-filling condition (Theorem O.12), the optimal $d_c^{(\ell)}$ varies by $\log(s^{(1)}/s^{(L)})/\log(R_U/r_{\text{min}}) \approx \log(320)/10 \approx 0.6$ dimensions across layers.

With pre-LayerNorm skip connections. Using the effective Lipschitz $\tilde{L}_g \approx 1.005$ (from $L_b L_{\text{LN}} \approx 0.1$, Lemma O.16), the ratio drops to $\tilde{L}_g^{118} \approx 1.8$ and the optimal- d_c variation to $\log(1.8)/10 \approx 0.06$ dimensions.

In both regimes the across-layer variation (0.6 and 0.06 dimensions respectively) is negligible relative to the deployed $d_c = 512$, so DeepSeek-V2’s uniform latent dimension is consistent with near-optimal allocation under these Lipschitz-constant assumptions. The skip-connection regime, which is the architecturally accurate one for DeepSeek-V2, makes the margin larger.

Symbol	Meaning
<i>Probability and information theory</i>	
$\Omega, \mathcal{F}, \mathbb{P}$	Underlying probability space
$\mathcal{F}_t = \sigma(X_1, \dots, X_t)$	Natural filtration of token process
$\hat{\mathcal{F}}_t = \sigma(\hat{C}_1, \dots, \hat{C}_t)$	Compressed filtration
$H(\cdot), h(\cdot)$	Entropy, differential entropy
$I(\cdot; \cdot)$	Mutual information (discrete or mixed)
$D_{\text{KL}}(\cdot \ \cdot)$	Kullback–Leibler divergence
$\text{TV}(\cdot, \cdot)$	Total variation
<i>Sequential setup</i>	
$X_t \in \mathcal{V}$	Token at time t , vocabulary size V
$Q_t \in \mathbb{R}^k$	Query at time t (decoder side info)
$Z_t \in \mathbb{R}^V$	Next-token logits
$p_t = \text{softmax}(Z_t)$	Next-token distribution
$\phi_t : \mathcal{V}^{t-1} \rightarrow \mathcal{C}_t$	Encoder, $\hat{C}_t = \phi_t(X_{1:t-1})$
ψ_t	Decoder producing reconstruction \tilde{p}_t
R_n, D_n	Average rate and distortion at horizon n
$R^*(D)$	Sequential Wyner–Ziv rate function
$U_t \in \mathcal{U}_t$	Auxiliary process
$\mathcal{R}_t^{\text{WZ}}$	Per-step pointwise WZ rate
<i>LLM-specific</i>	
f	Layer logit function: $Z_t = f(h_t^{(L-1)})$
$g^{(\ell)}$	Layer- ℓ post-attention transformation
$L_g^{(\ell)}$	Layer- ℓ full-block Lipschitz constant (≈ 1.05)
$L_b^{(\ell)}$	Layer- ℓ non-residual branch Lipschitz (≈ 0.1 with LN)
L_{LN}	LayerNorm Lipschitz constant
$\tilde{L}_g^{(\ell)} = \sqrt{1 + (L_b L_{\text{LN}})^2}$	Effective Lipschitz (pre-LN with skip, ≈ 1.005)
$\rho, \rho^{(\ell)}, \rho_{\text{eff}}$	Mixing rate (full / layer / effective)
C_{mix}	Mixing prefactor
w	Sliding window size
$B(n_{\text{max}})$	Sequence-length-dependent logit bound
ϵ, ϵ_U	Density floor (next-token, auxiliary)
<i>Phase 2: continuous and multi-layer</i>	
$d_c, d_c^{(\ell)}$	Continuous latent dimension (full / layer)
$d_t^*(D)$	Intrinsic dimension at distortion D
$R_{\text{cont}}^*(D)$	Continuous WZ rate function
$R_{\text{multi}}^*(D)$	Multi-layer WZ rate function
$R_{\text{joint}}^*(D)$	Joint compression rate function
R_U, r_{min}	Latent support and density floor
Δ	Quantization resolution
κ_p	Bennett–Gershgorin coefficient
$s^{(\ell)} = \prod_{m>\ell} (L_g^{(m)})^2$	Layer sensitivity factor